INFORMATION TO USERS

The most advanced technology has been used to photograph and reproduce this manuscript from the microfilm master. UMI films the text directly from the original or copy submitted. Thus, some thesis and dissertation copies are in typewriter face, while others may be from any type of computer printer.

The quality of this reproduction is dependent upon the quality of the copy submitted. Broken or indistinct print, colored or poor quality illustrations and photographs, print bleedthrough, substandard margins, and improper alignment can adversely affect reproduction.

In the unlikely event that the author did not send UMI a complete manuscript and there are missing pages, these will be noted. Also, if unauthorized copyright material had to be removed, a note will indicate the deletion.

Oversize materials (e.g., maps, drawings, charts) are reproduced by sectioning the original, beginning at the upper left-hand corner and continuing from left to right in equal sections with small overlaps. Each original is also photographed in one exposure and is included in reduced form at the back of the book.

Photographs included in the original manuscript have been reproduced xerographically in this copy. Higher quality 6" x 9" black and white photographic prints are available for any photographs or illustrations appearing in this copy for an additional charge. Contact UMI directly to order.

U·M·I

University Microfilms International
A Bell & Howell Information Company
300 North Zeeb Road Ann Arbor MI 48106-1346 USA
313 761-4700 800 521-0600

Order Number 9029964

Self-phase modulation and self-steepening in cubic and fifth-order dispersionless media with non-zero relaxation time

Mustafa, Mustafa Aref, Ph.D.

City University of New York, 1990

U·M·I
300 N. Zeeb Rd.
Ann Arbor, MI 48106

Self-Phase Modulation and Self-Steepening in Cubic and Fifth-order Dispersionless Media with Non-Zero Relaxation Time

By

Mustafa-Aref-Mustafa

A dissertation submitted to the Graduate Faculty in Engineering in partial fulfillment of the degree of Doctor of Philosophy, The City University of New York.

1990

This manuscript has been read and accepted for the Graduate Faculty in Engineering in satisfaction of the dissertation requirement for the degree of Doctor of Philosophy.

April 17, 1990
Date

Chairman of Examining Committee

April 17, 1990
Date

Executive Officer

Professor S. Ahmed

Professor R.R. Alfano

Professor G. Eichmann

Professor L. Roytman

Professor R. Tolimieri

Supervisory Committee

The City University of New York

ABSTRACT

Self-Phase Modulation and Self-Steepening in Cubic and Fifth-order Dispersionless Media with Non-Zero Relaxation Time

by

Mustafa-Aref-Mustafa

Adviser: Professor Jamal T. Manassah

The research presented here deals with some analytical solutions for self-phase modulation (SPM) and induced-phase modulation (IPM). In solving the electromagnetic wave equaitons, the method of multiple-scales is utilized. New sets of quasi-linear partial differential equations to describe the pulse shape and the phase associated with the propagation of an ultrashort intense pulse through a cubic nonlinear $\chi^{(3)}$ and a fifth-order nonlinear $\chi^{(5)}$- media, are summerized. The treatment neglects group velocity dispersion and therefore is valid for thin medium.

The solution of the quasi-linear differential equations show that the pulse shape is skewed towards the trailing edge, and that this asymmetry can give rise to optical shock deformation unless balanced by dispersion. The intensity and medium thickness required for the pulse

amplitude and phase to steepen are analysed. The pulse phase is shown to be asymmetric and its maximum is shifted from the maximum corresponding to the amplitude. The spectral distribution of the pulse is computed for different pulse intensities. We find that the anti-Stokes extent of the spectrum is larger than the Stokes side. With nonzero relaxation time, additional asymmetry and downshift towards the Stokes side of the spectrum appear.

We also show that the interference patterns produced by an SPM ultrafast pulse have their fringe positions shifted with respect to that of a plane wave due to the existence of the amplitude-phase maxima time shift. Further discussions center on the Fourier transform of the Young interferometric intensity distribution. We show that its range is determined by the same parameters as those of the spectral extents.

We then analyse the effect of an amplitude filter on the outgoing pulse shape (i.e., width, amplitude, and position of its maximum). Our research specifies the conditions under which the amplitude filter can be used to compress pulses.

The effects of strong pump signal on a weak second harmonic probe signal propagating simultaneously into a nonlinear medium (IPM) is examined. The superbroadening of the spectrum of a weak probe signal and the deformation of its pulse shape are investigated analytically. Finally a numerical method is used to determine the amplitude and phase of the pump signal and probe, when the probe signal is of comparable magnitude to that of the pump.

ACKNOWLEDGEMENTS

It is a great pleasure to acknowledge my deep indebtedness to Professor Jamal T. Manassah for his continued support, encouragement, instruction, and patient guidance during the course of this research. I benefited also greatly from Professors R. Alfano and P.P. Ho with whom we collaborated on a number of joint papers. I am grateful to the faculty of the Electrical Engineering Department for their instruction and help, especially to Professors S. Ahmed, L. Roytman, G. Eichmann, and R. Tolimieri members of my guidance and examining committees.

I would like to take this opportunity to express my sincere thanks to my parents and my sister who made it possible for me to pursue my education all through to the Ph.D degree at great personal sacrifies.

To My Family

TABLE OF CONTENTS

Page

LIST OF TABLES

LIST OF FIGURES

Page

Page

Page

Page

Page

Page

CHAPTER 1

INTRODUCTION

1.1 Background

Supercontinuum [1, 2, 3, 4, 5, 6, 7, 8, 9, 10, 11, 12, 13] generation is the production of nearly white continuous spectrum by propagating picosecond and subpicosecond laser pulses through nonlinear media. This superbroadening is used to produce intense, ultrashort pulses in the spectral range from the ultraviolet to the infrared. The amplitude, phase and extent of spectrum generated are functions of the nonlinear index of refraction of the medium, the initial shape, wavelength, width, intensity, and relaxation time of the material, and the propagation length of the pulse in the medium. Experimentally it is observed that the spectral extent is shifted more towards the blue than the red by a factor of approximately two [1]. The generated superbroad frequency band is used for time-resolved absorption spectroscopy [14] and nonlinear optical effects [15]. The supercontinuum finds several applications [11], in ranging, 3-D imaging, atmospheric remote sensing, and optical fiber characteristics.

Induced supercontinuum [16] is the superbroadening of the spectrum of a weak pulse due to the presence of a strong pulse propagating simultaneously with it in a nonlinear medium.

Self-phase modulation was first observed, by Shimuzu [17], when a modulated spectrum occurred after self-focusing has taken place in a liquid-filled cell. Shimuzu explained his observation as phase modulation due to the intensity-dependent refractive index. Shimuzu's experiment was followed by Alfano's et al observation [8, 18] in crystals and gases. The asymmetry in the Stokes and anti-Stokes region [1, 2, 3, 4, 5, 15, 19, 20] is attributed to contributions from plasmas [21] , self-steepening of the pulse amplitude and/or the time response of the nonlinear index of refraction.

The self-steepening, or the deformation of the pulse, [1, 2, 3, 4, 5] is generated in the non-linear medium because the pulse peak [21, 22] faces a larger refractive index than the leading and trailing edges; therefore, the pulse peak travels at a slower velocity than the edges. Consequently, as the pulse propagates in the medium, its trailing edge become steepened. This deformation can give rise to an asymmetry in the spectrum. De Martini et al [23] showed that, this self-steepening leads to an asymmetry in the spectrum [1, 2, 3, 4, 5, 24]. Likewise, Gustafson et al [25] showed that the incorporation of finite relaxation time in the expression of the Kerr index of refraction also generates an asymmetry and a downshift (towards the Stokes side) of its spectrum.

In this research, detailed results are shown for the self-steepening pulse amplitude, phase, spectral shape and shift in the spectral distribution maximum intensity in $\chi^{(3)}$ and $\chi^{(5)}$ media. The calculation is performed in the plane-wave approximation for dispersionless media but with self-steepening and material relaxation.

We show that the amplitude-phase time shift present in the SPM signal is responsible for the shifts in the positions of the SPM interferometric intensity extrema. Furthermore, we derived an expression for the Fourier transform of this interferometric intensity distribution and related its range parameters to the spectral distribution extents and frequency shift of the supercontinuum.

The effects of amplitude filters on ultrafast self-phase modulated pulses in $\chi^{(3)}$ and $\chi^{(5)}$- media are computed. We analyse the dependence of the outgoing pulse shape (i.e., width, amplitude, and maximum position) on the self-phase modulation parameters and filter characteristics. In particular, we show that amplitude filters can be used in certain conditions to compress pulses.

An analytical solution of the IPM in $\chi^{(3)}$- medium is obtained to compute the amplitude, phase and the spectral distribution of the probe pulse.

Finally, a numerical solution of the IPM in $\chi^{(3)}$- medium is derived to examine the amplitude and phase of a pump and a probe when the relative strength of the second-harmonic signal to the primary is approximately unity.

1.2 Thesis Work

This thesis summarizes in chapter 2 through 10 recent work done at City College in which the author participated and in chapter 11 presents new numerical results by the author.

In chapter 2, the nonlinear w e equation and the method of Multiple-Scales in $\chi^{(3)}$ and $\chi^{(5)}$- media are presented

In chapter 3, the quasi-linear form for the wave equation in $\chi^{(3)}$ and $\chi^{(5)}$ media are obtained.

In chapter 4, the solution for the pulse amplitude in $\chi^{(3)}$ and $\chi^{(5)}$- media are calculated.

In chapter 5, the solutions for the pulse phase and instantaneous frequency sweep in $\chi^{(3)}$ and $\chi^{(5)}$- media are computed.

In chapter 6, the pulse spectral distribution in $\chi^{(3)}$ and $\chi^{(5)}$- media are illustrated.

A method for direct time measurement of the phase in $\chi^{(3)}$ and $\chi^{(5)}$- media is examined in chapter 7.

In chapter 8, the interference pattern of the superocontinuum generated by SPM in $\chi^{(3)}$ and $\chi^{(5)}$- media are determined.

The filter transform of a pulse outgoing from $\chi^{(3)}$ and $\chi^{(5)}$- media are described in chapter 9.

In chapter 10, the analytical solution of the induced phase modulation in $\chi^{(3)}$ medium of a weak probe is obtained.

Finally in chapter 11, a numerical solution to compute the amplitudes and phase of a probe and a pump pulse of approximately equal amplitudes, in the presence of induced phase modulation is presented.

CHAPTER 2

NONLINEAR WAVE EQUATION AND METHOD OF MULTIPLE-SCALES IN $\chi^{(3)}$ AND $\chi^{(5)}$- DISPERSIONLESS MEDIA

2.1 Nonlinear wave equation and method of multiple-scales in $\chi^{(3)}$- medium

The Maxwell's equation in a $\chi^{(3)}$- nonlinear medium [1, 3], where the dispersion of the index of refraction and its imaginary part are neglected, is given by:

$$\nabla^2\vec{E} - \frac{n^2}{c^2}\frac{\partial^2\vec{E}}{\partial t^2} = \frac{2nn_2}{c^2}\frac{\partial^2}{\partial t^2}\left[<\vec{E}.\vec{E}>\vec{E} - c_1\vec{E}\frac{\partial}{\partial t}<\vec{E}.\vec{E}>\right] \qquad (2.1\text{-}1)$$

The last term in the above equation represents the material relaxation term. In Gordon's notation [27], we are considering the first two terms of the noninstantaneous nonlinear polarization, where c_1 is the first moment of the delayed response Kernel which is related to the Raman gain coefficient. Practically, c_1 is, up to a numerical factor of 0(1), equal to the material relaxation time [3], n is the linear index of refraction, n_2 is the nonlinear index of refraction and c is the speed of light in vacuum. In this research, we neglect diffraction effects (i.e we suppose an infinite transverse extent for the pulse) and group velocity dispersion. i.e. our results are valid for thin medium and for large beam sizes.

The above equation reduces to

$$\frac{\partial^2 E}{\partial z^2} - \frac{1}{v_g^2}\frac{\partial^2 E}{\partial t^2} = \frac{nn_2}{c^2}\frac{\partial^2}{\partial t^2}\left[|E|^2 E - c_1 E \frac{\partial}{\partial t}|E|^2\right] \qquad (2.1\text{-}2)$$

under the assumption that one component of $\vec{E}$ is only present and the transverse variation of $\vec{E}$ is neglected and where

$$\langle \vec{E}.\vec{E} \rangle = |E|^2/2$$

To convert the above differential equation to a dimensionless form [1], we bring in the new dimensionless variation Φ, T, Z defined as:

$$T = t/\tau_L, \quad Z = z/v_g \tau_L, \quad E = E_0 \phi \qquad (2.1\text{-}3)$$

where τ_L is the characteristic time associated with the pulse (pulse width), v_g is the group velocity in the medium, and E_0 is the maximum value of the electric field amplitude at the entrance plane of the medium. ε is the dimensionless nonlinear coupling constant, defined as:

$$\varepsilon = \frac{n_2 |E_0|^2}{n}$$

and

$$\varepsilon V = n_2 |E_0|^2 z/c\tau \qquad (2.1\text{-}4)$$

γ is defined as

$$\gamma = c_1/\tau \qquad (2.1\text{-}5)$$

By using the above assumptions, equation [2.1-2] reduces to the following dimensionless form

$$\left(\frac{\partial^2}{\partial Z^2} - \frac{\partial^2}{\partial T^2}\right) \phi = \epsilon \frac{\partial^2}{\partial T^2} \left\{ |\phi|^2 \Phi - \gamma \phi \frac{\partial}{\partial T} |\phi|^2 \right\} \tag{2.1-6}$$

Typical values for the above parameters are

$$\tau_L \approx 10^{-13} \text{ sec}$$
$$n_2 \approx 10^{-22} - 10^{-20} \text{ MKS} \quad \left[10^{-13} - 10^{-11} \text{ esu}\right]$$
$$v_g \approx 2 \times 10^8 \text{ m/sec}$$

The critical power for self-focusing [28] is

$$P_C = \frac{\pi \epsilon_0 c^3}{n_2 \omega^2} \tag{2.1-7}$$

and the distance from the input plane to the self-focusing point is (for $P \gg P_c$)

$$S_f \approx \frac{Ka^2}{2} \sqrt{\frac{P_c}{P}} \tag{2.1-8}$$

Consequently, if the sample thickness is much smaller than S_f one can declare that the supercontinuum observed does not have its origin in self-

focusing or optical breakdown. In Table 2.1-1, we summarize the values of the different experimentally pertinent parameters for an incoming pulse with the following characteristics: $\lambda = 10^{-6}$m, $\tau_L \approx 10^{-13}$s, and spot size $a \approx 10^{-3}$m.

The method of multiple-scales [1, 3, 29] is used to obtain a new set of quasi-linear partial differential equations. The method is summarized as follows:

The functional dependence of Φ on Z, T, and ε in the solution of equation (2.1-6) is not disjoint. To first order in ε, Φ depends on the combinations εT and εZ, as well as on the particular T, Z, and ε. Carrying the perturbation to higher orders, Φ depends additionally on $\varepsilon^2 T$, $\varepsilon^2 Z$, $\varepsilon^3 T$, $\varepsilon^3 Z$ etc. Therefore, it is suitable to write $\Phi(Z, T; \varepsilon)$ as

$$\Phi(Z, T; \varepsilon) = \Phi\left(Z_0, T_0, Z_1, T_1, Z_2, T_2, \ldots\ldots, \varepsilon\right) \qquad (2.1\text{-}9)$$

where the new scaled variables Z_1, T_1, Z_2, T_2, etc., are defined as

$$T_0 = T, \; T_1 = \varepsilon T, \quad T_2 = \varepsilon^2 T, \ldots\ldots\ldots, \; T_n = \varepsilon^n Z \qquad (2.1\text{-}10)$$

$$Z_0 = Z, \; Z_1 = \varepsilon Z, \quad Z_2 = \varepsilon^2 Z, \ldots\ldots\ldots, \; Z_n = \varepsilon^n T \qquad (2.1\text{-}11)$$

T_n's and Z_n's describe different time and distance scales.

Φ is defined as a function of the old and new variables.

Additionally, we search for a uniform expansion solution to Φ in the form

$$\Phi = \Phi_0\left(T_0, Z_0, T_1, Z_1, T_2, Z_2, ..\right) + \varepsilon\Phi_1\left(T_0, Z_0, T_1, Z_1, T_2, Z_2, ..\right)$$

$$+ \varepsilon^2 \Phi_2(T_0, Z_0, T_1, Z_1, T_2, Z_2, \ldots) \qquad (2.1\text{-}12)$$

To represent the drivatives in (2.1-6) as functions of the new variables, we make use of the chain rules for derivatives; then

$$\frac{\partial}{\partial T} = \frac{\partial}{\partial T_0} + \varepsilon \frac{\partial}{\partial T_1} + \varepsilon^2 \frac{\partial}{\partial T_2} + \ldots\ldots$$

$$\frac{\partial}{\partial Z} = \frac{\partial}{\partial Z_0} + \varepsilon \frac{\partial}{\partial Z_1} + \varepsilon^2 \frac{\partial}{\partial Z_2} + \ldots\ldots$$

$$\frac{\partial^2}{\partial T^2} = \frac{\partial}{\partial T_0^2} + 2\varepsilon \frac{\partial^2}{\partial T_0 \partial T_1} + \varepsilon^2 \left(2 \frac{\partial^2}{\partial T_0 \partial T_2} + \frac{\partial^2}{\partial T_1^2} \right) + \ldots\ldots$$

$$\frac{\partial^2}{\partial Z^2} = \frac{\partial}{\partial Z_0^2} + 2\varepsilon \frac{\partial^2}{\partial Z_0 \partial Z_1} + \varepsilon^2 \left(2 \frac{\partial^2}{\partial Z_0 \partial Z_2} + \frac{\partial^2}{\partial Z_1^2} \right) + \ldots\ldots$$

(2.1-13)

If an asterisk denotes a complex conjugate

$$\phi^* = \phi_0^* + \varepsilon \phi_1^* + \varepsilon^2 \phi_2^* \qquad (2.1\text{-}14)$$

then

$$|\phi|^2 = \phi . \phi^* = |\phi_0|^2 + \varepsilon \phi_0 \phi_1^* + \varepsilon \phi_0^* \phi_1 + \varepsilon^2 \phi_0 \phi_2^* + \varepsilon^2 |\phi_1|^2 + \varepsilon^2 \phi_0^* \phi_2 \qquad (2.1\text{-}15)$$

and

$$|\phi|^2\phi = |\phi_0|^2\phi_0 + 2\varepsilon|\phi_0|^2\phi_1 + \varepsilon\phi_0^2\phi_1^* + 2\varepsilon^2|\phi_0|^2\phi_2 + 2\varepsilon^2\phi_0|\phi_1|^2 + \varepsilon^2\phi_0^2\phi_2^* + \varepsilon^2\phi_0^*\phi_1^* \tag{2.1-16}$$

The first term on the R.H.S of equation (2.1-6) becomes

$$\varepsilon\frac{\partial}{\partial T^2}\left[|\phi|^2\phi\right] = \varepsilon\frac{\partial}{\partial T_0^2}|\phi_0|^2\phi_0 + 2\varepsilon^2\frac{\partial^2}{\partial T_0^2}|\phi_0|^2\phi_1 + \varepsilon^2\frac{\partial^2}{\partial T_0^2}\phi_0^2\phi_1^* + 2\varepsilon^2\frac{\partial^2}{\partial T_0\partial T_1}|\phi_0|^2\phi_0 + \varepsilon^3(0) + \varepsilon^4(0) \tag{2.1-17}$$

also

$$\phi\frac{\partial}{\partial T}\left[|\phi|^2\right] = \varepsilon\frac{\partial}{\partial T_0}|\phi_0|^2\phi_0 + \varepsilon^2\frac{\partial^2}{\partial T_0}\left(\phi_0\phi_1^*\right) + \varepsilon^2\frac{\partial}{\partial T_0}\phi_0^*\phi_1 + \varepsilon^2\frac{\partial}{\partial T_1}|\phi_0|^2 + \theta\left(\varepsilon^3\right) \tag{2.1-18}$$

The second term on the R.H.S. of equation (2.1-6) becomes

$$\varepsilon\frac{\partial^2}{\partial T^2}\left[\phi\frac{\partial}{\partial T}|\phi|^2\right] = \varepsilon\frac{\partial}{\partial T_0^2}\left(\phi_0\frac{\partial}{\partial T_0^2}|\phi_0|^2\right) + \varepsilon^2\frac{\partial}{\partial T_0^2}\left(\phi_0\frac{\partial}{\partial T_0}\phi_0\phi_1^*\right)$$

$$+ \varepsilon^2 \frac{\partial^2}{\partial T_0^2} \left[\phi_0 \frac{\partial}{\partial T_0} \phi_0^* \phi_1 \right] + \varepsilon^2 \frac{\partial^2}{\partial T_0^2} \left(\phi_0 \frac{\partial^2}{\partial T_1} |\phi_0|^2 \right)$$

$$+ \varepsilon^2 \frac{\partial^2}{\partial T_0^2} \left(\phi_1 \frac{\partial^2}{\partial T_0} |\phi_0|^2 \right) + 2\varepsilon^2 \frac{\partial^2}{\partial T_0 \partial T_1} \left(\phi_0 \frac{\partial}{\partial T_0} |\phi_0|^2 \right)$$

(2.1-19)

The terms on the L.H.S. of equation (2.1-6) become

$$\left(\frac{\partial^2}{\partial Z^2} - \frac{\partial^2}{\partial T^2} \right) = \frac{\partial^2}{\partial Z_0^2} + 2\varepsilon \frac{\partial^2}{\partial Z_0 \partial Z_1} + \varepsilon^2 \left(2 \frac{\partial^2}{\partial Z_0 \partial Z_2} + \frac{\partial^2}{\partial Z_1^2} \right)$$

$$- \frac{\partial^2}{\partial T_0^2} - 2\varepsilon \frac{\partial^2}{\partial T_0 \partial T_1} - \varepsilon^2 \left(2 \frac{\partial^2}{\partial T_0 \partial T_2} + \frac{\partial^2}{\partial T_1^2} \right) . \qquad (2.1\text{-}20)$$

Using the equations (2.1-12) through (2.1-20) in the partial equation (2.1-16), and equating the respective coefficient of ε^n, one obtains the following equations for the terms multiplying ε^0, ε^1, and ε^2 respectively:

$$\left(\frac{\partial^2}{\partial Z_0^2} - \frac{\partial^2}{\partial T_0^2} \right) \Phi_0 = 0 \qquad (2.1\text{-}21)$$

$$\left(\frac{\partial^2}{\partial Z_0^2} - \frac{\partial^2}{\partial T_0^2}\right)\Phi_1 + 2\left(\frac{\partial^2}{\partial Z_1 \partial Z_0} - \frac{\partial^2}{\partial T_1 \partial T_0}\right)\Phi_0 = \frac{\partial^2}{\partial T_0^2}\left|\Phi_0\right|^2 \Phi_0$$

$$- \gamma \frac{\partial}{\partial T_0^2}\left(\phi_0 \frac{\partial}{\partial T_0}\left|\phi_0\right|^2\right) \qquad (2.1\text{-}22)$$

$$\left(\frac{\partial^2}{\partial Z_0^2} - \frac{\partial^2}{\partial T_0^2}\right)\Phi_2 + 2\left(\frac{\partial^2}{\partial Z_1 \partial Z_0} - \frac{\partial^2}{\partial T_1 \partial T_0}\right)\Phi_1$$

$$+ \left(\frac{\partial^2}{\partial Z_1^2} - \frac{\partial^2}{\partial T_1^2} + 2\frac{\partial^2}{\partial Z_0 \partial Z_2} - 2\frac{\partial^2}{\partial T_0 \partial T_2}\right)\Phi_0$$

$$= 2\frac{\partial^2}{\partial T_0 \partial T_1}\left|\Phi_0\right|^2 \Phi_0 + 2\frac{\partial^2}{\partial T_0^2}\left|\Phi_0\right|^2 \Phi_1 + \frac{\partial^2}{\partial T_0^2}\Phi_0^2 \Phi_1^*$$

$$- \gamma \left[\frac{\partial^2}{\partial T_0^2}\left(\Phi_0 \frac{\partial}{\partial T_1}\left|\Phi_0\right|^2\right) + \frac{\partial^2}{\partial T_0^2}\left(\Phi_0 \frac{\partial}{\partial T_0}\Phi_0^* \Phi_1\right)\right.$$

$$\left. + \frac{\partial^2}{\partial T_0^2}\left(\Phi_0 \frac{\partial}{\partial T_0}\Phi_0 \Phi_1^*\right) + \frac{\partial^2}{\partial T_0^2}\left(\Phi_1 \frac{\partial}{\partial T_0}\left|\Phi_0\right|^2\right)\right.$$

$$\left[+ 2 \frac{\partial^2}{\partial T_0 \partial T_1} \left(\Phi_0 \frac{\partial^2}{\partial T_0} |\Phi_0|^2 \right) \right] \qquad (2.1\text{-}23)$$

The incoming pulse is represented by

$$\Phi_{in} = f(Z - T) \exp(iKZ - iWT) \qquad (2.1\text{-}24)$$

Where $W = \omega\tau$ and $f(Z - T)$ is the pulse form function, for a Gaussian pulse

$$f^2(Z - T) = \exp\left[-(Z - T)^2 \right] \qquad (2.1\text{-}25a)$$

and for a hyperbolic secant pulse

$$f^2(Z - T) = \operatorname{sech}^2(Z - T) \qquad (2.1\text{-}25b)$$

It is convenient to use a new coordinate system which is moving with the pulse, denoting the new coordinates by U_n and V_n where the U_n's and V_n's families are defined by:

$$\begin{aligned} U_0 &= Z_0 - T_0 & V_0 &= Z_0 \\ U_1 &= Z_1 - T_1 & V_1 &= Z_1 \\ U_2 &= Z_2 - T_2 & V_2 &= Z_2 \\ &\vdots & &\vdots \\ U_n &= Z_n - T_n & V_n &= Z_n \end{aligned} \qquad (2.1\text{-}26)$$

The partial derivatives can be described in the new coordinates as:

$$\frac{\partial}{\partial Z_n} = \frac{\partial}{\partial U_n} + \frac{\partial}{\partial V_n} \tag{2.1-27}$$

$$\frac{\partial}{\partial T_n} = - \frac{\partial}{\partial U_n} \tag{2.1-28}$$

$$\frac{\partial^2}{\partial Z_n^2} = \frac{\partial^2}{\partial U_n^2} + \frac{\partial^2}{\partial V_n^2} + 2 \frac{\partial^2}{\partial U_n \partial V_n} \tag{2.1-29}$$

$$\frac{\partial^2}{\partial T_n^2} = - \frac{\partial^2}{\partial U_n^2} \tag{2.1-30}$$

$$\frac{\partial^2}{\partial Z_n \partial Z_m} = \frac{\partial^2}{\partial U_n \partial U_m} + \frac{\partial^2}{\partial V_n \partial V_m} + \frac{\partial^2}{\partial U_n \partial V_m} + \frac{\partial^2}{\partial U_m \partial V_n} \tag{2.1-31}$$

Equation (2.1-17) can be simplified as

$$\varepsilon \frac{\partial^2}{\partial U^2} \left[|\phi|^2 \phi \right] = \varepsilon \frac{\partial^2}{\partial U_0^2} |\phi_0|^2 \phi_0 + 2\varepsilon^2 \frac{\partial^2}{\partial U_0^2} |\phi_0|^2 \phi_1 + \varepsilon^2 \frac{\partial}{\partial U_0^2} \phi_2^2 \phi_1^*$$

$$+ 2\varepsilon^2 \left(\frac{\partial^2}{\partial U_0 \partial U_1} + \frac{\partial^2}{\partial V_0 \partial V_1} + \frac{\partial^2}{\partial U_0 \partial V_1} + \frac{\partial^2}{\partial U_1 \partial V_0} \right) |\phi_0|^2 \phi_0 \tag{2.1-32}$$

and equation (2.1-19) is simplified to

$$\varepsilon \frac{\partial^2}{\partial T^2}\left[\phi \frac{\partial}{\partial T}|\phi|^2\right] = -\varepsilon \frac{\partial^2}{\partial U_0^2}\left[\phi_0 \frac{\partial}{\partial U_0}|\phi_0|^2\right] - \varepsilon^2 \frac{\partial^2}{\partial U_0^2}\left[\phi_0 \frac{\partial}{\partial U_0}\phi_0 \phi_1^*\right]$$

$$-\varepsilon^2 \frac{\partial^2}{\partial U_0^2}\left[\phi_0 \frac{\partial}{\partial U_0}\phi_1^* \phi_0\right] - \varepsilon^2 \frac{\partial^2}{\partial U_0^2}\left[\phi_0 \frac{\partial}{\partial U_1}|\phi_0|^2\right]$$

$$-\varepsilon^2 \frac{\partial^2}{\partial U_0^2}\left[\phi_1 \frac{\partial}{\partial U_0}|\phi_0|^2\right] - 2\varepsilon^2 \frac{\partial^2}{\partial U_0 \partial U_1}\left[\phi_0 \frac{\partial}{\partial U_0}|\phi_0|^2\right] \tag{2.1-33}$$

In a similar manner, we can make the same substitution in equation (2.1-20). The partial differential equations (2.1-21) through (2.1-23) can, respectively, be written as

$$\left[\frac{\partial}{\partial V_0^2} + 2\frac{\partial}{\partial U_0}\frac{\partial}{\partial V_0}\right]\Phi_0 = 0 \tag{2.1-34}$$

$$\left[\frac{\partial^2}{\partial V_0^2} + 2\frac{\partial}{\partial U_0}\frac{\partial}{\partial V_0}\right]\Phi_1 + 2\left[\frac{\partial}{\partial U_1}\frac{\partial}{\partial V_0} + \frac{\partial}{\partial U_0}\frac{\partial}{\partial V_1} + \frac{\partial}{\partial V_1}\frac{\partial}{\partial V_0}\right]\Phi_0$$

$$= \frac{\partial^2}{\partial U_0^2}|\Phi_0|^2 \Phi_0 + \gamma \frac{\partial^2}{\partial U_0^2}\left[\Phi_0 \frac{\partial}{\partial U_0}|\Phi_0|^2\right] \tag{2.1-35}$$

$$\left[\frac{\partial^2}{\partial V_0^2} + 2\,\frac{\partial}{\partial U_0}\,\frac{\partial}{\partial V_0}\right]\Phi_2 + 2\left[\frac{\partial}{\partial U_1}\,\frac{\partial}{\partial V_0} + \frac{\partial}{\partial U_0}\,\frac{\partial}{\partial V_1} + \frac{\partial}{\partial V_1}\,\frac{\partial}{\partial V_0}\right]\Phi_1$$

$$+\left[\frac{\partial^2}{\partial V_1^2} + 2\,\frac{\partial}{\partial U_1}\,\frac{\partial}{\partial V_1} + 2\frac{\partial}{\partial U_0}\,\frac{\partial}{\partial V_2} + 2\,\frac{\partial}{\partial U_2}\,\frac{\partial}{\partial V_0} + 2\,\frac{\partial}{\partial V_2}\,\frac{\partial}{\partial V_0}\right]\Phi_0$$

$$= 2\frac{\partial}{\partial U_0}\,\frac{\partial}{\partial U_1}\left|\Phi_0\right|^2\Phi_0 + 2\frac{\partial^2}{\partial U_0^2}\left|\Phi_0\right|^2\Phi_1 + \frac{\partial^2}{\partial U_0^2}\,\Phi_0^2\,\Phi_1^*$$

$$+\gamma\left[\frac{\partial^2}{\partial U_0^2}\left(\Phi_0\,\frac{\partial}{\partial U_0}\,\Phi_0\Phi_1^*\right) + \frac{\partial^2}{\partial U_0^2}\left(\Phi_0\,\frac{\partial}{\partial U_0}\,\Phi_0^*\Phi_1\right)\right.$$

$$+\frac{\partial^2}{\partial U_0^2}\left(\Phi_0\,\frac{\partial}{\partial U_1}\left|\Phi_0\right|^2\right) + \frac{\partial^2}{\partial U_0^2}\left(\Phi_1\,\frac{\partial}{\partial U_0}\left|\Phi_0\right|^2\right)$$

$$\left.+2\,\frac{\partial^2}{\partial U_0\,\partial U_1}\left(\Phi_0\,\frac{\partial}{\partial U_0}\left|\Phi_0\right|^2\right)\right] \qquad (2.1\text{-}36)$$

The above simultaneous differential equations can be solved through the ansatz

$$\Phi_0 = A\,(U_1,\ V_1,\ U_2,\ V_2)\ \exp(i\,KU_0)$$

$$\Phi_1 = 0$$

$$\Phi_2 = C\,(U_1,\ V_1,\ U_2,\ V_2)\ \exp(i\,KU_0) \qquad (2.1\text{-}37)$$

Where $K = \omega\tau = W$, ω is the pulse center frequency.

It is worth noting that the specific form of C cannot be obtained from the above equations. For cases under consideration, $\varepsilon < 1$ and Φ can be sufficiently approximated by Φ_0. Thus, the solutions are obtained for $\varepsilon V \approx 0(1)$.

2.2 Nonlinear wave equation and method of Multiple-Scales in $\chi^{(5)}$- medium

The Maxwell's equation in a $\chi^{(5)}$- nonlinear medium [4,5] where the dispersion of the index of refraction and its imaginary part are neglected, is given by:

$$\nabla^2 \vec{E} - \frac{n^2}{c^2} \frac{\partial^2 \vec{E}}{\partial t^2} = \frac{4n\, n_4}{c^2} \frac{\partial^2}{\partial t^2} \left[\langle \vec{E}.\vec{E} \rangle^2 \vec{E} - C_2 \vec{E} \frac{\partial}{\partial t} \langle \vec{E}.\vec{E} \rangle^2 \right] \tag{2.2-1}$$

The last term in the above equation represents the material relaxation term. We are considering the first two terms of the noninstantaneous nonlinear polarization, n_4 is the quartic nonlinear Kerr coefficient, C_2, is the relaxation time, C and all the assumptions are the same as in section (2.1)

The above equation becomes

$$\frac{\partial^2 \vec{E}}{\partial z^2} - \frac{1}{v_g^2} \frac{\partial^2 \vec{E}}{\partial t^2} = \frac{n\, n_4}{c^2} \frac{\partial^2}{\partial t^2} \left[|E|^4 E - C_2 E \frac{\partial}{\partial t} |E|^4 \right] \tag{2.2-2}$$

this equation reduces to

$$\left(\frac{\partial^2}{\partial Z^2} - \frac{\partial^2}{\partial T^2}\right)\phi = \varepsilon' \frac{\partial^2}{\partial T^2}\left\{ |\phi|^4 \phi - \gamma' \phi \frac{\partial}{\partial T} |\phi|^4 \right\}$$

(2.2-3)

where the dimensional parameters ε' and γ' are given by

$$\varepsilon' = \frac{n_4 |E_0|^4}{n}$$

(2.2-4)

and

$$\varepsilon' V = n_4 |E_0|^4 z/c\tau$$

(2.2-5)

Relaxation time is defined as

$$\gamma' = C_2/\tau \qquad (2.2\text{-}6)$$

Equation (2.2-3) is parallel to equation (2.1-6) in the previous section.

The method of multiple-scales is used to obtain a new set of quasi-linear partial differential equations as in section (2.1).

The terms in equation (2.2-3) can be simplified as follows

$$|\phi_0|^4 = |\phi_0|^4 + \varepsilon' |\phi_0|^2 \phi_0 \phi_1^* + \varepsilon' |\phi_0|^2 \phi_0^* \phi_1 + \varepsilon'^2 |\phi_0|^2 \phi_0 \phi_2^*$$

$$+ \varepsilon'^2 |\phi_0|^2 \phi_0^* \phi_2 + \varepsilon'^2 |\phi_0|^2 |\phi_1|^2 + \varepsilon' |\phi_0|^2 \phi_0 \phi_1^* + \varepsilon'^2 \phi_0^2 \phi_1^{*2}$$

$$+ \varepsilon'^2 |\phi_0|^2 |\phi_1|^2 + \varepsilon' |\phi_0|^2 \phi_0^* \phi_1 + \varepsilon^2 |\phi_0|^2 |\phi_1|^2 + \varepsilon' \phi_0^{*2} \phi_1^2 \tag{2.2-7}$$

and

$$|\phi|^4 \phi = |\phi_0|^4 \phi_0 + 2\varepsilon' |\phi_0|^2 \phi_0^2 \phi_1^* + 3\varepsilon' |\phi_0|^4 \phi_1 + \varepsilon'^2 |\phi_0|^2 \phi_0^2 \phi_2^*$$

$$+ 3\varepsilon'^2 |\phi_0|^2 \phi_0 |\phi_1|^2 + 2\varepsilon' |\phi_0|^4 \phi_2 + \varepsilon'^2 \phi_0^3 \phi_2^{*2} + 3\varepsilon^2 |\phi_0|^2 \phi_0^* \phi_1^*$$

$$+ 2\varepsilon' |\phi_0|^2 \phi_0 |\phi_1|^2 \tag{2.2-8}$$

The first term on the R.H.S. of equation (2.2-3) becomes

$$\varepsilon' \frac{\partial^2}{\partial T^2} |\phi|^4 \phi = \varepsilon' \left[\frac{\partial^2}{\partial T_0^2} |\phi_0|^4 \phi_0 \right] + \varepsilon'^2 \left[2 \frac{\partial^2}{\partial T_0^2} |\phi_0|^2 \phi_0^2 \phi_1^* \right.$$

$$\left. + 3 \frac{\partial^2}{\partial T_0^2} |\phi_0|^4 \phi_1 + 2 \frac{\partial^2}{\partial T_0 \partial T_1} |\phi_0|^4 \phi_0 \right] \tag{2.2-9}$$

then, the second term on the R.H.S of equation (2.2-3) becomes

$$\varepsilon' \frac{\partial^2}{\partial T^2}\left(\phi \frac{\partial^2}{\partial T}\left|\phi_0\right|^4\right) = \varepsilon' \frac{\partial^2}{\partial T_0^2}\left(\phi_0 \frac{\partial^2}{\partial T_0}\left|\phi_0\right|^4\right) + 2\varepsilon' \frac{\partial^2}{\partial T_0 \partial T_1}\left(\phi_0 \frac{\partial^2}{\partial T_0}\left|\phi_0\right|^4\right)$$

$$+ \varepsilon'^2 \frac{\partial^2}{\partial T_0^2}\left(\phi_0 \frac{\partial^2}{\partial T_1}\left|\phi_0\right|^4\right) \qquad (2.2\text{-}10)$$

The Ts and Zs partial differential equations are

$$\left(\frac{\partial^2}{\partial Z_0^2} - \frac{\partial^2}{\partial T_0^2}\right)\phi_0 = 0 \qquad (2.2\text{-}11)$$

$$\left(\frac{\partial^2}{\partial Z_0^2} - \frac{\partial^2}{\partial T_0^2}\right)\phi_1 + 2\left(\frac{\partial^2}{\partial Z_1 \partial Z_0} - \frac{\partial^2}{\partial T_1 \partial T_0}\right)\phi_0 = \frac{\partial^2}{\partial T_0^2}\left|\phi_0\right|^2 \phi_0$$

$$- \gamma' \frac{\partial^2}{\partial T_0^2}\left(\phi_0 \frac{\partial^2}{\partial T_0^2}\left|\phi_0\right|^4\right) \qquad (2.2\text{-}12)$$

$$\left(\frac{\partial^2}{\partial Z_0^2} - \frac{\partial^2}{\partial T_0^2}\right)\phi_2 + 2\left(\frac{\partial^2}{\partial Z_1 \partial Z_0} - \frac{\partial^2}{\partial T_1 \partial T_0}\right)\phi_1$$

$$+\left(\frac{\partial^2}{\partial Z_1^2} - \frac{\partial^2}{\partial T_1^2} + 2\frac{\partial^2}{\partial Z_0 \partial Z_2} - 2\frac{\partial^2}{\partial T_0 \partial T_2}\right)\phi_0$$

$$= 2\frac{\partial^2}{\partial T_0 \partial T_1}\left|\phi_0\right|^4 \phi_0 + 2\frac{\partial^2}{\partial T_0^2}\left|\phi_0\right|^2 \phi_0^2 \phi_1^* + 3\frac{\partial^2}{\partial T_0^2}\left|\phi_0\right|^4 \phi_1$$

$$- \gamma' \left[2\frac{\partial^2}{\partial T_0 \partial T_1}\left(\phi_0 \frac{\partial^2}{\partial T_0}\left|\phi_0\right|^4\right) + \frac{\partial^2}{\partial T_0^2}\left(\phi_0 \frac{\partial^2}{\partial T_1}\left|\phi_0\right|^4\right)\right]$$

(2.2-13)

By using equations (2.1-27) through (2.1-31), the final partial differential equations, which are respectively parallel to equations (2.1-34) through (2.1-36), are given by:

$$\left[\frac{\partial^2}{\partial V_0^2} + 2\frac{\partial}{\partial U_0}\frac{\partial}{\partial V_0}\right]\phi_0 = 0$$

(2.2-14)

$$\left[\frac{\partial^2}{\partial V_0^2} + 2\,\frac{\partial}{\partial U_0}\,\frac{\partial}{\partial V_0}\right]\phi_1 + 2\left[\frac{\partial}{\partial U_1}\,\frac{\partial}{\partial V_0} + \frac{\partial}{\partial U_0}\,\frac{\partial}{\partial V_1} + \frac{\partial}{\partial V_1}\,\frac{\partial}{\partial V_0}\right]$$

$$= \frac{\partial^2}{\partial U_0^2}\left|\phi_0\right|^4 \phi_0 + \gamma' \frac{\partial^2}{\partial U_0^2}\left(\phi_0 \frac{\partial}{\partial U_0}\left|\phi_0\right|^4\right) \qquad (2.2\text{-}15)$$

$$\left[\frac{\partial^2}{\partial V_0^2} + 2\frac{\partial}{\partial U_0}\,\frac{\partial}{\partial V_0}\right]\phi_2 + 2\left[\frac{\partial}{\partial U_1}\,\frac{\partial}{\partial V_0} + \frac{\partial}{\partial U_0}\,\frac{\partial}{\partial V_1} + \frac{\partial}{\partial V_1}\,\frac{\partial}{\partial V_0}\right]\phi_1$$

$$+ \left[\frac{\partial^2}{\partial V_1^2} + 2\,\frac{\partial}{\partial U_1}\,\frac{\partial}{\partial V_1} + 2\,\frac{\partial}{\partial U_0}\,\frac{\partial}{\partial V_2} + 2\,\frac{\partial}{\partial U_2}\,\frac{\partial}{\partial V_0} + 2\,\frac{\partial}{\partial V_2}\,\frac{\partial}{\partial V_0}\right]\phi_0$$

$$= 2\,\frac{\partial^2}{\partial U_0^2}\left|\phi_0\right|^2 \phi_0^2\,\phi_1^* + 3\,\frac{\partial^2}{\partial U_0^2}\left|\phi_0\right|^4 \phi_1 + 2\,\frac{\partial^2}{\partial U_0 \partial U_1}\left|\phi_0\right|^4 \phi_0$$

$$+ \gamma'\left[2\,\frac{\partial}{\partial U_0 \partial U_1}\left(\phi_0\,\frac{\partial}{\partial U_0}\left|\phi_0\right|^4\right) + \left(\frac{\partial^2}{\partial U_0^2}\,\phi_0\,\frac{\partial}{\partial U_1}\left|\phi_0\right|^4\right)\right]$$

(2.2-16)

The above differential equation can be solved through the same ansatz in equation (2.1-37).

The value of ε' is less than 1.

CHAPTER 3

QUASI-LINEAR FORM FOR THE WAVE EQUATION IN $\chi^{(3)}$ AND $\chi^{(5)}$- DISPERSIONLESS MEDIA

3.1 Quasi-Linear Form in $\chi^{(3)}$- Dispersionless Medium

In this chapter, we will derive the quasi-linear form for the wave equation [1, 3]. Beginning with equations (2.1-34, 2.1-35, and 2.1-36), we obtain a system of quasi-linear partial differential equations for the amplitude and phase of the pulse.

Denote A by:

$$A = a\, e^{i\alpha} \tag{3.1-1}$$

Where a is the amplitude and α is the phase of the pulse; a and α are functions of (U_1, V_1, U_2, V_2).

Substituting equations (3.1-1) and (2.1-37) in equations (2.1-34) through (2.1-36)

where

$$\frac{\partial \phi_0}{\partial V_0} = 0 \tag{3.1-2}$$

$$\frac{\partial \phi_0}{\partial U_0 \partial V_0} = 0 \tag{3.1-3}$$

$$\frac{\partial}{\partial U_0} \cdot \frac{\partial}{\partial V_1} \phi_0 = e^{i\alpha} e^{iKU_0} \left(iK \frac{\partial a}{\partial V_1} - K a \frac{\partial \alpha}{\partial V_1} \right)$$

(3.1-4)

$$\frac{\partial^2}{\partial U_0^2} \left(\phi_0 \frac{\partial}{\partial U_0} \left| \phi_0 \right|^4 \right) = 0$$

(3.1-5)

$$\frac{\partial^2}{\partial U_0^2} \left(\phi_0 \frac{\partial}{\partial U_1} \left| \phi_0 \right|^4 \right) = -4 K^2 e^{i\alpha} e^{iKU_0} \left(a^4 \frac{\partial a}{\partial u_1} \right)$$

(3.1-6)

$$\frac{\partial^2}{\partial U_0^2} \left| \phi_0 \right|^2 \phi_0 = -K^2 a^3 e^{i\alpha} e^{iKU_0}$$

(3.1-7)

$$\frac{\partial^2}{\partial V_1^2} \phi_0 = e^{i\alpha} e^{iKU_0} \left[i a \frac{\partial^2 \alpha}{\partial V_1^2} - a \left(\frac{\partial \alpha}{\partial V_1} \right)^2 + 2i \frac{\partial a}{\partial V_1} \cdot \frac{\partial \alpha}{\partial V_1} + \frac{\partial^2 a}{\partial V_1^2} \right]$$

(3.1-8)

$$\frac{\partial}{\partial U_1} \cdot \frac{\partial}{\partial V_1} \phi_0 = e^{i\alpha} e^{iKU_0} \left[ia \frac{\partial^2 \alpha}{\partial V_1 \partial U_1} + \frac{\partial^2 a}{\partial V_1 \partial U_1} + i \frac{\partial a}{\partial V_1} \cdot \frac{\partial \alpha}{\partial U_1} \right.$$

$$\left. + i \frac{\partial \alpha}{\partial V_1} \left(ia \frac{\partial a}{\partial U_1} + \frac{\partial a}{\partial U_1} \right) \right]$$

(3.1-9)

$$\frac{\partial}{\partial U_0} \cdot \frac{\partial}{\partial V_2} \phi_0 = iK e^{i\alpha} e^{iKU_0} \left[ia \frac{\partial \alpha}{\partial V_2} + \frac{\partial a}{\partial V_2} \right]$$

(3.1-10)

$$\frac{\partial}{\partial U_1} \cdot \frac{\partial}{\partial U_0} |\phi_0|^2 \phi_0 = iK e^{i\alpha} e^{iKU_0} \left[ia^3 \frac{\partial \alpha}{\partial U_1} + 3a^2 \frac{\partial a}{\partial U_1} \right]$$

(3.1-11)

When we equate the real and imaginary parts in equations (2.1-34) through (2.1-36), the new set of partial differential equations are:

$$\frac{\partial a}{\partial V_1} = 0$$

(3.1-12)

$$\frac{\partial \alpha}{\partial V_1} = \frac{K}{2} a^2 \tag{3.1-13}$$

$$3 a^2 \frac{\partial a}{\partial U_1} = 2 \frac{\partial a}{\partial V_2} \tag{3.1-14}$$

$$\frac{K}{4} a^4 + 2 \frac{\partial \alpha}{\partial V_2} = a^2 \frac{\partial \alpha}{\partial U_1} + 2 K \gamma a \frac{\partial a}{\partial U_1} \tag{3.1-15}$$

The above four equations can be represented as functions of the variables U and V, using the chain rule technique

$$\frac{\partial}{\partial V} = \frac{\partial}{\partial V_0} + \varepsilon \frac{\partial}{\partial V_1} + \varepsilon^2 \frac{\partial}{\partial V_2} \tag{3.1-16}$$

$$\frac{\partial}{\partial U} = \frac{\partial}{\partial U_0} + \varepsilon \frac{\partial}{\partial U_1} + \varepsilon^2 \frac{\partial}{\partial U_2} \tag{3.1-17}$$

we obtain

$$\frac{\partial \alpha}{\partial V_1} = \frac{1}{\varepsilon} \frac{\partial \alpha}{\partial V} - \frac{1}{\varepsilon} \frac{\partial \alpha}{\partial V_0} - \frac{\varepsilon^2}{\varepsilon} \frac{\partial \alpha}{\partial V_2} \tag{3.1-18}$$

and

$$\frac{\partial \alpha}{\partial V_2} = \frac{1}{\varepsilon^2} \frac{\partial \alpha}{\partial V} - \frac{1}{\varepsilon^2} \frac{\partial \alpha}{\partial V_0} - \frac{\varepsilon}{\varepsilon^2} \frac{\partial \alpha}{\partial V_1} \tag{3.1-19}$$

and the same technique can be used for the pulse amplitude a.

Hence equations (3.1-12) through (3.1-15) can be reduced to

$$\frac{\partial a}{\partial V} - \frac{3\epsilon}{2} a^2 \frac{\partial a}{\partial U} = 0 \qquad (3.1\text{-}20)$$

$$\frac{\partial \alpha}{\partial V} - \frac{\epsilon}{2} a^2 \frac{\partial \alpha}{\partial U} = \frac{K\epsilon}{2} a^2 - \frac{K}{8} \epsilon^2 a^4 + \gamma K \epsilon a \frac{\partial a}{\partial U} \qquad (3.1\text{-}21)$$

Equations (3.1-20) and (3.1-21) are the quasi-linear partial differential equations corresponding to the propagation of a pulse in a $\chi^{(3)}$ medium where dispersion and absorption have been neglected, correct to order ϵ^2 [3].

The partial differential equations for zero relaxation time ($\gamma = 0$) are given by [1]:

$$\frac{\partial a}{\partial V} - \frac{3}{2} \epsilon a^2 \frac{\partial a}{\partial U} = 0 \qquad (3.1\text{-}22)$$

$$\frac{\partial \alpha}{\partial V} - \frac{\epsilon}{2} a^2 \frac{\partial \alpha}{\partial U} = \frac{K\epsilon}{2} a^2 - \frac{K\epsilon^2}{8} a^4 \qquad (3.1\text{-}23)$$

The above equations represent the quasi-linear partial differential equations correlating with the propagation of a pulse in a nonlinear $\chi^{(3)}$ medium where

absorption and dispersion have been neglected, correct to order ε^2, with zero relaxation time.

The previous quasi-linear partial differential equations are listed below:

A - Traditional Theory (Conventional theory) [8]

$$\frac{\partial a}{\partial V} = 0 \tag{3.1-24}$$

$$\frac{\partial \alpha}{\partial V} = 0 \tag{3.1-25}$$

The above two equation do not include the self-steepening term $\left(\frac{\partial a}{\partial U} \text{ term}\right)$.

B - Slowly Varying approximation [26]

$$\frac{\partial a}{\partial V} - 3\varepsilon a^2 \frac{\partial a}{\partial U} = 0 \tag{3.1-26}$$

$$\frac{\partial \alpha}{\partial V} - \varepsilon a^2 \frac{\partial \alpha}{\partial U} = \frac{K\varepsilon}{2} a^2 \tag{3.1-27}$$

C - Yang and Shen Approximation [13]

$$\frac{\partial a}{\partial V} - \frac{\varepsilon}{2} a^2 \frac{\partial a}{\partial U} = 0 \qquad (3.1\text{-}28)$$

$$\frac{\partial \alpha}{\partial V} - \frac{\varepsilon}{2} a^2 \frac{\partial \alpha}{\partial U} = \frac{K\varepsilon}{2} a^2 \qquad (3.1\text{-}29)$$

Table 3.1-1, summarizes the above equations.

3.2 Quasi-Linear Form in $\chi^{(5)}$- Dispersionless Medium

In this section [4, 5], the same method and assumptions have been used as in section (3.1).

Substituting equations (3.1-1) and (3.1-37) in equations (2.2-14) through (2.2-16), where

$$\frac{\partial^2}{\partial U_0^2} \left|\phi_0\right|^4 \phi_0 = - K^2 a^5 e^{i\alpha} e^{iKU_0} \tag{3.2-1}$$

$$\frac{\partial}{\partial U_2} \frac{\partial}{\partial V_0} \phi_0 = 0 \tag{3.2-2}$$

$$\frac{\partial}{\partial V_2} \cdot \frac{\partial}{\partial V_0} \phi_0 = 0 \tag{3.2-3}$$

$$\frac{\partial^2}{\partial U_0 \partial U_1} \left(\phi_0 \frac{\partial^2}{\partial U_0} \left|\phi_0\right|^4 \right) = 0 \tag{3.2-4}$$

$$\frac{\partial^2}{\partial U_0^2} \left(\phi_0 \frac{\partial}{\partial U_1} \left|\phi_0\right|^4 \right) = - 4 K^2 a^4 \frac{\partial a}{\partial U_1^2} e^{i\alpha} e^{iKU_0} \tag{3.2-5}$$

Then, equating the real and imaginary parts in equations (2.2-14) through (2.2-16), a new set of first order partial differential equations are obtained:

$$\frac{\partial a}{\partial V_1} = 0 \tag{3.2-6}$$

$$\frac{\partial \alpha}{\partial V_1} = \frac{K}{2} a^4 \tag{3.2-7}$$

$$5 a^4 \frac{\partial a}{\partial U_1} = 2 \frac{\partial a}{\partial V_2} \tag{3.2-8}$$

$$\frac{K}{4} a^8 - a^4 \frac{\partial \alpha}{\partial U_1} + 2 \frac{\partial \alpha}{\partial V_2} = 4 K \gamma' a^3 \frac{\partial a}{\partial U_1} \tag{3.2-9}$$

By using the chain-rule technique in equations (3.1-18) and (3.1-19), the final partial differential equations [4, 5] for a and α are given by:

$$\frac{\partial a}{\partial V} - \frac{5}{2} \varepsilon' a^4 \frac{\partial a}{\partial U} = 0 \tag{3.2-10}$$

$$\frac{\partial \alpha}{\partial V} - \frac{\varepsilon'}{2} a^4 \frac{\partial \alpha}{\partial U} = \frac{K}{2} \varepsilon' a^4 - \frac{K}{8} \varepsilon'^2 a^8 + 2 K \gamma' \varepsilon' a^3 \frac{\partial a}{\partial U} \tag{3.2-11}$$

These equations are the parallel equations to (3.1-20) and (3.1-21) respectively.

The U-partial derivatives, on the left-hand side of the above equations, are responsible for self-steepening and γ' term represents the relaxation term in $\chi^{(5)}$- medium.

We can notice, from equation (3.2-10), that the relaxation time does not affect the amplitude equation.

The partial differential equations for zero relaxation time (γ') are [4]:

$$\frac{\partial a}{\partial V} - \frac{5}{2}\,\varepsilon'\, a^4\, \frac{\partial a}{\partial U} = 0 \qquad (3.2\text{-}12)$$

$$\frac{\partial \alpha}{\partial V} - \frac{\varepsilon'}{2}\, a^4 \frac{\partial \alpha}{\partial U} = \frac{K}{2}\,\varepsilon' a^4 - \frac{K}{8}\,\varepsilon'^2 a^8 \qquad (3.2\text{-}13)$$

The above equations represent the quasi-linear partial differential equations corresponding to the propagation of .a pulse in a nonlinear $\chi^{(5)}$ medium where absorption and dispersion have been neglected, correct to order ε'^2, with zero relaxation time.

The general solution of equations (3.1-20), (3.1-21) and (3.2-12), (3.2-13) will be given in the next section.

CHAPTER 4

SOLUTION FOR PULSE AMPLITUDE IN $\chi^{(3)}$ AND $\chi^{(5)}$- DISPERSIONLESS MEDIA

4.1. Solution for Pulse Amplitude $\chi^{(3)}$- in Medium

In this section, specific solutions [1, 3] to equation (3.1-20) will be found whose shape function at the input plane is either Gaussian or secant hyperbolic. The quantity εV will repeatedly occur in the original coordinates $\varepsilon V = \left(n_2 |E_0|^2 z/c \tau_1 \right)$.

The general solution of equation (3.1-20) can be represented by [30]:

$$\frac{dV}{1} = \frac{-2dU}{3\varepsilon a^2} = \frac{da}{0} \qquad (4.1\text{-}1)$$

$$a = c_1 \qquad (4.1\text{-}2)$$

and

$$U + \frac{3}{2}\varepsilon V a^2 = c_2 \qquad (4.1\text{-}3)$$

The general solution will be in the form of

$$c_1 = f(c_2) \qquad (4.1\text{-}4)$$

hence

$$a = f\left(U + \frac{3}{2}\,\varepsilon V a^2\right) \tag{4.1-5}$$

A. Gaussian Pulse [1]

The pulse amplitude a is given by the transcendental equation:

$$a^2 = \exp\left[-\left(U + \frac{3}{2}\,\varepsilon V a^2\right)^2\right] \tag{4.1-6}$$

The Gaussian pulse shapes, as a function of εV, are plotted. In Fig. 4.1-2 the trail of the pulse steepens as εV increases. This pulse is deformed as it propagates. The maximum of the pulse takes effect when $\partial a/\partial U = 0$ at

$$U_M = \frac{-3}{2}\varepsilon V \tag{4.1-7}$$

The (amplitude)^2 of the pulse at U = 0 is given by the solution of

$$(\varepsilon V)^2 = -\frac{4}{9}\,\frac{\ln a^2(0, V)}{a^4(0, V)} \tag{4.1-8}$$

This solution is valid as long as no shock wave is formed [24], i.e., $\partial a^2 / \partial U$ is finite; this implies that V at the exit plane, signified by V_e, should fulfill the inequality:

$$\varepsilon V_e < \frac{(2e)^{1/2}}{3} \approx 0.777 \tag{4.1-9}$$

The way to determine the value of εV_e at the shock is explained next in the derivation for an initial hyperbolic secant pulse. For a larger value of εV, the above solution needs to be modified near the curve sharp edge by including higher derivatives in the approximate differential equation.

B. Hyperbolic secant Pulse [1]

The pulse amplitude solution is given by:

$$a^2 = \operatorname{sech}^2 \left[U + \frac{3}{2} \varepsilon V a^2 \right] \tag{4.1-10}$$

for the boundary condition

$$a(U, 0) = \operatorname{sech}(U) \tag{4.1-11}$$

The amplitude is maximum ($a_M = 1$)

$$U_s = -3/2 \, \varepsilon V \tag{4.1-12}$$

The $(\text{amplitude})^2$ of the pulse at $U = 0$ is given by the solution of

$$a_0^2 = \operatorname{sech}^2\left(\tfrac{3}{2}\,\varepsilon V a_0^2\right) \tag{4.1-13}$$

or

$$\varepsilon V = \frac{2}{3a_0^2}\ln\left[\frac{1}{a_0} + \left(\frac{1}{a_0^2} - 1\right)^{1/2}\right] \tag{4.1-14}$$

where $a_0 = a\,(0, V)$

In Fig. 4.1-1, $a^2(0, V)$ is plotted as a function of εV.

In Fig. 4.1-2, a^2 is plotted as a function of U for different pulse intensities (εV). This figure shows more asymmetry as the pulse energy increases (i.e, εV increasing).

The partial derivative of the pulse amplitude with respect to U can be derived by taking:

$$a = \operatorname{sech}\left(U + \frac{3}{2}\,\varepsilon V a^2\right) \tag{4.1-15}$$

from which we write

$$\operatorname{sech}^{-1} a = U + \frac{3}{2}\,\varepsilon V a^2 \tag{4.1-16}$$

giving:

$$\frac{1}{+\,a\sqrt{1 - a^2}}\,\frac{\partial a}{\partial U} = 3\,\varepsilon V a\,\frac{\partial a}{\partial U} \tag{4.1-17}$$

and $\frac{\partial a}{\partial U}$ is then:

$$\frac{\partial a}{\partial U} = \frac{-a\left(1 - a^2\right)}{3\varepsilon V a^2\left(1 - a^2\right)^{1/2} \pm 1} \qquad (4.1\text{-}18)$$

where (+) refers to $U > -3/2$ and (-) to $U < -3/2$.

The general solution for the pulse amplitude is valid only for $\varepsilon V < (\sqrt{3}/2)$. This inequality can be derived by setting $\partial a/\partial U$ to infinity and finding the value of εV which leads to an optical shock in the pulse amplitude, i.e.,

$$3\varepsilon V a^2\left(1 - a^2\right)^{1/2} - 1 = 0 \qquad (4.1\text{-}19)$$

Hence

$$\varepsilon V = \frac{1}{3}\left[\frac{1}{a^2\left(1 - a^2\right)^{1/2}}\right] \qquad (4.1\text{-}20)$$

then, we take the derivative of the numerator in the above equation to find the max value of a which leads to the shock.

Hence,

$$2a\left(1 - a^2\right)^{1/2} + \frac{1}{2}\, a^2 \frac{(2a)}{\left(1 - a^2\right)^{1/2}} = 0 \qquad (4.1\text{-}21)$$

From the above equation, the pulse amplitude at the shock is equal

$$a = \sqrt{\frac{2}{3}} \tag{4.1-22}$$

Substituting equation (4.1-22) into equation (4.1-20), we get

$$\varepsilon V_{crit} = \frac{\sqrt{3}}{2} \approx 0.866 \tag{4.1-23}$$

For, $\varepsilon V \geq (\sqrt{3}/2)$ an optical shock [24] in the trailing part of the pulse will develop. This shock is smoothed by including the higher time derivatives in Maxwell's equation [24, 31]. These terms are neglected in our approximation.

In Fig. 4.1-3, $\partial a / \partial u$ is plotted as a function of U, for different pulse intensities.

The U-partial derivatives, on the left-hand side of equations (3.1-20) and (3.1-21), are responsible for self-steepening and, the term proportional to γ represents finite material relaxation time. To illustrate the impact of the above two effects, we shall index the parameter (a) by two indices where the first index refers to self-steepening and the second to finite relaxation time. Each index takes the value (0, 1) for the effect being (absent, present). We introduce four cases $a_{0,0}$, $a_{1,0}$, $a_{0,1}$, $a_{1,1}$ [1, 3]

$$a_{0,0} = \operatorname{sech}(U) \tag{4.1-24}$$

$$a_{0,1} = a_{0,0} = \operatorname{sech}(U) \tag{4.1-25}$$

$$a_{1,0}^2 = \operatorname{sech}^2\left[U + \frac{3}{2}\varepsilon V a^2\right] \tag{4.1-26}$$

$$a_{1,1}^2 = a_{1,0}^2 \tag{4.1-27}$$

The $a_{1,1}$ is the general solution to equation (3.1-20) and (3.1-21) It is clear, from equation (4.1-25) and (4.1-26), that the nonzero relaxation time does not affect form of the pulse amplitude solution.

4.2. Solution for Pulse Amplitude in $\chi^{(5)}$. Medium

In this section, we determine the general solution of equation (3.2-10) by using the same techniques as those of section (4.1). Therefore, the pulse amplitude a solution is given by:

$$a^2 = f\left(U + \frac{5}{2}\,\varepsilon V a^4\right) \tag{4.2-1}$$

We consider the case that the initial pulse shape is a hyperbolic secant.

The pulse amplitude a is given by:

$$a^2 = \operatorname{sech}^2\left[U + \frac{5}{2}\,\varepsilon' V a^4\right] \tag{4.2-2}$$

The pulse amplitude is maximum $a_M = 1$ when $\partial a / \partial U = 0$ at

$$U_a = \frac{-5}{2}\varepsilon' V \tag{4.2-3}$$

The $(\text{amplitude})^2$ of the pulse at $U = 0$ is given by the solution of

$$a_0^2 = \operatorname{sech}^2\left[\frac{5}{2}\,\varepsilon' V a_0^4\right] \tag{4.2-4}$$

or

$$\varepsilon' V = \frac{2}{5 a_0^4} \ln \left[\frac{1}{a_0} + \left(\frac{1}{a_0^2} - 1 \right)^{1/2} \right] \tag{4.2-5}$$

where $a_0 = a(0, V)$

In Fig. 4.2-1, the steepened pulse amplitude is plotted as a function of U for different pulse intensities. This figure shows that, as $\varepsilon' V$ increases, the pulse is skewed more toward the left-hand-side of U = 0 and becomes more asymmetric.

The partial derivative of the pulse amplitude with respect to U can be derived in a similar manner as in equations (4.1-15) through (4.1-17). Therefore, the slope of the pulse amplitude is given by

$$\frac{\partial a}{\partial U} = \frac{-a\left(1 - a^2\right)^{1/2}}{10 \varepsilon' V a^4 \left(1 - a^2\right)^{1/2} \mp 1} \tag{4.2-6}$$

where (-, +) corresponds respectively to U (smaller, larger) than $\frac{-5}{2}\varepsilon' V$. The solution of equation (4.2-2) is deduced under the condition of no dispersion and no absorption and is valid for all values of $V < V_{crit}$; V_{crit} is the critical value of V at which the optical shock generates $\left(\text{i.e., } \partial a/\partial U \Rightarrow \infty\right)$. This shock is smoothed by including the

higher order derivative in Maxwell's equation. The value of V_{crit} can be derived in a similar manner as in section 4.1. $a = \sqrt{\frac{4}{5}}$ at the shock and,

$$\varepsilon' V_{crit} = \frac{5\sqrt{5}}{32} \approx 0.349 \tag{4.2-7}$$

It is worth noting that, as in χ^3- dispersionless medium, the nonzero relaxation time does not affect the amplitude solution.

In Fig. 4.2-2, the slope of the steepened amplitude pulse is plotted as a function of U for different pulse intensities.

The U-partial derivatives, on the left-hand side of equations (3.2-10) and (3.2-11) are responsible for self-steepening and, the term proportional to γ' is responsible for material relaxation. We index the parameter a by two indices as in section (4.1). The four possible cases are $a_{0,0}$, $a_{1,0}$, $a_{0,1}$, $a_{1,1}$, [4, 5]

$$a_{0,0} = \operatorname{sech}(U) \tag{4.2-8}$$

$$a_{0,1} = a_{0,0} \tag{4.2-9}$$

$$a_{1,0}^2 = \operatorname{sech}^2\left[U + \frac{5}{2}\varepsilon' V a^4\right] \tag{4.2-10}$$

$$a_{1,1}^2 = a_{1,0}^2 \tag{4.2-11}$$

CHAPTER 5

SOLUTIONS FOR PULSE PHASE AND INSTANTANEOUS FREQUENCY SWEEP IN $\chi^{(3)}$ AND $\chi^{(5)}$. DISPERSIONLESS MEDIA

5.1 Solutions for Pulse Phase and Instantaneous Frequency Sweep in $\chi^{(3)}$ Medium

In this section we will find the general solution of equation (3.1-23) the phase and its derivatives α, $\partial\alpha/\partial U$ and $\partial^2\alpha/\partial U^2$ will thus be determined [1, 3].

Let

$$\alpha' = \alpha + KU \tag{5.1-1}$$

the equation for α' is given by

$$\frac{\partial\alpha'}{\partial V} - \frac{\epsilon}{2} a^2 \frac{\partial\alpha'}{\partial U} = \frac{-K\epsilon^2}{8} a^4 \tag{5.1-2}$$

The above equation can be converted to the following form

$$\frac{\partial \alpha}{\partial V} - \frac{\varepsilon}{2} a^2 \frac{\partial \alpha}{\partial U} = \frac{K\varepsilon}{2} a^2 - \frac{K\varepsilon^2}{8} a^4 \qquad (5.1\text{-}3)$$

From equation (5.1-3), the solution for α is given by

$$\alpha = -KU - \frac{K\varepsilon}{2} \int_0^U a^2(p, V)\, dp - \frac{3}{8} K\varepsilon^2 \int_0^V a^4(0, q)\, dq + f \qquad (5.1\text{-}4)$$

The V and U partial derivatives of the above equation are

$$\frac{\partial \alpha}{\partial V} = -\frac{K\varepsilon}{2} \int_0^U \frac{\partial a^2(p, V)}{\partial V} dp - \frac{3K}{8} \varepsilon^2 a^4(0, V) + \frac{\partial f}{\partial V} \qquad (5.1\text{-}5)$$

and

$$\frac{\partial \alpha}{\partial U} = -K - \frac{K\varepsilon}{2} a^2(U, V) + \frac{\partial f}{\partial U} \qquad (5.1\text{-}6)$$

by substituting equations (5.1-5) and (5.1-6) into equation (5.1-3), the resultant becomes

$$\left\{ -\frac{K\varepsilon}{2}\left(\frac{3\varepsilon}{4}\right)\left[a^4(U,V) - a^4(0,V)\right] - \frac{3K}{8}\,\varepsilon^2\, a^4(0,V) + \frac{\partial f}{\partial V}\right\}$$

$$-\frac{\varepsilon}{2}\, a^2\left[-K - \frac{K\varepsilon}{2}\, a^2 + \frac{\partial f}{\partial U}\right] \quad = \frac{K\varepsilon}{2}\, a^2 - \frac{K\varepsilon^2}{8}\, a^4 \qquad (5.1\text{-}7)$$

and

$$\frac{\partial f}{\partial V} - \frac{\varepsilon}{2}\, a^2\, \frac{\partial f}{\partial U} = 0 \qquad (5.1\text{-}8)$$

The boundary condition imposed by the physical condition of no initial chirp is that, at the input plane (i.e., $V = 0$), α should be zero of all values of U. this implies that, for an incoming sech pulse,

$$\alpha(U,0) = 0 = -KU - \frac{K\varepsilon}{2}\int_0^U a^2(p,0)\, dp + f(U,0) \qquad (5.1\text{-}9)$$

where $$\int_0^U \operatorname{sech}^2 p\, dp = \tanh p|_{p=0}$$

Hence

$$f(U,0) = KU + \frac{K\varepsilon}{2}\tanh U \qquad (5.1\text{-}10)$$

for small V; $\frac{\partial \alpha}{\partial U}$, $\frac{\partial \alpha}{\partial V}$ and α are given by:

$$\frac{\partial \alpha}{\partial U} = -K - \frac{K\varepsilon}{2} + K + \frac{K\varepsilon}{2} = 0 \tag{5.1-11}$$

$$\frac{\partial \alpha}{\partial V} = \frac{K\varepsilon}{2} a^2(U,0) - \frac{K\varepsilon^2}{2} a^4(U,0)$$

$$= \frac{K\varepsilon}{2} \operatorname{sech}^2(U) - \frac{K\varepsilon^2}{2} \operatorname{sech}^4(U) \tag{5.1-12}$$

$$\alpha = \left[\frac{K\varepsilon}{2} \operatorname{sech}^2(U) - \frac{K\varepsilon^2}{2} \operatorname{sech}^4 U \right] U \tag{5.1-13}$$

To find f, we try the following formula

$$f = \int_0^V a^3(U,q)\,dq + \frac{2}{\varepsilon} \int_0^U a(p,0)\,dq \tag{5.1-14}$$

$$\frac{\partial}{\partial V} \int_0^U a(p,0)\,dp = 0 \tag{5.1-15}$$

$$\frac{\partial}{\partial U} \int_0^U a(p,0)\,dp = a(U,0) \tag{5.1-16}$$

$$\frac{\partial}{\partial V}\int_0^V a^3(U,q)\,dq = a^3(U,V) \tag{5.1-17}$$

$$\frac{\partial}{\partial U}\int_0^V a^3(U,q)\,dq = \frac{2}{\varepsilon}\left[a(U,V) - a(U,0)\right] \tag{5.1-18}$$

then

$$\frac{\partial f}{\partial V} - \frac{\varepsilon a^2}{2}\frac{\partial f}{\partial U} = 0 + a^3(U,V) - \frac{\varepsilon}{2}a^2\left[a(U,0)\,\frac{2}{\varepsilon} + \frac{2}{\varepsilon}a(U,V) - \frac{2}{\varepsilon}a(U,0)\right]$$

$$= 0 \tag{5.1-19}$$

The general solution of F(f) can be derived by

$$\frac{\partial F}{\partial V} = \frac{\partial F}{\partial f}\cdot\frac{\partial f}{\partial V} \tag{5.1-20}$$

and

$$\frac{\partial F}{\partial U} = \frac{\partial F}{\partial f}\cdot\frac{\partial f}{\partial U} \tag{5.1-21}$$

looking at V = 0, α (U, 0) = 0

$$f(U,0) = 0 + \frac{2}{\varepsilon}\int_0^U a(p,0)\,dp = \frac{2}{\varepsilon}\sin^{-1}(\tanh U) \tag{5.1-22}$$

and

$$\alpha(U,0) = 0 = -KU - \frac{K\varepsilon}{2}\tanh U + K F\left[\sin^{-1}(\tanh U)\right] \tag{5.1-23}$$

hence

$$F(y) = \tanh^{-1}(\sin y) + \frac{\varepsilon}{2}\sin y \tag{5.1-24}$$

To check the value of y which satisfies the above equation, try

$$F\left[\sin^{-1}(\tanh U)\right] = \tanh^{-1}\left(\sin\sin^{-1}\tanh U\right) + \frac{\varepsilon}{2}\sin\left(\sin^{-1}\tanh U\right)$$

$$= U + \frac{\varepsilon}{2}\tanh U \tag{5.1-25}$$

The final form of α is given by [1]

$$\alpha = -KU - \frac{K\varepsilon}{2}\int_0^U a^2(p,V)\,dp - \frac{3}{8}K\varepsilon^2\int_0^V a^4(0,q)\,dq$$

$$+ K\tanh^{-1}\sin f(U,V) + \frac{K\varepsilon}{2}\sin f(U,V) \tag{5.1-26}$$

where

$$f(U, V) = \frac{\varepsilon}{2} \int_0^V a^3(U, q)\, dq + \sin^{-1} \tanh U \qquad (5.1\text{-}27)$$

To check equation (5.1-26), the boundary condition $V = 0$, $\alpha = 0$

$$\alpha(U, 0) = 0 = -KU - \frac{K\varepsilon}{2} \tanh U + 0 + K \tanh^{-1} \sin\left[\sin^{-1} \tanh U\right]$$

$$+ \frac{K\varepsilon}{2} \sin\left[\sin^{-1} \tanh U\right] = 0$$

The maximum of α, expressed by α_M, and its position, expressed by U_α, are respectively given by

$$\alpha_M \approx \frac{K\varepsilon V}{2} \qquad (5.1\text{-}28)$$

and

$$U_\alpha \approx -\varepsilon V \qquad (5.1\text{-}29)$$

From the above two equations, we can observe that the positions of the maxima of a and α are shifted from each other. Additionally, this shift is linear in εV. Also, observe that the maximum of the amplitude is equal to (1) for all εV, α_M increases linearly with εV. In Fig. 5.1-1, the pulse phase is plotted for different pulse intensities. It can be observed, for small values of εV, α is symmetric and its maximum is centered at $U = 0$. However, as εV increases, the α-curves are skewed at its maximum to the

left-hand side of the comoving coordinate U = 0. In Fig. 5.1-2, the calculated values of α_M and U_α are plotted as function of εV. The computed coordinates of the maxima of the curves are in close agreement with equations [5.1-28 and 5.1-29].

The expression for the partial derivative of the pulse, with respect to U, is called the instantaneous frequency sweep and is given by [1]:

$$\frac{1}{K}\frac{\partial \alpha}{\partial U} = \overline{\alpha'} = -1 + a(U,V)\left[\cos f(U,V)\right]^{1} + \frac{\varepsilon}{2}\left\{a(U,V)\left[\cos f(U,V)\right] - a^{2}(U,V)\right\} \tag{5.1-30}$$

In Fig. 5.1-3, the instantaneous relative frequency sweep is plotted for different values of εV.

In Fig. 5.1-4, a, α, and $\partial\alpha/\partial U$ are plotted for $\varepsilon V = 0.4$; this figure shows that the $|U_\alpha|$ and $|U_a|$ do not coincide with each other which is the source of the fringe position shifts, as will be discussed in a later chapter. In Fig. (5.1-5), we plot the maximum and minimum instantaneous frequency sweep as a function of εV with different γ; this figure shows that as γ increases $\left(\frac{\partial\overline{\alpha}}{\partial U}\right)_{max}$ increases, especially for large values of εV.

In Fig. 5.1-6, we plot the maximum and minimum instantaneous frequency sweep for zero relaxation; this figure shows the comparison between the steepened pulse and the conventional SPM.

The second partial derivative of the pulse is given by

$$\frac{1}{K}\frac{\partial^2 \alpha}{\partial U^2} = \bar{\alpha}'' = \left[\frac{\partial a(U,V)}{\partial U} + a^2(U,V)\tan f(U,V)\right]\left[\cos f(U,V)\right]^{-1}$$

$$+ \frac{\varepsilon}{2}\left[\frac{\partial a(U,V)}{\partial U}\left[\cos f(U,V)\right] - a^2(U,V)\sin f(U,V)\right.$$

$$\left. - 2\,a(U,V)\frac{\partial a(U,V)}{\partial U}\right] \qquad (5.1\text{-}31)$$

In Fig. 5.1-7, we plot the second partial derivative of the pulse for different pulse intensities. It can be observed that $\bar{\alpha}'$ and $\bar{\alpha}''$ for a self-phase modulation pulse differ drastically from their respective expressions associated with a chirped Gaussian pulse, where in that instance α' is linear in U and α'' is constant. Consequently, the pulse, in the time domain for small εV, can be approximated by a chirped gaussian; in the frequency domain, however the detailed forms of values of $\bar{\alpha}'$ and $\bar{\alpha}''$ are critical, and such an approximation is not valid. This point will be discussed in the spectral distribution and the filter transform chapters.

The general solution of equation (3.1-21) which includes self-steepening and non-zero relaxation time is given by:

$$\alpha_T = \alpha + K\gamma\left[\ln a - \ln\left(\operatorname{sech}\left(\tanh^{-1}(\sin f)\right)\right)\right] \qquad (5.1\text{-}32)$$

where α_T is the total pulse phase with self-steepening and nonzero relaxation, and α is the pulse phase with self-steepening but zero relaxation.

To verify the above equation, we have to find the U and V partial derivatives of α_T.

$$\frac{\partial \alpha_T}{\partial U} = \frac{\partial \alpha}{\partial U} + K\gamma \left[\frac{1}{a} \frac{\partial a}{\partial U} + a \tan f \right] \tag{5.1-33}$$

$$\frac{\partial \alpha_T}{\partial V} = \frac{\partial \alpha}{\partial V} + K\gamma \left[\frac{1}{a} \frac{\partial a}{\partial V} + \frac{\varepsilon a^3}{2} \tan f \right] \tag{5.1-34}$$

By substituting the above two equations (5.1-33) and (5.1-34) into equation (3.1-21), the γ terms contributions on both sides will cancel each other. and the solution is verified.

We use the same representation of section 5.1 with the indices, to exhibit the different forms of α. The four possible cases are given by:

$$\bar{\alpha}_{0,0} = \frac{\varepsilon V}{2} \operatorname{sech}^2 U \tag{5.1-35}$$

$$\bar{\alpha}_{0,1} = \frac{\varepsilon V}{2} \operatorname{sech}^2(U) - \gamma \varepsilon V \operatorname{sech}^2(U) \tanh(U) \tag{5.1-36}$$

$$\bar{\alpha}_{1,0} = -U - \frac{\varepsilon}{2} \int_0^U a^2(p, V)\, dp - \frac{3}{8} \varepsilon^2 \int_0^V a^4(0, q)\, dq + \tanh^{-1} \sin f(U, V)$$

$$+\frac{\varepsilon}{2}\sin f(U,V) \tag{5.1-37}$$

$$\bar{\alpha}_{1,1} = \bar{\alpha}_{1,0} + \gamma \ln(a_{1,0}) - \gamma \ln\left[\operatorname{sech}\left[\tanh^{-1} \sin f(U,V)\right]\right] \tag{5.1-38}$$

where

$$\bar{\alpha}_{i,j} = \frac{1}{K}\,\bar{\alpha}_{i,j} \tag{5.1-39}$$

and

$$f(U,V) = \frac{\varepsilon}{2}\int_0^V a_{1,0}^3(U,q)\,dq + \sin^{-1}(\tanh U) \tag{5.1-40}$$

The (1, 1) solution is the general solution of the pulse phase with self-steepening and nonzero relaxation time material. We can observe that the nonzero relaxation time term affects the pulse phase solution. In Fig. 5.1-8, we plot $\frac{1}{\gamma}\left(\bar{\alpha}_{0,1} - \bar{\alpha}_{0,0}\right)$ as a function of U for selected values of pulse intensities. This figure shows that this quantity represents the part of the phase, due to nonzero relaxation time, which is approximately linear in U and with negative slope, which translates into a stokes shift in the instantaneous frequency as previously shown by Gordon [27]. In Fig. 5.1-9, we plot $\frac{1}{\gamma}\left(\bar{\alpha}_{1,1} - \bar{\alpha}_{1,0}\right)$ for different values of intensities (εV) and different relaxation times. This figure shows the effects of self-steepening on the Stoke's shift which will be discussed in section (5.2).

In Fig. 5.1-10, we plot $\bar{\alpha}_{1,1}$ which is the pulse phase including the relaxation and self-steepening, as a function of U for different pulse energies and different relaxation times. This figure shows that the presence of the relaxation term and self-steepening term, shifts the position of the pulse maximum more toward the left-hand side of U = 0. In Fig. 5.1-11, we plot the normalized total frequency sweep with respect to U for different pulse intensities (εV) and different relaxation times (γ). The maximum and minimum of this graph specify the spectral frequency extent on the anti-Stokes and Stokes side respectively.

5.2 Solutions for Pulse Phase and Instatantaneous Frequency Sweep in $\chi^{(5)}$- Medium

In this section, we will find the general solution of equation (3.2-13) to obtain $\alpha, \partial\alpha/\partial U$, and $\partial^2\alpha/\partial U^2$ [1, 4, 5].

Let

$$\alpha' = \alpha + KU \tag{5.2-1}$$

the equation for α' is given by

$$\frac{\partial\alpha'}{\partial V} - \frac{\varepsilon'}{2} a^4 \frac{\partial\alpha'}{\partial U} = -\frac{K}{8} \varepsilon'^2 a^8 \tag{5.2-2}$$

Hence

$$\frac{\partial\alpha}{\partial V} - \frac{\varepsilon'}{2} a^4 \frac{\partial\alpha}{\partial U} = \frac{-K\varepsilon'}{8} a^4 - \frac{K}{8} \varepsilon'^2 a^8 \tag{5.2-3}$$

From equations (5.2-3), the solution for (α) is given by

$$\alpha = -KU - \frac{K\varepsilon'}{2} x \int_0^U a^d(p, V)\, dp - \frac{5}{8} K\varepsilon'^2 y \int_0^V a^e(0, q)\, dq + g \tag{5.2-4}$$

where x, y, d and e are constants. We next determine the exact coefficient of each term in the above equation. The U and V partial derivatives of the above equation are

$$\frac{\partial \alpha}{\partial U} = -K - \frac{K\varepsilon'}{2} \times a^{d}(U, V) + \frac{\partial g}{\partial U} \tag{5.2-5}$$

$$\frac{\partial \alpha}{\partial V} = -\frac{5}{4}\frac{K\varepsilon' xd}{(d+4)}\alpha^{d+4}(U, V) + \frac{5}{4}\frac{K\varepsilon'^{2} xd}{(d+4)}a^{d+4}(0, V)$$

$$-\frac{5}{8}K\varepsilon'^{2} y\, a^{e}(0, V) + \frac{\partial g}{\partial V} \tag{5.2-6}$$

by substituting equations (5.2-1), (5.2-5), and (5.2-6), into equation (5.2-3), the we obtain:

$$\left\{-\frac{5}{4}\frac{K\varepsilon'^{2} xd}{(d+4)}\left[d^{d+4}(U, V) - a^{d+4}(0, V)\right] - \frac{5}{8}K\varepsilon'^{2} y\, a^{e}(0, V) + \frac{\partial g}{\partial V}\right\}$$

$$-\frac{\varepsilon'}{2}a^{4}\left[-K - \frac{K\varepsilon'}{2} \times a^{d}(U,V) + \frac{\partial g}{\partial U}\right] = \frac{K\varepsilon'}{2}a^{2} - \frac{K\varepsilon'^{2}}{8}a^{8} \tag{5.2-7}$$

by equating the power and the identical coefficients on each side, the values of x, y, d, and β are 1/3, 1/3, 4, and 8 respectively. The general solution for α is given by [4]

$$\alpha = -KU - \frac{K\varepsilon'}{6}\int_0^U a^4(p, V)\,dp - \frac{5}{24}K\varepsilon'^2\int_0^V a^8(0, q)\,dq + g \tag{5.2-8}$$

g obeys:

$$\frac{\partial g}{\partial V} - \frac{\varepsilon'}{2}a^4\frac{\partial g}{\partial U} = 0 \tag{5.2-9}$$

The boundary condition imposed by the physical condition of no initial chirp is that at V = 0, α should be zero of all values of U. This implies that, for an incoming sech pulse,

$$\alpha(U, 0) = 0 = -KU - \frac{K\varepsilon'}{6}\int_0^U a^4(p, 0)\,dp + g(U, 0) \tag{5.2-10}$$

$$\text{where} \int_0^U \operatorname{sech}^4 p\,dp = \left(\tanh p - \frac{\tanh^3 p}{3}\right)_{p=0}$$

and

$$g(U,0) = KU + \frac{K\varepsilon'}{6}\left(\tanh U - \frac{\tanh^3 U}{3}\right) \tag{5.2-11}$$

To find g, we try the following solution:

$$g = \int_0^V a^5(U, q)\,dq + \frac{2}{\varepsilon'}\int_0^U a(p, 0)\,dp \tag{5.2-12}$$

$$\frac{\partial}{\partial V}\int_0^V a^5(U, q)\,dq = a^5(U, V) \tag{5.2-13}$$

$$\frac{\partial}{\partial V}\int_0^U a(p, 0)\,dp = 0 \tag{5.2-14}$$

$$\frac{\partial}{\partial U}\int_0^U a(p, 0)\,dp = a(U, 0) \tag{5.2-15}$$

$$\frac{\partial}{\partial U}\int_0^V a^5(U, q)\,dq = \frac{2}{\varepsilon'}\left[a(U, V) - a(U, 0)\right] \tag{5.2-16}$$

The general solution of G(g) can be derived by noting that

$$\frac{\partial G}{\partial V} = \frac{\partial G}{\partial g} \cdot \frac{\partial g}{\partial V} \tag{5.2-17}$$

and $$\frac{\partial G}{\partial U} = \frac{\partial G}{\partial g} \cdot \frac{\partial g}{\partial U} \tag{5.2-18}$$

looking at $V = 0$, $\alpha(U, 0) = 0$

$$g(U,0) = 0 + \frac{2}{\varepsilon'}\int_0^U a(p,0)\,dp = \frac{2}{\varepsilon'}\sin^{-1}(\tanh U) \tag{5.2-19}$$

and

$$\alpha(U,0) = 0 = -KU - \frac{K\varepsilon'}{6}\tanh U + \frac{K\varepsilon'}{6}\frac{\tanh^3 U}{3}$$

$$+ K\,G\left[\sin^{-1}(\tanh U)\right] \tag{5.2-20}$$

$$G(y) = \tanh^{-1}(\sin y) + \frac{\varepsilon'}{6}\sin y - \frac{\varepsilon'}{6}\sin\left(\sin^{-1}\frac{\sin^3 y}{3}\right) \tag{5.2-21}$$

To check the value of y which satisfy the above equation, try

$$G\left[\sin^{-1}(\tanh U)\right] = \tanh^{-1}\left(\sin\sin^{-1}\tanh U\right) + \frac{\varepsilon'}{6}\sin\left[\sin^{-1}\tanh U\right]$$

$$- \frac{\varepsilon'}{6}\sin\left[\sin^{-1}\frac{\tanh^3 U}{3}\right]$$

$$= U + \frac{\varepsilon'}{6}\tanh U - \frac{\varepsilon'}{6}\frac{\tanh^3 U}{3} \tag{5.2-22}$$

The final form of α is then given by

$$\bar{\alpha} = -U - \frac{\varepsilon'}{6}\int_0^U a^4(p,V)\,dp - \frac{5}{24}\varepsilon'^2\int_0^V a^8(0,q)\,dq$$

$$+ \tanh^{-1}[\sin g(U,V)] + \frac{\varepsilon'}{6} \sin g(U,V) - \frac{\varepsilon'}{18} \sin^3 g(U,V)$$

(5.2-23)

where

$$g(U,V) = \frac{\varepsilon'}{2} \int_0^V a^5(U,q)\,dq + \sin^{-1} \tanh U$$

(5.2-24)

The above two equations (5.2-23) and (5.2-24) should satisfy the boundary condition that at V = 0, $\alpha = 0$. The maximum value of α expressedby α_M, and its position, expressed by U_α, are respectively given by

$$\alpha_M \approx \frac{K\varepsilon' V}{2}$$

(5.2-25)

and

$$U_\alpha \approx \frac{-3}{2}\varepsilon' V$$

(5.2-26)

The maxima of the amplitude and the phase are shifted with respect to each other. This result gives rise to a shift of the minima of the interference pattern which will be discussed in a subsequent chapter. The U_a and U_α are deduced by comparing equations (4.2-3) and (5.2-26). The first derivative of $\bar{\alpha}$ with respect to U is given by

$$\frac{\partial \bar{\alpha}}{\partial U} = -1 - \frac{\varepsilon'}{6} a^4 + \frac{a}{\cos g} + \frac{\varepsilon'}{6} a(\cos g) - \frac{\varepsilon'}{6} a\left(\sin^2 g\right)(\cos g)$$

(5.2-27)

In Fig. 5.2-1, the pulse phase α is plotted for different pulse intensities. These figures show that the pulse phase is asymmetric with respect to the U-axis. This is a consequence of the amplitude self-steepening.

In Fig. 5.2-2, we plot the instantaneous frequency sweep $\partial\bar{\alpha}/\partial U$ for different pulse intensities. This figure shows that the derivative of the pulse phase is asymmetric with respect to the U-axis. This is the reason for the asymmetry of the spectral distribution between the Stoke's and anti-Stoke's portion of the spectrum.

The absolute value of the maximum of $\frac{\partial\alpha}{\partial U}$ is always greater than that corresponding to its minimum value; therefore, the anti-Stokes extent is larger than the Stokes extent of the spectrum.

In Fig. 5.2-3, we plot α_M and $|U_\alpha|$ as a function of $\epsilon' V$ and, in Fig. 5.2-4, the maximum and minimum instantaneous frequency sweep are plotted for different values of relaxation time. The second derivative of the total pulse phase is given by

$$\bar{\alpha}'' = -\frac{2}{3}\epsilon' a^3 \frac{\partial a}{\partial U} + \frac{1}{\cos g}\frac{\partial a}{\partial U} + a^2 \frac{\sin g}{\cos^2 g} + \frac{\epsilon'}{6}\left[\cos g \frac{\partial a}{\partial U} - a^2 \sin^2 g\right]$$

$$- \frac{\epsilon'}{6}\left[\sin^2 g . \cos g \frac{\partial a}{\partial U} - a^2 \sin^3 g + 2 a \sin g . \cos^2 g\right]$$

(5.2-28)

In Fig. 5.2-5, we plot $\bar{\alpha}''$ for different pulse intensities ($\varepsilon' V$).

The general solution of equation (3.2-11) which includes self steepening and material relaxation [5], will follow the same procedures as in section(5.1), i.e., equations (5.1-32) to (5.1-36) will be the same as in $\chi^{(3)}$- dispersionless medium.

We use the same representation of the parameter α, with the indices, to represent the presence/absence of the nonzero relaxation time and self steepening. The four possible cases are given by:

$$\bar{\alpha}_{0,0} = \frac{\alpha_{0,0}}{K} = \frac{\varepsilon' V}{2} \operatorname{sech}^4(U) \tag{5.2-29}$$

$$\bar{\alpha}_{0,1} = \frac{\varepsilon' V}{2} \operatorname{sech}^4(U) - 2\gamma' \varepsilon' V \operatorname{sech}^4(U) \tanh(U) \tag{5.2-30}$$

$$\bar{\alpha}_{1,0} = -U - \frac{\varepsilon'}{6} \int_0^U a_{1,0}^4(p, V)\, dp - \frac{5}{24} \int_0^V a_{1,0}^8(0, q)\, dq$$

$$+ \tanh^{-1} \sin g(U, V) + \frac{\varepsilon'}{6} \sin g(U, V) - \frac{\varepsilon'}{18} \sin^3[g(U, V)] \tag{5.2-31}$$

$$\bar{\alpha}_{1,1} = \bar{\alpha}_{1,0} + \gamma' \ln(a_{1,1}) - \gamma' \ln\left[\operatorname{sech}\left[\tanh^{-1}(\sin g(U, V))\right]\right] \tag{5.2-32}$$

Where

$$\bar{\alpha}_{i,j} = = \frac{1}{K}\,\alpha_{i,j} \tag{5.2-33}$$

and

$$g(U,V) = \frac{\varepsilon'}{2}\int_0^V a^5_{1,0}(U,q)\,dq + \sin^{-1}(\tanh U) \tag{5.2-34}$$

The (1, 1) solution is the general solution of pulse phase with self-steepening and nonzero relaxation time. We can observe that the nonzero relaxation time affects the pulse phase. In Fig. 5.2-6, we plot $\frac{1}{\gamma'}\left(\bar{\alpha}_{0,1} - \bar{\alpha}_{0,0}\right)$ as a function U. This figure shows that the phase with nonzero relaxation time for $\varepsilon'V < 1$ is approximately linear in U with a negative slope; this causes a Stokes shift in the instantaneous frequency. This shift is equivalent to Gordon's self frequency, derived for $\chi^{(3)}$ medium In Fig. 5.2-7, we plot $\frac{1}{\gamma'}\left(\bar{\alpha}_{1,1} - \bar{\alpha}_{1,0}\right)$ for different values of intensities ($\varepsilon'V$) to illustrate the effects of self-steepening on this Stoke's shift.

In Fig. 5.2-8, we plot $\bar{\alpha}_{1,1}$ which is the pulse phase including the self-steepening and nonzero relaxation time as a function of U. This figure shows that the existance of self-steepening and nonzero relaxation time term shifts the pulse maximum more toward the left-hand side of U = 0.

The expression of the normalized frequency sweep, for this pulse, is derived by taking the U-partial derivative of $\bar{\alpha}$ and is given by:

$$\frac{\partial \bar{\alpha}}{\partial U} = -1 - \frac{\varepsilon'}{6} a^4 + \frac{a}{\cos g} + \frac{\varepsilon'}{6} a(\cos g) - \frac{\varepsilon'}{6} a(\sin^2 g)(\cos g)$$

$$+ \gamma' \left[a(\tan g) + \frac{1}{a} \frac{\partial a}{\partial U} \right] \qquad (5.2\text{-}35)$$

In Fig. 5.2-9, we plot the normalized total frequency sweep with respect to U. The maximum and minimum of this graph specify the spectral frequency extent on the anti-Stokes and Stoke's side respectively.

CHAPTER 6

PULSE SPECTRAL DISTRIBUTION IN $\chi^{(3)}$ AND $\chi^{(5)}$. DISPERSIONLESS MEDIA

6.1 Pulse Spectral Distribution in $\chi^{(3)}$ Medium

The spectral distribution for the signal at the exit plane is proportional to the magnitude squared of the time Fourier transform of the electric field, which is given by [1]

$$S(\omega', z_e) \alpha \left|\tilde{E}(\omega', z_e)\right|^2 \qquad (6.1\text{-}1)$$

Where $\tilde{E}(\omega', z_e)$ is the Fourier transform of the electric field at the plane $z = z_e$

$$\tilde{E}(\omega', z_e) = \frac{1}{2\pi} \int_{-\infty}^{\infty} \exp(i\omega' t)\ E(t, z)\, dt \qquad (6.1\text{-}2)$$

Where z_e is the coordinate of the exit plane. In the U - V coordinates, where $W = \omega \tau_L$ and , $W' = \omega' \tau_L$, the expression for $\tilde{E}$ is given by [2, 6, 7, 32, 33, 34]

$$\tilde{E}(W', V_e) = \frac{E_0 \tau_L}{2\pi} \int_{-\infty}^{\infty} dU \cdot \exp\left[i(W - W')U\right] \; a(U, V_e) \cdot \exp\left(i\alpha(U, V_e)\right) \tag{6.1-3}$$

Where V_e corresponds to the V of the exit plane

The general equation of the spectral distribution is given by:

$$\tilde{E}(K') = \int_{-\infty}^{\infty} \exp(-iK'U)\, E(U)\, dU \tag{6.1-4}$$

The spectral intensity of self-phase modulation was computed from the specific values of a and α, previously found. However, to obtain an intuitive feeling for this spectrum structure, we used the method of stationary phase [35, 36] to simplify $\tilde{E}(K)$ as follows;

$$\tilde{E}(K') = \int_{-\infty}^{\infty} a(U) \exp(-iK'U) \cdot \exp\left(i\alpha(U)\right) \cdot \exp(iKU) \cdot dU \tag{6.1-5}$$

hence

$$\tilde{E}(K') = \int_{-\infty}^{\infty} a(U)\, e^{iK\left[\delta + \bar{\alpha}(U)\right]}\, du \tag{6.1-6}$$

Here $a(U)$ and $\left[\delta + \bar{\alpha}(U)\right]$ are real functions (no analyticity is necessary).

Assume that there is one point U_0 in the interior of $(-\infty, \infty)$, having the property that; $\left(\delta + \bar{\alpha}(U_0)\right)' = 0$. also, let $\left(\delta + \bar{\alpha}(U_0)\right)'' \neq 0$. In accordance with the above assumption of the method of stationary phase, we assume that only the neighborhood of the point U_0 is of significance, and we can expand

$$iK\left[\delta + \bar{\alpha}(U)\right] \equiv iK\left[\left(\delta + \bar{\alpha}(U_0)\right) + \frac{1}{2}\left(\delta + \bar{\alpha}(U_0)\right)''(U - U_0)^2\right] \tag{6.1-7}$$

Substituting (6.1-7) into (6.1-6), new equation of $\tilde{E}(k)$ becomes

$$\tilde{E}(K) \approx \int_{-}^{-} a(U_0) \exp\left\{ iK\left[\left(\delta + \bar{\alpha}(U_0)\right) + \frac{1}{2}\left(\delta + \bar{\alpha}(U_0)\right)''(U - U_0)^2\right] \right\} x\, dU \tag{6.1-8}$$

then

$$\tilde{E}(K) \approx \left[\frac{2\pi}{K\left|\bar{\alpha}''(U_0)\right|}\right]^{1/2} a(U_0) \exp\left[iK\left(\delta + \bar{\alpha}(U_0)\right) \pm i\frac{\pi}{4}\right] \tag{6.1-9}$$

where the + or - sign is chosen for $\bar{\alpha}''(U_0) > 0$ or < 0, respectively. Since we have two stationary points (U_1 & U_2) for each value of δ, the approximate solution for the pulse spectral distribution becomes [2]

$$\tilde{E}(K) = \left(\frac{2\pi}{K}\right)^{1/2} \left\{ \frac{a(U_1)\exp\left[ik\left(\delta + \bar{\alpha}(U_1)\right) + i\pi/4\right]}{\left[\bar{\alpha}''(U_1)\right]^{1/2}} \right.$$

$$\left. + \frac{a(U_2)\exp\left[iK\left(\delta + \bar{\alpha}(U_2)\right) - i\pi/4\right]}{\left|\bar{\alpha}''(U_2)\right|^{1/2}} \right\} \qquad (6.1\text{-}10)$$

where $K - K' = \delta K$, U_1 and U_2 are the roots of the equation:

$$\delta + \bar{\alpha}'(U) = 0 \qquad (6.1\text{-}11)$$

i.e., the stationary points, and U_1 and U_2 are chosen such that: $\alpha''(U_1) > 0$ and $\alpha''(U_2) < 0$. Two stationary points exist for any $(-\delta)$ in the interval spanning the domain of α'. The chirped gaussian pulse, on the other hand, has only one solution for the equivalent equation (6.1-11), the function α' has no finite maximum and minimum, and the function α is symmetric. These differences is responsible for the qualitative differences of the self-phase modulation spectrum from the spectral distribution of a chirped gaussian pulse.

In Fig. 6.1-1, we plot the spectral distribution $|\tilde{E}|^2$ for different pulse intensities with $\gamma = 0$. From the above figure, we can observe the

following features for the spectral distribution of the self-phase modulated supercontinuum:

(1) The spectral extents are given by:

$$\left|W' - W\right|_{\text{anti-Stokes}} \approx \text{Max}\left(\frac{\partial\alpha}{\partial U}\right) \tag{6.1-12}$$

$$\left|W' - W\right|_{\text{Stokes}} \approx \text{Min}\left(\frac{\partial\alpha}{\partial U}\right) \tag{6.1-13}$$

since $\text{Max}\left(\frac{\partial\alpha}{\partial U}\right) > \left|\text{Min}\left(\frac{\partial\alpha}{\partial U}\right)\right|$ as in Figs. 5.1-5 and 5.1-6, the spectral extent on the anti-stokes side ($\delta < 0$), is larger than the corresponding quantity on the stokes side. This is clearly understood by observing the results in Figs. 6.1-1 and 6.1-2.

(2) The existence of two stationary points in the integrand of equation (6.1-5) or, equivalently, the existence of two solutions to equation (6.1-11) for all δ in the domain limited by the maximum and minimum of α' implies the existence of an interference-like pattern in the spectral intensity distribution.

(3) The shallowness of the $\frac{\partial \alpha}{\partial U}$ curve near its minimum values, causes the existence of the peak on the edge of the stoke's portion of the spectrum.

(4) The number of oscillations in the spectral distribution (M), is estimated by the method of stationary phase approximation to be given by equation (6.1-10) as:

$$M \approx \frac{\overset{M}{\alpha}}{\pi} \approx \frac{K \varepsilon V}{2\pi} \qquad (6.1\text{-}14)$$

which is in a good agreement with the numerical computed values. The above equation is derived by using equation (5.1-28).

From equation (6.1-14), it is worth mentioning that M increases with both K (i.e., τ) and εV. The modulation frequency of these oscillations is then approximately given by the frequencey extent (proportional to the extrema of α') divided by the number of oscillations. Combining equations (6.1-12) through (6.1-13) we conclude that this quantity depends on εV and is independent of K.

(5) The envelope of the maxima of the spectral distribution can be directly estimated from equation (6.1-10), and is given by [2]

$$\left|\xi\right|^2 \approx \frac{2\pi}{K}\left[\frac{a(U_1)}{\left(\bar{\alpha}''(U_1)\right)^{1/2}} + \frac{a(U_2)}{\left|\bar{\alpha}''(U_2)\right|^{1/2}}\right]^2 \qquad (6.1\text{-}15)$$

The cutoff points for the envelope are determined by $(\max \bar{\alpha}')$ and $(\min \bar{\alpha}')$. The envelope maximum is in the shallow region of the α' curve; as observed in Fig. 5.1-3, this shallowness is in region of (min α'). Physically, this translates into the spectrum having a sharp band edge close to its Stokes maximum extent. In Fig. 6.1-3, the envelope of the spectral maximum is plotted for selected values of εV, using the approximate expression of equation (6.1-15). We will refer to the displacement of the spectral maximum from the incoming pulse center frequency as the SPM-spectral Maximum shift. For all practical purposes, the magnitude of this shift follows closely the stokes frequency extent to within half a modulation curve.

Physically, the SPM spectral-Maximum-shift can be explained by noting that the $\chi^{(3)}$ *nonlinearity does not change* the total number of photons in the pulse, thus since the the spectral anti-Stokes extent is larger than the stokes extent, in order to conserve energy it is necessary that the peak of the spectral intensity be shifted to the Stokes side. Mathematically the SPM-spectral Maximum shift can be approximated as function of εV by

$$\frac{\Delta_M}{K} \approx \frac{\varepsilon V}{4} \qquad (6.1\text{-}16)$$

In Fig. 6.1-2, the pulse spectral distribution in the presence of self-steepening and material relaxation, is plotted versus Δ. The important features of Fig. 6.1-2, are that:

(1) as εV increases the spectrum is more asymmetric, the spectral maximum is shifted to the stokes side, and near the stokes maximum extent the spectrum falls off rapidly.

(2) as γ increases, the spectrum is further shifted to the Stokes side and the maximum frequency extents are consistent with the result in Fig. 5.1-5.

In Fig. 6.1-4, we plot the spectral maximum peak position as a function of εV for different values of relaxation times. This peak's stokes shift increases, for a fixed value of εV, with an increase of γ as will be shown in the following analysis.

The mean frequency of the pulse normalized to the original center frequency can be shown to be given by [3]

$$\frac{\bar{K}'}{K} = \frac{\int_{-\infty}^{\infty} \left(1 + \frac{\partial \bar{\alpha}}{\partial U}\right) a^2 \, dU}{\int_{-\infty}^{\infty} a^2 \, dU} \qquad (6.1\text{-}17)$$

for small εV, this quantity, for $\chi^{(3)}$ medium, is given by:

$$\lim_{\varepsilon V << 1} \frac{\overline{K'}}{K} = 1 - \frac{4}{15}\gamma(\varepsilon V) \qquad (6.1\text{-}18)$$

this corresponding to the stokes shift discussed earlier.

6.2 Pulse Spectal Distribution in $\chi^{(5)}$. Medium

The spectral distribution of the supercontinuum is obtasined by taking the amplitude square of the fourier transform of the electric field [1, 2]. In this section we used the same equations for the spectral distribution as in section (6.1).

In Fig. 6.2-1, we plot the spectral distribution $|\tilde{E}|^2$ for different pulse intensities with $\gamma' = 0$ [5]. From the spectral extent figures, we observe the following features:

(1) The calculated spectral extents are in a good agreement with the estimated values of equations (6.1-12 and 6.1-13).

(2) The number of oscillations in the spectral distribution can be estimated, using the stationary phase approximation to the Fourier transform of the electric field, to be:

$$N \approx \frac{\alpha_M}{\pi} \approx \frac{k\,\varepsilon' V}{2\pi} \qquad (6.2\text{-}1)$$

This estimated value is in close agreement with the computed values.

(3) The existence of the spectral peak on the edge of the stoke's portion of the spectrum is a result of the shallowness of the $\partial\alpha/\partial U$ curve near its minimum value.

(4) The envelope of the maxima of the spectral distribution is given as in equation (6.1-15) of section 6.1.

In Fig. 6.2-2, the spectral maximum shift can be approximately as function of $\varepsilon' V$ by

$$\frac{\Delta_M}{K} \approx \frac{\varepsilon' V}{3} \qquad (6.2\text{-}2)$$

In Fig. 6.2-1, the $|\tilde{E}|^2$ is plotted for $\gamma' = 0$, a spectral peak at $\Delta = 0$ is observed, which will be discussed later. In Fig. 6.2-3, the pulse spectral distribution in the presence of self-steepining and material relaxation is plotted for $\gamma' = 0.2$. The important features found from the spectrum are that:

(1) As $\varepsilon' V$ increases, the spectrum is more asymmetric, and near the Stokes maximum extent the spectrum falls off rapidly;

(2) As γ' increases, the spectrum is further shifted to the Stokes side and the maximum frequency extents are consistent with the result in Fig. 5.2-4.

(3) The spectral shape has a peak at the center frequency, a new feature not present in the $\chi^{(3)}$- dispersionless media. This is the result that the instanteneous frequency in the $\chi^{(5)}$ medium has more roots than the corresponding one in $\chi^{(3)}$ medium.

The role of the non-zero relaxation time in the Stokes shift is illustrated by claculating the mean frequency of the pulse normalized to the original center frequency. The normalized first moment of the frequency can be expressed in the time domain form as [5]:

$$\frac{\overline{K'}}{K} = \frac{\int_{-}^{-} \left(1 + \frac{\partial \overline{\alpha}}{\partial U}\right) a^2 \, dU}{\int_{-}^{-} a^2(U)\, dU} \qquad (6.2\text{-}3)$$

for small $\varepsilon' V$, this quantity, for the $\chi^{(5)}$ medium, is given by:

$$\lim_{\varepsilon' V << 1} \frac{\overline{K'}}{K} = 1 - 0.3\ \gamma' \left(\varepsilon' V\right) \qquad (6.2\text{-}4)$$

the second term on the right hand side corresponds to the numerically computed Stokes shifts. This shift is linear in the thickness of the material, and in the relaxation time and is quadratic in the intensity.

CHAPTER 7

DIRECT TIME MEASUREMENT OF THE PHASE IN $\chi^{(3)}$ AND $\chi^{(5)}$ DISPERSIONLESS MEDIA

7.1 Introduction

In order to characterize an optical pulse completely, one must measure the slowly varying phase $\alpha(U)$. The phase of the pulse can be directly mesured using the interference technique [37]. Rothenberg and Grischkowsky were the first to apply this technique. A Mach-Zehnder interferometer with Fabry-Perot étalon in one arm, is used. The étalon, tuned to resonant with the input pulse, provides the monochromatic reference pulse. The delay and the alignment of the interferometer are adjusted to ensure that this reference pulse interferes (heterodynes) with the input pulse, which passes unaltered through the other arm of the interferometer. Furthermore, because of the ease of adjustment of the delay of the interferometer, the phase of the entire pulse can be obtained.

7.2 Direct Time Measurement of the Phase in $\chi^{(3)}$ – Medium

The direct technique to measure the phase of the pulse consists of adding two pulses, a reference pulse of given width and zero chirp and a signal pulse described by the amplitude (a) and phase (α) which we found previously, then subtracting the sum of the intensities of the signal pulse and the measured reference pulse from the modulated pulse. The resultant intensity is given by [2]

$$I(U) = 2\,R(U).\ a(U)\ .\ \cos\left[\alpha(U)\right] \qquad (7.2\text{-}1)$$

If the reference pulse R(U) is a part of the incoming pulse i.e., sech U, then the intensity I(U) is given by

$$I(U) = 2\,\mathrm{sech}(U)\ a(U)\ \cos\left[\alpha(U)\right] \qquad (7.2\text{-}2)$$

For conventional SPM, where

$$a(U) = \mathrm{sech}\,U \qquad (7.2\text{-}3)$$

and

$$\alpha(U) = \frac{K\,\varepsilon\,V}{2}\,\mathrm{sech}^2\,U \qquad (7.2\text{-}4)$$

The intensity for conventional SPM is

$$I(U) = 2\,\mathrm{sech}^2 U \,.\, \cos\left[\frac{K\varepsilon V}{2}\,\mathrm{sech}^2 U\right] \qquad (7.2\text{-}5)$$

In Fig. 7.2-1, I(U) for the conventional SPM and self-steepened effect are plotted as function of U. The intensity of the conventional SPM is symmetric due to neglecting the self-steepening effect. The shift between the maxima of the amplitude and phase and the asymmetry in their shapes produce an asymmetry in I(U). The degree of asymmetry increases with increasing εV.

7.3 Direct Time Measurement of the Phase in $\chi^{(5)}$ – Medium

In this section the same technique is used as in section (7.2). Equations (7.2-1) through (7.2-3) are valid.

For conventional SPM,

$$\alpha(U) = \frac{K\varepsilon' V}{2} \operatorname{sech}^4 U \qquad (7.3\text{-}1)$$

The intensity for conventional SPM is

$$I(U) = 2 \operatorname{sech}^2 U \cdot \cos\left[\frac{K\varepsilon' V}{2} \operatorname{sech}^4 U\right] \qquad (7.3\text{-}2)$$

In Fig. 7.3-1, I(U) for the conventional SPM and self-steepened effect are plotted as a function of U. From this figure, I(U) of the conventional SPM is symmetric due to neglecting the self-steepening effect. The shift between the maxima of the amplitude and phase and the asymmetry in their shapes translate an asymmetry in I(U). The degree of asymmetry increases with increasing $\varepsilon' V$.

CHAPTER 8

INTERFERENCE PATTERN OF THE SUPERCONTINUUM GENERATED BY SELF-PHASE MODULATION IN $\chi^{(3)}$AND $\chi^{(5)}$ - DISPERSIONLESS MEDIA

8.1 Introduction

In this chapter, we compute the interference pattern generated by a plane-wave self-phase-modulated ultrafast pulse [5]. We prove that for high intensities, the presence of the time shift between the maxima of the amplitude and the phase of the SPM pulse leads to a shift in the position of the interferometric intensity extrema (fringe position shifts) as in Fig. 5.1-4. These shifts are functions of a parameter related to the pulse energy and the pulse width and to the nonlinear index of refraction and the thickness of the nonlinear medium that generated the SPM signal. Furthermore, we calculate the Fourier transform [38] of the interferometric intensity distribution and relate its range to the extrema of the frequency sweep (i.e, the derivative of the pulse-phase funtion,) which were shown to identify the supercontinuum spectral extents and the spectral maximum shift.

In all interferometric problems [6, 39, 40, 41] , the method of analysis of non-monochromatic light is to find first the intensity distribution for specific frequency as function of the paths diferences (or time delays) of

the particular geometry, then to sum incoherently over all frequency components intensities. The general expression for the interferometric intensity for ultrashort pulse characterization is summarized in [6].

8.2 Interference Pattern of the Supercontinuum Generated by Self-Phase Modulation $\chi^{(3)}$. Dispersionless Medium.

The interference pattern can be derived as follows; The incident light on an interferometric system has an input spectral distribution given by $I_{in}(\omega)$, the resultant (output) intensity is given by [6]

$$I_{out}(\Delta) = \int I_{in}(\omega)\, H(\omega,\Delta)d\omega \qquad (8.2\text{-}1)$$

where Δ is the set of time delays associated with the problem's geomtry, and $H(\omega, \Delta)$ is the response of the system to an incoming field of unit amplitude and frequency ω. The monochromatic response function for the Young double-slit configuration is given by:

$$H(\omega,\Delta) = 2\{1+\cos(\omega\,\Delta)\} \qquad (8.2\text{-}2)$$

where $\Delta = dx(Lc)^{-1}$, d is the separation between the slit centers, L is the distance to the screen, x is the distance of the observation point from the center of the screen, and C is the velocity of light.

The electric field of the incoming pulse is parameterized as follows:

$$E_{in}(t) = \exp\left(i\omega_0 t\right) a(t) \exp\left[i\,\alpha(t)\right] \qquad (8.2\text{-}3)$$

where ω_0 is the carrier frequency, a(t) is the envelope function, and $\alpha(t)$ is the phase function.

The Fourier transform of the pulse is given by

$$E_{in}(\omega) = \frac{1}{(2\pi)^{1/2}} \int_{-\infty}^{\infty} \exp(-i\omega t)\, E_{in}(t)\, dt \qquad (8.2\text{-}4)$$

From equations (8.1-3) and (8.1-4)

$$E_{in}(\omega) = \frac{1}{(2\pi)^{1/2}} \left[\int_{-\infty}^{\infty} a(t) \cos\left[(\omega - \omega_0)t - \alpha(t)\right] dt - \int_{-\infty}^{\infty} a(t) \sin\left[(\omega - \omega_0)t - \alpha(t)\right] dt \right] \qquad (8.2\text{-}5)$$

The intensity $I_{in}(\omega)$ is equal to

$$\left|E_{in}(\omega)\right|^2 = I_{in}(\omega) = \frac{1}{2\pi} \int_{-\infty}^{\infty} a(t) \exp\left\{ -i\left[(\omega - \omega_0)t - \alpha(t)\right]\right\} dt \times \left[\int_{-\infty}^{\infty} a(t') \exp\left\{ -i\left[(\omega - \omega_0)t' - \alpha(t')\right]\right\} dt' \right]^* \qquad (8.2\text{-}6)$$

The output intensity becomes

$$I_{out}(\Delta) = I(\Delta) \qquad (8.2\text{-}7)$$

Hence from equations (8.2-2), (8.2-6) and (8.2-7)

$$I(\Delta) = \frac{1}{2\pi} \int_{-\infty}^{\infty} d\omega \int_{-\infty}^{\infty} dt \int_{-\infty}^{\infty} dt' \; a(t)\; a(t') \exp\left\{ i\left[\alpha(t) - \alpha(t')\right] \right.$$

$$\left. + i\omega(t' - t) + i\omega_0 (t - t') \right\} \left[2 + \exp(i\omega\Delta) + \exp(-i\omega\Delta) \right] \tag{8.2-8}$$

By interchanging the order of integration and using the Fourier representation of the Dirac delta function, the intensity $I(\Delta)$ can then be written as

$$I(\Delta) = I_1(\Delta) + I_2(\Delta) + I_3(\Delta) \tag{8.2-9}$$

where

$$I_1(\Delta) = 2 \int_{-\infty}^{\infty} a^2(t)\, dt \tag{8.2-10}$$

$$I_2(\Delta) = \int_{-\infty}^{\infty} a(t) .\; a(t - \Delta)$$

$$x \exp\left\{ i\left[\alpha(t) - \alpha(t - \Delta) + \omega_0 \Delta\right] \right\} dt \tag{8.2-11}$$

$$I_3(\Delta) = \int_{-\infty}^{\infty} a(t) \cdot a(t + \Delta)$$

$$x \exp\left\{i\left[\alpha(t) - \alpha(t + \Delta) - \omega_0 \Delta\right]\right\} dt \qquad (8.2\text{-}12)$$

The relative intensity for any Δ normalized to the intensity at the center is given by

$$\frac{I(\Delta)}{I(0)} = \frac{1}{2} + \frac{1}{2}$$

$$x \frac{\int_{-\infty}^{\infty} a(t)\ a(t - \Delta) \cos\left\{\omega_0 \Delta + \alpha(t) - \alpha(t - \Delta)\right\} dt}{\int_{-\infty}^{\infty} a^2(t)\, dt} \qquad (8.2\text{-}13)$$

where (a) is the pulse amplitude, (α) is its phase, and ω_0 is its center frequency. For cw radiation, the minima of the interferometric intensity are located at:

$$\Delta(n) = \frac{(2n + 1)\,\pi}{\omega_0} \qquad (8.2\text{-}14)$$

In normalized time T (i.e., time measured in units of τ, the pulse width), the normalized frequency $K = \omega_0 \tau$ and the normalized time delay Δ/τ is parameterized as y/K. In these units the cw minima correspond to [6]

$$y(n) = (2n + 1)\,\pi \tag{8.2-15}$$

and the expression for the relative intensity of the interference pattern reduces to [6]:

$$I_R(y) = \frac{1}{2} + \frac{1}{2} \times \frac{\int_{-\infty}^{\infty} dT\; a(T)\, a\left(T - {}^{y}/_{K}\right) \cos\left[y + \alpha(T) - \alpha\left(T - {}^{y}/_{K}\right)\right]}{\int_{-\infty}^{\infty} a^2(T)\, dT} \tag{8.2-16}$$

In Fig. 8.2-1 we plot $I_R(y)$ for fixed K (i.e., fixed pulse width) but with different pulse intensities (εV). From the above figure, we can observe that, both the values and positions of the extrema change with εV. Furthermore, for large n, the ratio of the magnitudes of a maximum intensity to its neighboring minimum intensity decreases with increasing εV. This ratio goes asymptotically, for large n, to 1.

In Fig. 8.2-2, we plot the shifts in the position of the third minimum (i.e., the minimum that corresponds to $y(2) = 5\pi$ for cw radiation) as function of K, but fixed εV. From the above graph, it is clear that this shift depends only weakly on K. This approximate scaling (i.e., the strong dependence of the shift in fringe positions on εV, the ratio of the pulse intensity over the pulse width alone) will be discussed later.

The phase that we have derived earlier, depends only on the parameter K through a multiplication factor, i.e., $\alpha = K\bar{\alpha}$, where $\bar{\alpha}$ depends only on the parameter εV. Consequently, if for $y/K < 1$ we approximate equation (8.2-16) by the leading term of its Taylor series, we obtain [6]

$$I_R^A(y) \approx \frac{1}{2} + \frac{1}{2} \frac{\int_{-\infty}^{\infty} dU\ a^2(U) \cos\left[y\left(1 + \frac{\partial\bar{\alpha}}{\partial U}\right)\right]}{\int_{-\infty}^{\infty} dU\ a^2(U)} \qquad (8.2\text{-}17)$$

This approximate expression for I_R does not have an explicit dependence on K. From Fig. 8.2-2, we can observe that this asymptotic value for I_R is already within 2% of its exact value for $K \approx 90$ (i.e., a 30 fs pulse for $\lambda \approx 0.628\,\mu m$). Furthermore, from equation (8.2-17), it is clear that εV dependent amplitude-phase time shifts is responsible for the interferometric minima shifts, in effect $\frac{\partial\bar{\alpha}}{\partial U} \neq 0$ for $U = U_s$, and the argument of the cosine function at that point is εV dependent.

In Table 8.21, the shifts in the position of the I_R^A minima are tabulated as functions of the order of the minima and of the parameter εV. The shift is defined as the difference between the actual minimum of $I_R^A(Y)$ and the cw minimum as defined in equation (8.2-14). As can be noticed, each εV has a distinct signature for the shifts.

An alternative nonspectroscopic method to derive εV is by analysing the fourier transform of I_R^A. The expression for the Fourier transform can be directly derived from equation (8.2-17), and the integral representation of the Dirac delta function, and the delta function property:

$$\int g(y)\,\delta\left[f(y) - a\right] dy = \frac{g(y)}{\left|\frac{\partial f}{\partial y}\right|}\Bigg|_{y = y_0,\ f(y_0) = a} \tag{8.2-18}$$

where g(y) and f(y) are any mathematical functions

Consequently the spatial Fourier transform of the interferometric intensity defined by:

$$F(x) = \int_{-\infty}^{\infty} e^{ixy}\left[I_R^A(y) - \frac{1}{2}\right] dy \tag{8.2-19}$$

is then given by:

$$F(x) = \frac{\pi}{2N}\left[\sum_i \left|\frac{a^2(U)}{\frac{\partial^2 \bar{\alpha}}{\partial U^2}}\right|_{U = U_i} + \sum_j \left|\frac{a^2(U)}{\frac{\partial^2 \bar{\alpha}}{\partial U^2}}\right|_{U = U_j}\right]$$

(8.2-20)

where U_i and U_j are respectively the solutions of:

$$x + 1 + \frac{\partial \bar{\alpha}}{\partial U} = 0 \tag{8.2-21}$$

$$x - 1 - \frac{\partial \bar{\alpha}}{\partial U} = 0 \tag{8.2-22}$$

and N is the a^2 integral normalization factor. F(x) is even function of x. For $x > 0$, only equation (8.2-22) has a solution since $\left|\frac{\partial \bar{\alpha}}{\partial U}\right| < 1$. The function F(x) is not identically zero in the interval [a, b],where:

$$a = \min\left(\frac{\partial \bar{\alpha}}{\partial U}\right) + 1 \tag{8.2-23}$$

$$b = \max\left(\frac{\partial \bar{\alpha}}{\partial U}\right) + 1 \tag{8.2-24}$$

(i.e., a determination of the range of F(x) specifies the value of the parameter εV).

In Fig. 8.2-3, we plot F(x) for specific value of εV with different relaxation times and in Fig. 8.2-4, F(x) is plotted for different pulse intensities. From the F(x) figures, we can observe that as εV increases (high pulse energy), the broadening increases and there will be no peak on the R.H.S. of the

curves. This happens, due to the fact, that the pulse spreads its energy in the broadening and it does not have enough energy to show on the R.H.S. peak (due to the energy observe law). Also, we have previously observed in chapter 6, that the spectral distribution extents on the stokes and the anti-stokes sides are also determined by the extrema of $\partial\alpha/\partial U$. Furthermore, the SPM frequency shift is also determined by $\min\left(\partial\alpha/\partial U\right)$.

8.3 Interference Pattern of the Supercontinuum Generated by Self-phase Modulation in $\chi^{(5)}$- Dispersionless Medium

The interference pattern in $\chi^{(5)}$- medium can be derived in the same fashion as in section (8.2). Equations (8.2-1) through (8.2-24) are used here to find the relative intensity for any Δ normalized to the intensity at the center and the Fourier transform of I_R^A.

In Fig. 8.3-1, $I_R(Y)$ of fixed K is plotted for different pulse intensities $\varepsilon'V$. From the above figure, the values and positions of the extrema change with $\varepsilon'V$. Additionally, for large n, the ratio of the magnitudes of a maximum intensity to its neighboring minimum intensity decreases with increasing the pulse intensity $\varepsilon'V$. This ratio becomes asymptotically, for large n, to 1.

In Fig. 8.3-2, the Fourier transform of F(x) is plotted for specific value of ($\varepsilon'V$) with different relaxation times and in Fig. 8.3-3, F(x) is plotted for different pulse intensities. From the F(x) figures, as $\varepsilon'V$ increases the broadening increases and the magnitude of the peak on the R.H.S. of the curves decreases. From Fig. 8.3-3, the following features can be observed:-

1. As we explained in chapter 5, $\max \frac{\partial \alpha}{\partial U}$ is greater than $\min \frac{\partial \alpha}{\partial U}$. This inequality leads for $x > 0$, the left peak of the F(x) closer in notation to the peak at $x = 1$ than the right peak.
2. The spectral shape has a peak at $x = 1$. This peak is associated with the spectral peak at the center frequency.

CHAPTER 9

FILTER TRANSFORM OF A PULSE OUTGOING FROM $\chi^{(3)}$ AND $\chi^{(5)}$-DISPERSIONLESS MEDIA

9.1 INTRODUCTION

In this chapter, we compute the effect of amplitude filters on ultrafast self-phase modulated pulses [7]. We find the dependence of the outgoing pulse shape (i.e., width, amplitude, and maximum position) as functions of the self-phase modulation parameters and filter characteristics. Specially, we show that the amplitude filters can be used in certain conditions to compress pulses. The physical setup we are considering consists of an SPM pulse passing through a nondispersive Kerr media ($\chi^{(3)}$ and $\chi^{(5)}$- individually) following which the pulse passes through an amplitude filter. We denote by superscript 1 quantities at the entrance plane of the nonlinear medium, by superscript 2 quantities at the input of the filter, and by subscript 3 quantities at the output of the filter.

9.2 Filter Transform in $\chi^{(3)}$- Medium

It was shown in [7] that if the amplitude filter transfer function is given by

$$H(K') = \exp\left\{-\left[(K' - K_f)/2\Delta_f\tau\right]^2\right\} \tag{9.2-1}$$

where $K = \omega\tau$, Δ_f is the filter spectral halfwidth, ω_f is the filter center frequency, τ is the initial pulse width and ω is the incoming pulse center frequency. $E^{(2)}(U)$ is given by

$$E^{(2)}(U) = E_0\, a(U) \exp\left[i\alpha(U)\right] \exp\left[iKU\right] \tag{9.2-2}$$

the outgoing electric field from the filter $E^{(3)}$ is given by [7]

$$E^{(3)}(U) = E_0 \frac{\Delta_f\tau}{\sqrt{\pi}} \exp(iK_fU) \int_{-\infty}^{\infty} dU'\, a(U') \exp\left[i\alpha(U')\right]$$

$$x \exp\left[i(K - K_f)U'\right] \exp\left[-(U' - U)^2(\Delta_f\tau)^2\right] \tag{9.2-3}$$

where U is the pulse comoving coordinate that we defined previously, E_0 is the magnitude of $E^{(1)}$, a and α are the amplitude and phase of the pulse exiting from the nonlinear medium, as defined before. In Fig. 9.2-1, we plot the numerical values of $|E^{(3)}|^2$ for different values of the filter's center frequency and specific εV.

We assume $E^{(1)}$ to be given by:

$$E^{(1)}(U) = E_0 \operatorname{sech}(U) \exp(i K U) \qquad (9.2\text{-}4)$$

i.e., the initial pulse is taken to have a secant hyperbolic shape.

In the case of very large $(\Delta_f \tau)$, specially $(\Delta_f \tau)^2 >> K(\varepsilon V)$, and using the following representation of the dirac delta function:

$$\delta(U - U') = \lim_{\gamma \Rightarrow 0} \frac{1}{\gamma\sqrt{\pi}} \exp\left\{-\left[\frac{(U' - U)^2}{\gamma^2}\right]\right\} \qquad (9.2\text{-}5)$$

$E^{(3)}$ reduces to $E^{(2)}$. This physically, means that the filter is transparent to all frequencies, i.e., there is no modification to the pulse.

On the other hand, if, $1 << (\Delta_f \tau)^2 << K(\varepsilon V)$ we can evaluate equation (9.2-3) by the method of the stationary phase [35, 36], as follows:

$$E^{(3)}(U) = E_0 \frac{\Delta_f \tau}{\sqrt{\pi}} \int_{-\infty}^{\infty} a(U') \cdot \exp\left[-(U' - U)^2 (\Delta_f \tau)^2\right]$$

$$x \exp\left\{i K\left[\delta + \bar{\alpha}(U')\right]\right\} \cdot dU' \qquad (9.2\text{-}6)$$

Here a(U') and $\left[\delta + \bar{\alpha}(U')\right]$ are real functions. Suppose that there is one point U_0 in the interior of $(-\infty, \infty)$, having the property that $\left(\delta + \bar{\alpha}(U_0)\right)' = 0$; also, let $\left(\delta + \bar{\alpha}(U)\right)'' \neq 0$. In accordance with the above

assumption of the method of stationary phase we assume that only the neighborhood of the point U_0 is of significance, and we can expand

$$iK\left[\delta + \bar{\alpha}(U')\right] \cong iK\left[\left(\delta + \bar{\alpha}(U_0)\right) + \frac{1}{2}\left(\delta + \bar{\alpha}(U_0)\right)''(U' - U_0)^2\right] \tag{9.2-7}$$

substituting equation (9.2-7) into (9.2-6), the new equation of $\tilde{E}(U)$ becomes

$$\tilde{E}(U) \approx E_0 \frac{\Delta_f \tau}{\sqrt{\pi}} \int_{-\infty}^{\infty} a(U_0) \cdot \exp\left[-(U_0 - U)^2 (\Delta_f \tau)^2\right]$$

$$x \exp\left[iK\left[\delta + \bar{\alpha}(U_0) + \frac{1}{2}\left(\delta + \bar{\alpha}(U_0)\right)''(U' - U_0)^2\right]\right] dU' \tag{9.2-8}$$

then

$$\tilde{E}(U) \approx E_0 \frac{\Delta_f \tau}{\sqrt{\pi}} \left[\frac{2\pi}{K\left|\bar{\alpha}''(U_0)\right|}\right]^{1/2} \left[a(U_0)\, x \exp\left[iK\left(\delta + \bar{\alpha}(U_0)\right)\right] \pm i\frac{\pi}{4}\right]$$

$$x \exp\left[-(U_0 - U)^2 (\Delta_f \tau)^2\right] \tag{9.2-9}$$

where the + or - sign is chosen for, $\bar{\alpha}''(u_0) > 0$ or < 0 respectively. Since we have two stationary points (U_1, U_2) for each value of δ, the approximate solution for the pulse spectral distribution becomes [6]

$$E^{(3)}(U) \approx E_0(\Delta_f\tau)\left(\frac{2}{K}\right)^{1/2}\left(\frac{a(U_1)\cdot\exp\left[i K\left[\delta + \bar{\alpha}(U_1)\right] + i\pi/4\right]}{\left[\bar{\alpha}''(U_1)\right]^{1/2}}\right.$$

$$\times \exp\left[-(U_1 - U)^2(\Delta_f\tau)^2\right] + \exp\left[-(U_2 - U)^2(\Delta_f\tau)^2\right]$$

$$\left.\times\frac{a(U_2)\cdot\exp i K\left[\delta + \bar{\alpha}(U_2)\right] - i\pi/4}{\left|\bar{\alpha}''(U_2)\right|^{1/2}}\right) \qquad (9.2\text{-}10)$$

where U_1 and U_2 are the roots of

$$\delta + \bar{\alpha}(U) = 0 \qquad (9.2\text{-}11)$$

i.e., the stationary points of the integral, and where

$$K - K_f \equiv \delta_f K \qquad (9.2\text{-}12)$$

U_1 and U_2 are selected so that $\alpha''(U_1) > 0$ and $\alpha''(U_2) > 0$. There are two stationary points exist for any $(-\delta_f)$ in the interval spanning the values of α'. From equation (9.2-10), we can observe the following features:

(1) $E^{(3)}$ decribes two pulses centered at U_1 and U_2 and of width $\Delta_f\tau$.

(2) When $\left(-\delta_f\right)$ is close to the maximum or minimum of $\bar{\alpha}'$, the stationary points are very close to each other and the two pulses merge into one pulse, which is called daughter pulse.

The above results are different from that associated with chirped gaussian (CG) pulses, these are

(1) For small (εV), although the phase function α for SPM and CG pulses ($\alpha = -K\varepsilon V\ U^2$) coincides in the region around the maximum of α, the respective derivative function α' and α'' are quiet seperate.

(2) For CG pulses, α' is linear in U ($\alpha' = -2\ K\varepsilon V\ U$) and its magnitude is symmetric with respect to an axis of symmetry and α'' is constant ($\alpha'' = -2\ K\varepsilon V$). While for the SPM pulses, as we have previously seen, α' is asymmetric and is bounded, it has two extrema.

(3) Approximating α for SPM pulse by the CG pulse can be acceptable in the time domain in certain specific instances, it is never so in the frequency domain.

(4) The transformation by the filter is a frequency domain calculation, so there should be major differences between the SPM and the CG pulses going through the amplitude filters, namely:

(4.1) For CG pulses, equation (9.2-12) has one solution whereas for SPM pulses, it has two, one or zero solutions depending on the value of δ_f. Physically, while the CG pulse produces only a single daughter pulse by passing through the filter. For an SPM pulse input, two pulses are the normal output from the filter. See Fig. 9.2-1 .

(4.2) The output from two filters with center frequencies equidistant from the pulse center frequency (ex: in $\chi^{(3)}$- medium, we are using $K - K_f = -30$ and $K - K_f = 30$) have a similar shape for a CG input pulse, but they are not for an SPM input pulse. This asymmetry is demonstrated through the amplitude, shape and width of the outgoing pulses. See Fig. 9.2-1 (iv) and (x).

(4.3) In the SPM spectrum, the α' asymmetry leads to different Stokes and anti-Stokes, while for a CG pulse the spectral distribution is symmetric. The axis of symmetry is the line passing through the pulse carrier frequency.

(4.4) In the CG case, the time of arrival of the pulse peak for different filter center frequencies is a linear function of the detuning with the pulse carrier frequency. For SPM pulses this curve is given by the α' graph. This curve for SPM does not intersect the U axis at zero detuning [7].

An effective compression scheme [7] will occur for values of K_f where a single daughter pulse is produced (i.e., near the frequency

maximum extent). The values for the position of the pulse maximum and width are in good agreement to 10% with the approximate values of the stationary phase approximation from equation (9.2-5).

In the intermediate region, i.e., when $(\Delta_f\tau)^2 \approx K(\epsilon V)$, the stationary phase approximation should be replaced by the method of steepest descent [35] which is applicable in case that the argument of the exponent in the integrand is complex and the exponent is multiplied by a large number, in this case, K.

In Fig. 9.2-2, we plot the compression ratio (C) and the intensity magnitude of SPM pulses outgoing form the filter $\left(I_0^{(3)}\right)$ as a function of $(\Delta_f\tau)$ in the case of efficient compression.

It can be observed from the above figure, as the filter is broadened, i.e., more light passes through, then the magnitude of $\left|E^{(3)}\right|^2$ is increased. The compression ratio is defined as the ratio of the pulse width of $\left|E^{(1)}\right|^2$ (i.e., sech pulse width) divided by the pulse width of $\left|E^{(3)}\right|^2$, increases to a maximum then decreases. As $(\Delta_f\tau)$ becomes very large (i.e.,$((\Delta_f\tau) >> K\epsilon V)$ the compression ration approaches 1. An approximate value of the compression ratio for the case of one daughter pulse can be estimated by the method of steepest descent. It is given by [2, 7]

$$C^2 \approx (\Delta_f\tau)^2 - \frac{(\Delta_f\tau)^4\left[(\Delta_f\tau)^2 + 1\right]}{\left[(\Delta_f\tau) + 1\right]^2 g^2} \qquad (9.2\text{-}13)$$

where, $g \approx K\alpha''(U_s)$, U_s is the average value of the two colapsing stationary points. This approximate expression for the compression ratio (C) agrees to better than 20% with the computed values in Fig. 9.2-2.

Finally, we study the effect of εV (i.e., the laser source fluctuations) on the shape of the filter output. In Fig. (9.2-3, it can be observed that changing (εV) by $\pm 25\%$, which corresponds to $\pm 25\%$ fluctuation in the incoming laser intensity $I_0^{(1)}$. By keeping ($\Delta_f\tau$) constant, the effect of increasing (εV) is to create two daughter pulses. This could be explained by observing that the maximum of α' increases with (εV). Consequently, an increase of εV means the reappearance of two well-separated stationary points. On the other hand, as (εV) decreases, $E^{(3)}$ magnitude will be extremely reduced but with only slight variations to the shape. Consequently, in designing a physical set-up for specific compressor [7], the experimental nonlinear parameters should be selected to overcompensate the positive fluctuation.

We note that the above compression scheme produces ultrashort pulses but with center frequency different from that of the incoming laser signal. The above scheme permits, inter alia, the generation of femtosecond pulse in new regions (ultraviolet) of the spectral domain using a laser pulse, with center frequency in the visible region.

Finally, in Fig. (9.2-4), the computed normalized intensity, shape and position of SPM pulse outgoing from an optimum compression filter and the normalized intensity shape of the incoming pulse prior to SPM and filtering.

9.3 Filter Transform in $\chi^{(5)}$- Medium

The filter transform in $\chi^{(5)}$- medium can be deduced by the same technique as in section (9.2). Equations (9.2-1) through (9.2-11) are used here to determine the pulse spectral distribution $E^{(3)}(U)$ and the compression ratio C. The same discussions and comparisions between the CG pulses and SPM are valid as in section (9.2).

In Fig. 9.3-1, we plot the normalized values of $|E^{(3)}|^2$ for different values of the filter's center frequency and specific $\varepsilon'V$. From the above figure, two, one, or zero solutions are produced depending on the value of δ in equation 9.2-11, whereas for CG pulses has a single solution.

From Fig. 9.3-1, the output from two filters with center frequencies equidistant from the pulse center frequency, i.e., $K - K_f = 20$ and $K - K_f = -20$ also $K - K_f = 30$ and $K - K_f = -30$ have similar shapes for a CG input pulse, but they are not for an SPM input pulse. This asymmetry is proved through the amplitude, shape and width of the outgoing pulses.

In Fig. 9.3-2, we plot the compression ratio (C) and the intensity magnitude of SPM pulses outgoing from the filter $I_0^{(3)}$ as a function of $\Delta_f\tau$.

In Fig. 9.3-3, $|E|^2$ is plotted for different pulse intensities ($\varepsilon'V$), to study the effect of the laser source fluctuations on the shape of the filter output.

From Fig. 9.3-3, we can observe the effects of fluctuation in $\varepsilon'V$ on the shape of the filter output. By keeping $\Delta_f\tau$ constant then increasing the pulse intensity ($\varepsilon'V$) will create two daughter pulses. This can be demonstrated by observing that the maximum of α' increases with ($\varepsilon'V$), then any increase of ($\varepsilon'V$) means the reappearance of two well-seperated stationary points. On the other hand, as ($\varepsilon'V$) decreases, $|E^{(3)}|$ will be reduced with slight variations to the shape. The same discussion about designing a physical set-up for specific compressor is carried-out as in section (9.2).

CHAPTER 10

ANALYTICAL SOLUTION FOR SMALL SIGNAL INDUCED-PHASE MODULATION IN $\chi^{(3)}$- MEDIUM

10.1 Introduction

When a weak probe pulse and an intense pump pulse of different frequencies are introduced together into a nonlinear medium, the pump pulse can modulate the refractive index of the weak pulse [16, 42, 43]. In this analysis, we neglect the following:

(1) the pump shape distortion due to group velocity dispersion

(2) higher derivatives beyond the first derivative of the index of refraction.

In this chapter, we consider induced phase modulation when the pump intensity produces self-steepening [16]. The partial differential equation describing this case can be solved by the method of multiple scales [1, 2, 3, 16, 29] used in chapter 2. By using the same notation as in chapter (2), we specialize our treatment to the case of the probe at the second harmonics frequency of the pump.

10.2 Induced Supercontinuum and Steepening of an Ultrafast Laser Pulse

The analytical solution for induced-phase modulation in $\chi^{(3)}$. medium is summarized as follows;

The boundary condition at the entrance plane is

$$\phi_{in} = \text{sech}\, U\ e^{iKU} + \delta\ \text{sech}\ (1.76\, U) e^{2iKU_0} \qquad (10.2\text{-}1)$$

where δ measures the relative strength of the second harmonic signal to the primary frequency signal. In equation (10.2-1), the incoming primary mode pulse from function is assumed to be given by sech(U) and the incoming second harmonic pulse form function is assumed to be given by sech (1.76U).

Equations (2.1-34) through (2.1-36) can be solved for this case through [44]

$$\phi_0 = A(U_1, V_1, U_2, V_2)\ e^{iKU_0} + \delta\ B\ (U_1, V_1, U_2, V_2)\ e^{2iKU_0}$$

$$\phi_1 = C(V_1, U_1, U_2, V_2)\ e^{3iKU_0}$$

$$\phi_2 = \sum_n D_n(U_1, V_1, U_2, V_2)\ e^{niKU_0} \qquad (10.2\text{-}2)$$

where A corresponds to the pump and B to the probe. C and D_n are complex amplitudes associated with ω and $n\omega$ signals respectively. Assuming the velocity of propagation of the wave to be the same for ω and 2ω in the medium. The pump pulse A and the weak probe B are represented by [16, 42].

$$A = a e^{i\alpha} \tag{10.2-3}$$

$$B = b e^{i\beta} \tag{10.2-4}$$

where a, b are the pump and probe amplitude respectively, and α, β are the pump and probe phase respectively.

Consider the polarization to be proportional to $|\phi|^2 \phi$, the term-by-term solutions of equations (2.1-34) through (2.1-36) with $\gamma = 0$ are:

$$\frac{\partial^2}{\partial U_0^2} |\phi_0|^2 \phi_0 = \frac{\partial}{\partial U_0^2} \left[\left(a^3 e^{i\alpha} + 2\delta^2 a b^2 e^{i\alpha} \right) e^{iKU_0} \right.$$

$$\left. + \left(\delta^3 b^3 e^{i\beta} + 2\delta a^2 b e^{i\beta} \right) e^{i2KU_0} \right]$$

$$= - K^2 \left(a^3 + 2\delta^2 a b^2 \right) e^{i\alpha} e^{iKU_0}$$

$$- 4K^2 \left(\delta^3 b^3 + 2\delta a^2 b \right) e^{i\beta} e^{i2KU_0} \tag{10.2-5}$$

and

$$2\frac{\partial}{\partial V_1}\frac{\partial}{\partial U_0}\left[A\, e^{iKU_0} + \delta\, B\, e^{i2KU_0} \right] = -2\,Ka\,\frac{\partial \alpha}{\partial V_1}\, e^{i\alpha}\, e^{iKU_0}$$

$$- 4\,K\,\delta\, b\,\frac{\partial \beta}{\partial V_1}\, e^{i\beta}\, e^{i2KU_0} + i\left(2K\,\frac{\partial a}{\partial V_1} \right) e^{i\alpha}\, e^{iKU_0}$$

$$+ i\left(4\,K\,\delta\,\frac{\partial b}{\partial V_1} \right) e^{i\beta}\, e^{i2KU_0} \qquad (10.2\text{-}6)$$

The rest of the terms of equations (2.1-34) and (2.1-35) are zero. By equating the real and Imaginary terms of $e^{i\alpha}\, e^{iKU_0}$ and $e^{i\beta}\, e^{i2KU_0}$ of equation (2.1-35), the following equaitons are given by:

$$\frac{\partial \alpha}{\partial V_1} = \frac{K}{2}\left(a^2 + 2\delta^2 b^2 \right) \qquad (10.2\text{-}7)$$

and

$$\frac{\partial a}{\partial V_1} = 0 \qquad (10.2\text{-}8)$$

then

$$\frac{\partial \beta}{\partial V_1} = K\left(2a^2 + \delta^2 b^2\right) \tag{10.2-9}$$

and

$$\frac{\partial b}{\partial V_1} = 0 \tag{10.2-10}$$

The term-by-term solutions of equation (2.1-36) with $\gamma = 0$ are:

$$2\frac{\partial^2}{\partial U_0 \partial U_1}\left|\Phi_0\right|^2 \Phi_0 = -2K\left(a^3 + 2\delta^2 ab\right)\frac{\partial \alpha}{\partial U_1} \quad e^{i\alpha}\ e^{iKU_0}$$

$$+ i\left[2K\left(3a^2 + 2\delta^2 b^2\right)\frac{\partial a}{\partial U_1} + 8K\delta^2 ab\frac{\partial b}{\partial U_1}\right] e^{i\alpha}\ e^{iKU_0}$$

$$-4K\delta b\left(2a^2 + \delta^2 b^2\right)\frac{\partial \beta}{\partial U_1} \quad e^{i\alpha}\ e^{i2KU_0}$$

$$+ i\left[\left(2a^2 + 3\delta^2 b^2\right)\frac{\partial b}{\partial U_1} + 4ab\frac{\partial a}{\partial U_1}\right] 4K\delta\ e^{i\beta}\ e^{i2KU_0} \tag{10.2-11}$$

and

$$\frac{\partial}{\partial V_1^2}\,\phi_0 = \frac{\partial^2}{\partial V_1^2}\left[\, a\ e^{i\alpha}\, e^{iKU_0} + \delta\, b\, e^{i\beta}\, e^{i2KU_0}\right]$$

$$= \left[-a\left(\frac{\partial \alpha}{\partial V_1}\right)^2 + \frac{\partial^2 a}{\partial V_1^2}\right] e^{i\alpha}\, e^{iKU_0}$$

$$+ i\left(2\,\frac{\partial a}{\partial V_1}\cdot\frac{\partial \alpha}{\partial V_1} + a\,\frac{\partial^2 \alpha}{\partial V_1^2}\right) e^{i\alpha}\, e^{iKU_0}$$

$$+ \left[-\delta b\left(\frac{\partial \beta}{\partial V_1}\right)^2 + \delta\,\frac{\partial^2 b}{\partial V_1^2}\right] e^{i\beta}\, e^{i2KU_0}$$

(10.2-12)

then

$$2\,\frac{\partial}{\partial U_1}\ \frac{\partial}{\partial V_1}\left[\phi_0\right] = \left[-2a\,\frac{\partial^2 \alpha}{\partial V_1 \partial U_1} + 2\,\frac{\partial^2 a}{\partial U_1 \partial V_1}\right] e^{i\alpha}\, e^{iKU_0}$$

$$+ i\left[2\,\frac{\partial a}{\partial V_1}\ \frac{\partial \alpha}{\partial U_1} + 2a\,\frac{\partial^2 \alpha}{\partial U_1 \partial V_1} + 2\,\frac{\partial a}{\partial U_1}\cdot\frac{\partial \alpha}{\partial V_1}\right] e^{i\alpha}\, e^{iKU_0}$$

$$+\left[2\delta\,\frac{\partial^2 b}{\partial U_1\,\partial V_1}-2\delta b\,\frac{\partial^2\beta}{\partial V_1\,\partial U_1}\right]\,e^{i\beta}\,e^{i2KU_0}$$

$$+i\left[2\delta b\,\frac{\partial^2\beta}{\partial U_1\,\partial V_1}+2\delta\,\frac{\partial b}{\partial U_1}\,\frac{\partial\beta}{\partial V_1}\right]\,e^{i\beta}\,e^{i2KU_0}$$

(10.2-13)

and

$$2\,\frac{\partial}{\partial U_0}\,\frac{\partial a}{\partial V_2}\,[\phi_0]=\left(-2Ka\,\frac{\partial\alpha}{\partial V_2}\right)e^{i\alpha}\,e^{iKU_0}+i\left(2K\,\frac{\partial a}{\partial V_2}\right)\,e^{i\alpha}\,e^{iKU_0}$$

$$-\left(4\delta kb\,\frac{\partial\beta}{\partial V_2}\right)\,e^{i\beta}\,e^{i2KU_0}$$

$$+i\left(4\delta K\,\frac{\partial b}{\partial V_2}\right)\,e^{i\beta}\,e^{i2KU_0}$$

(10.2-14)

The rest of the terms of equation (2.1-36) are zero

By equating the real and imaginary coefficients of $e^{i\alpha}\, e^{iKU_0}$ and $e^{i\beta}\, e^{i2KU_0}$ of equation (2.1-36), the following set of partial differential equations are given by:

$$-a\left(\frac{\partial\alpha}{\partial V_1}\right)^2 + \frac{\partial^2 a}{\partial V_1^2} - 2a\,\frac{\partial\alpha}{\partial V_1}\,\frac{\partial\alpha}{\partial U_1} + 2\,\frac{\partial^2 a}{\partial U_1 \partial V_1} - 2Ka\,\frac{\partial\alpha}{\partial V_2}$$

$$= -2K\left(a^3 + 2\delta^2 a b^2\right)\frac{\partial\alpha}{\partial U_1} \qquad (10.2\text{-}15)$$

$$2\,\frac{\partial a}{\partial V_1}\,\frac{\partial\alpha}{\partial V_1} + a\,\frac{\partial^2\alpha}{\partial V_1^2} + 2\,\frac{\partial a}{\partial V_1}\cdot\frac{\partial\alpha}{\partial U_1} + 2a\,\frac{\partial^2\alpha}{\partial U_1 \partial V_1} + 2\,\frac{\partial a}{\partial U_1}\cdot\frac{\partial\alpha}{\partial V_1}$$

$$+ 2K\,\frac{\partial a}{\partial V_2} = \left[\,2K\left(3a^2 + 2\delta^2 b^2\right)\frac{\partial a}{\partial U_1}\right.$$

$$\left. + 8K\delta^2 a b\,\frac{\partial b}{\partial U_1}\,\right] \qquad (10.2\text{-}16)$$

$$-\delta b\left(\frac{\partial\beta}{\partial V_1}\right)^2 + \delta\,\frac{\partial^2 b}{\partial V_1^2} + 2\delta\,\frac{\partial^2 b}{\partial U_1 \partial V_1} - 2\delta b\,\frac{\partial^2\beta}{\partial V_1 \partial U_1} - 4\delta K b\,\frac{\partial\beta}{\partial V_2}$$

$$= -4K\delta b\left(2a^2 + \delta^2 b^2\right)\frac{\partial \beta}{\partial U_1} \qquad (10.2\text{-}17)$$

$$2\delta\frac{\partial b}{\partial V_1}\frac{\partial \beta}{\partial V_1} + \delta b\frac{\partial^2 \beta}{\partial V_1^2} + 2\delta b\frac{\partial^2 \beta}{\partial U_1 \partial V_1} + 2\delta\frac{\partial b}{\partial U_1}\cdot\frac{\partial \beta}{\partial V_1}$$

$$+ 4K\delta\frac{\partial b}{\partial V_2} = \left(2a^2 + 3\delta^2 b^2\right)\frac{\partial b}{\partial U_1} + 2ab\frac{\partial a}{\partial U_1} \qquad (10.2\text{-}18)$$

Substituting equations (10.2-7) through (10.2-10) into equations (10.2-14) through (10.2-18), another set of partial differential equations are given by:

$$2\frac{\partial a}{\partial V_2} - \left[\left(3a^2 + 2\delta b^2\right)\frac{\partial a}{\partial U_1} + 4\delta^2 ab\frac{\partial b}{\partial U_1}\right] = 0 \qquad (10.2\text{-}19)$$

$$2\frac{\partial \alpha}{\partial V_2} - \left(a^2 + 2\delta^2 b^2\right)\frac{\partial \alpha}{\partial U_1} = -\frac{1}{4}K\left(a^2 + 2\delta^2 b^2\right)^2 \qquad (10.2\text{-}20)$$

$$2\frac{\partial b}{\partial V_2} - \left[\left(2\delta^2 b^2 + 2a^2\right)\frac{\partial b}{\partial U_1} + 4ab\frac{\partial a}{\partial U_1}\right] = 0 \qquad (10.2\text{-}21)$$

$$2\frac{\partial \beta}{\partial V_2} - \left(\delta^2 b^2 + 2a^2\right)\frac{\partial \beta}{\partial U_1} = -\frac{1}{2}K\left(2a^2 + \delta^2 b^2\right)^2 \qquad (10.2\text{-}22)$$

By using chain rule technique that is given in equations (3.1-18) and (3.1-19), the partial differential equations for the amplitude and phase of the pump and probe pulses are given by [16]:

$$\frac{\partial a}{\partial V} - \frac{1}{2}\varepsilon\left[\left(3a^2 + 2\delta^2 b^2\right)\frac{\partial a}{\partial U} + 4\delta^2 ab\frac{\partial b}{\partial U}\right] = 0 \qquad (10.2\text{-}23)$$

$$\frac{\partial \alpha}{\partial V} - \frac{1}{2}\varepsilon\left(a^2 + 2\delta^2 b^2\right)\frac{\partial \alpha}{\partial U} = \frac{1}{2}K\varepsilon\left(a^2 + 2\delta^2 b^2\right) - \frac{1}{8}\varepsilon^2 K\left(a^2 + 2\delta^2 b^2\right)^2 \qquad (10.2\text{-}24)$$

$$\frac{\partial b}{\partial V} - \frac{1}{2}\varepsilon\left[\left(2\delta^2 b^2 + 2a^2\right)\frac{\partial b}{\partial U} + 4ab\frac{\partial a}{\partial U}\right] = 0 \qquad (10.2\text{-}25)$$

$$\frac{\partial \beta}{\partial V} - \frac{1}{2}\varepsilon\left(\delta^2 b^2 + 2a^2\right)\frac{\partial \beta}{\partial U} = K\varepsilon\left(2a^2 + \delta^2 b^2\right) - \frac{1}{4}\varepsilon^2 K\left(\delta^2 b^2 + 2a^2\right)^2 \tag{10.2-26}$$

The above four equations cannot be solved analytically, in the general case. A numerical method [44, 45, 46, 47] that will be introduced in the next chapter will be used to solve this set of partial differential equation. However, in the case of, $\delta^2 << 1$, the above equations reduce to [16] .

$$\frac{\partial a}{\partial U} - \frac{3}{2}\varepsilon a^2 \frac{\partial a}{\partial U} = 0 \tag{10.2-27}$$

$$\frac{\partial \alpha}{\partial V} - \frac{1}{2}\varepsilon a^2 \frac{\partial \alpha}{\partial U} = \frac{1}{2}K\varepsilon a^2 - \frac{1}{8}K\varepsilon^2 a^4 \tag{10.2-28}$$

$$\frac{\partial b}{\partial V} - \varepsilon a^2 \frac{\partial b}{\partial U} - 2\varepsilon ab\frac{\partial a}{\partial U} = 0 \tag{10.2-29}$$

$$\frac{\partial \beta}{\partial V} - \varepsilon a^2 \frac{\partial \beta}{\partial U} = 2K\varepsilon a^2 - \varepsilon^2 K a^4 \tag{10.2-30}$$

The equations of a and α are similar to those corresponding in chapters (3 and 4), and the solutions for b and β are respectively given by:

$$b(U,V) = a^4(U,V)\ L_1(U,V) \tag{10.2-31}$$

and

$$\beta(U,V) = -2KU + 4\varepsilon K\int_0^U a^2(p,V)\,dp$$

$$+ 3K\varepsilon^2 + 4\varepsilon K\int_0^V a^4(0,q)\,dq + K L_2(U,V) \tag{10.2-32}$$

Where L_1 and L_2 satisfy the partial differential equation

$$\frac{\partial L_i}{\partial V} - \varepsilon a^2\frac{\partial L_i}{\partial U} = 0 \tag{10.2-33}$$

The solution of equation (10.2-33) is given by

$$L(U,V) = L\left(\varepsilon\int_0^V a^6(U,q)\,dq + \int_0^V a^4(p,0)\,dp\right)$$

$$= L(r)$$

$$= L\left(\varepsilon \int_0^V a^6(U,q)\,dq + \tanh U - \frac{1}{3}\tanh^3 U \right) \qquad (10.2\text{-}34)$$

The initial conditions for the parameters a, b, α, and β are:

$$a(U,0) = \operatorname{sech}(U) \qquad (10.2\text{-}35)$$

$$b(U,0) = \operatorname{sech}(n\,U) \qquad (10.2\text{-}36)$$

$$\alpha(U,0) = 0 \qquad (10.2\text{-}37)$$

$$\beta(U,0) = 0 \qquad (10.2\text{-}38)$$

The function L_1 and L_2 are given by the following parametric representation (where s is the parameter):

$$L_1(X) = \left(\cosh^4 s\right) \operatorname{sech}(ns) \qquad (10.2\text{-}39)$$

where $n = 1.76$

$$L_2(X) = 2s - 4\varepsilon \tanh s \qquad (10.2\text{-}40)$$

$$X = \tanh s - \frac{1}{3}\tanh^3 s \qquad (10.2\text{-}41)$$

The frequency extent of the induced supercontinuum centered at the probe frequency (i.e., 2ω) is given by the maximum and minimum of $\left(\frac{1}{2K}\frac{\partial\beta}{\partial U}\right)$ where:

$$\left(\frac{1}{2k}\frac{\partial\beta}{\partial U}\right) = -1 + 2\varepsilon\, a^2(U,V) + \frac{1}{2}\left[\frac{\partial L_2(r)}{\partial r}\right] a^4(U,V) \qquad (10.2\text{-}42)$$

and the derivative of L_2 in parametric form is:

$$\frac{\partial L_2}{\partial X} = \frac{2 - 4\varepsilon\,\mathrm{sech}^2 s}{\mathrm{sech}^2 s - (\tanh^2 s)(\mathrm{sech}^2 s)} \qquad (10.2\text{-}43)$$

10.3 Results and Discussions

In this chapter, the analytical solution for induced-phase modulation in $\chi^{(3)}$- medium is investigated for weak pulses. The probe (weak signal) amplitude, phase, derivative of the phase, and spectral distribution are plotted for selected values of εV.

In Figure 10.2-1, the probe amplitude is plotted as a function of U for different vaules of εV with n = 1.76. From this figure, the probe amplitude is asymmetric and skewed towards the trailing edge, also that the induced steepening of the probe signal depends on the intensity of the strong wave.

In Figure 10.2-2, the normalized probe phase is plotted as a function of U for selected values of εV with n = 1.76. From this figure, the probe phase is asymmetric with respect to the U axis. This is a result of the amplitude self-steepening. Both the amplitude and the phase of the probe pulse are driven by the amplitude of the strong wave.

In Figure 10.2-3, the derivative of the probe phase is asymmetric with respect to the U axis. This results in an asymmetry of the spectral distribution between the Stokes and the anti-Stokes portions of the spectrum. The absolute value of the maximum of β' is always bigger than that corresponding to its minimum value. Given that the spectral extents on the Stokes and anti-Stokes sides are given, respectively, by

$$|W' - W|_{\text{anti-Stokes}} \approx 2 \times \max \frac{\partial \beta}{\partial U} \qquad (10.3\text{-}1)$$

$$|W' - W|_{Stokes} \approx 2 \times \min \frac{\partial \beta}{\partial U} \qquad (10.3\text{-}2)$$

The anti-Stokes extent is larger than the Stokes extent of the spectrum.

In Figures 10.2-4 and 10.2-5, the probe spectral distributions are plotted for $\varepsilon V = .5$ and $\varepsilon V = .8$ respectively. the important features found that

1. As εV increases the spectrum is more asymmetric, the spectral maximum is shifted to the stokes side, and near the Stokes maximum extent the spectrum falls off rapidly.
2. The existence of the spectral peak on the edge of the Stokes portion of the spectrum is a result of the shallowness of β' curve near its minimum value.
3. The detailed features of the calculated spectral extents conform well with the estimated values of relations (10.3-1) and (10.3-2).

In figure 10.2-6, the induced frequency extents are plotted as a function of εV. This figure shows that, the induced supercontinuum frequency extents as a function of εV grow faster than those corresponding to SPM.

CHAPTER 11

NUMERICAL SOLUTION FOR INDUCED SUPERCONTINUUM OF AN ULTRAFAST LASER PULSE IN χ^3- MEDIUM

11.1 Introduction

In this chapter, we summarize the basic concept of the Grid (Mesh) method [44, 45, 46, 47] in its simplest possible form. We use a finite-difference technique to solve the partial differential equations (with bounary and initial conditions), expressed in rectangular coordinates. A network of grid point is employed to solve the set of four, simultaneous, nonlinear partial differential given by equations (10.2-23) through (10.2-26).

In this set of partial differential equations, we have two independent variables U and V, and four dependent variables a, b, α, and β. The respective grid spacing are ΔU and ΔV. Subscripts, i and j are used to denote the space point having coordinate $i\Delta U$, $j\Delta V$, and also called the grid-point (i, j). Let the exact solution to the partial-differential equations be $a = a(U, V)$, $b = b(U, V)$, $\alpha = \alpha(U, V)$, and $\beta = \beta(U, V)$. The analysis for (a) is shown. similar analysis for b, α and β were also performed.

Assuming that (a) possesses a sufficient number of well defined partial derivatives, the values of (a) at the two points (U, V) and (U + h, V + k) are related by Taylor's expression:

$$a(U + h, V + k) = a(U, V) + \left(h \frac{\partial}{\partial U} + K \frac{\partial}{\partial V}\right) a(U, V)$$

$$+ \frac{1}{2!} \left(h \frac{\partial}{\partial U} + K \frac{\partial}{\partial V}\right)^2 a(U, V) + \ldots\ldots$$

$$+ \frac{1}{(n-1)!} \left(h \frac{\partial}{\partial U} + K \frac{\partial}{\partial V}\right)^{n-1} a(U, V) + R_n$$

(11.1-1)

where the remainder term is given by

$$R_n = \frac{1}{n!} \left(h \frac{\partial}{\partial U} + K \frac{\partial}{\partial V}\right)^n a(U + \xi h, V + \xi k) \qquad 0 < \xi < 1$$

(11.1-2)

That is,

$$R_n = 0\left[(|h| + |k|)^n \right]$$

(11.1-3)

By equation (11.1-3), we mean there is a positive constant M such that $|R_n| \leq M(|h| + |k|)^n$ as both h and k tend to zero.

The space point ($i\Delta U$, $j\Delta V$) is surrounded by the neighboring grid points down in Fig. 11.1-1. Expanding in Taylor's series for $a_{i-i,j}$ about $a_{i+i,j}$ about the central value $a_{i,j}$, we obtain

$$a_{i-i,j} = a_{i,j} - \Delta U \cdot a_U + \frac{(\Delta U)^2}{2!} a_{UU} - \frac{(\Delta U)^3}{3!} a_{UUU}$$

$$+ \frac{(\Delta x)^3}{4!} a_{UUUU} \qquad (11.1\text{-}4)$$

and

$$a_{i+i,j} = a_{i,j} + \Delta U \cdot a_U + \frac{(\Delta U)^2}{2!} a_{UU} + \frac{(\Delta U)^3}{3!} a_{UUU}$$

$$+ \frac{(\Delta x)^4}{4!} a_{UUUU} \qquad (11.1\text{-}5)$$

where, $a_U = \partial a/\partial U$, $a_{UU} = \partial^2 a/\partial U^2$ etc., and all derivatives are evaluated at the grid-point (i, j). By taking these equations singly, and by adding or subtracting one from the other, we obtain the following finite-difference formulas for the first-and second-order derivatives at (i, j):

$$\frac{\partial a}{\partial U} = \frac{a_{i+1,j} - a_{i,j}}{\Delta U} + 0(\Delta U) \qquad (11.1\text{-}6)$$

$$\frac{\partial a}{\partial U} = \frac{a_{i,j} - a_{i-1,j}}{\Delta U} + 0(\Delta U) \qquad (11.1\text{-}7)$$

$$\frac{\partial a}{\partial U} = \frac{a_{i+1,j} - a_{i-1,j}}{2\,\Delta U} + 0\left[(\Delta U)^2\right] \qquad (11.1\text{-}8)$$

$$\frac{\partial^2 a}{\partial U^2} = \frac{a_{i-1,j} - 2\,a_{i,j} + a_{i+1,j}}{(\Delta U)^2} + 0\left[(\Delta U)^2\right] \qquad (11.1\text{-}9)$$

Equations (11.1-6) through (11.1-8) are known as the forward, backward, and central difference forms respectively. Similar forms exist for $\partial a/\partial V$ and $\partial^2 a/\partial V^2$. It may also be shown that

$$\frac{\partial^2 a}{\partial U\,\partial V} = \frac{a_{i+1,j+1} - a_{i-1,j+1}\,a_{i+1,j-1} + a_{i-1,j+1}}{4\,\Delta U \,.\, \Delta V}$$

$$+ 0\left[(\Delta U + \Delta V)^2\right] \qquad (11.1\text{-}10)$$

For a square grid ($\Delta U = \Delta V$), the following nine-point approximation is available for the Laplacian in two dimensions and will have the specified truncation error, provided that $a_{U\,U} + a_{V\,V} = 0$ is being solved:

$$\frac{\partial^2 a}{\partial U^2} + \frac{\partial^2 a}{\partial V^2} = \frac{\left[\begin{array}{l} a_{i-1,j+1} + 4a_{i,j+1} + a_{i+1,j+1} \\ + 4a_{i-1,j} - 20a_{i,j} + 4a_{i+1,j} \\ + a_{i-1,j+1} + 4a_{i,j-1} + a_{i+1,j-1} \end{array}\right]}{6(\Delta U)^2}$$

$$+ 0\left[(\Delta U)^4\right] \qquad (11.1\text{-}11)$$

By taking more and more neighboring points, an unlimited number of other approximations can be obtained, but the above forms are the most compact.

For convenience, the central-difference operation δ_x will be used occasionally. It is defined by

$$\delta_x a_{i,j} = \frac{a_{i+\frac{1}{2},j} - a_{i-\frac{1}{2},j}}{\Delta U} \qquad (11.1\text{-}12)$$

whence

$$\delta_x^2 a_{i,j} = \frac{a_{i-1,j} - 2a_{i,j} + a_{i+1,j}}{(\Delta U)^2} \qquad (11.1\text{-}13)$$

11.2 Difference Equations for the Amplitude and Phase of the Probe and Pump Pulses

In this section, we derived the difference equations for a, b, α, and β. The term-by-term solution for equations (10.2-22) through (10.2-25) are:

$$\frac{\partial a}{\partial V} = \frac{a_{i,j+1} - a_{i,j}}{\Delta V} \tag{11.2-1}$$

$$a = a_{i,j} \tag{11.2-2}$$

$$\frac{\partial a}{\partial U} = \frac{a_{i+1,j} - a_{i,j}}{\Delta U} \tag{11.2-3}$$

The same technique is applicable for b, α, and β.

Therefore, equation (10.2-23) become

$$a_{i,j+1} = \Delta V \Big(0.5\ \varepsilon \left(3a_{i,j}^2 + 2\delta^2 b_{i,j}^2\right) \left(a_{i+1,j} - a_{i,j}\right)/\Delta U + 4\delta^2 a_{i,j}\ b_{i,j} \left(b_{i+1,j} - b_{i,j}\right)/\Delta U \Big) + a_{i,j} \tag{11.2-4}$$

Equation (10.2-24) becomes

$$\alpha_{i,j+1} = \Delta V \left(\left(0.5\ \varepsilon \left(a_{i,j}^2 + 2\delta^2 b_{i,j}^2 \right) \left(\alpha_{i+1,j} - \alpha_{i,j} \right) / \Delta U \right) \right.$$

$$+ 0.5\ \varepsilon\ K \left(a_{i,j}^2 + 2\delta^2 b_{i,j}^2 \right)$$

$$\left. - \tfrac{1}{8}\ K\ \varepsilon^2 \left(a_{i,j}^2 + 2\delta^2 b_{i,j}^2 \right)^2 \right) + \alpha_{i,j} \qquad (11.2\text{-}5)$$

Equation (10.2-25) becomes

$$b_{i,j+1} = \Delta V \left(0.5\ \varepsilon \left(2\ \delta^2\ b_{i,j}^2 + 2\ a_{i,j}^2 \right) \left(b_{i+1,j} - b_{i,j} \right) / \Delta U \right.$$

$$\left. + 4\ a_{i,j}\ b_{i,j} \left(a_{i+i,j} - a_{i,j} \right) / \Delta U \right) + b_{i,j}$$

(11.2-6)

Equation (10.2-26) becomes

$$\beta_{i,j+1} = \Delta V \left(\left(0.5\ \varepsilon \left(\delta^2\ b_{i,j}^2 + 2\ a_{i,j}^2 \right) \left(\beta_{i+1,j} - \beta_{i,j} \right) / \Delta U \right) \right.$$

$$+ K \varepsilon \left(2\ a_{i,j}^2 + \delta^2 b_{i,j}^2 \right)$$

$$\left. - \tfrac{1}{4}\ K\ \varepsilon^2 \left(\delta^2 b_{i,j}^2 + 2\ a_{i,j}^2 \right)^2 \right) + \beta_{i,j} \qquad (11.2\text{-}7)$$

The initial conditions are:

$$\text{at} \quad V=0 \qquad a_{i,1} = \operatorname{sech}(U), \qquad b_{i,1} = \operatorname{sech}(\sigma U),$$

where the cases $\sigma = 0.5$ and 1 are treated

$$\alpha_{i,1} = 0, \qquad \beta_{i,1} = 0$$

The set of four simultaneous, nonlinear partial differential equations (10.2-23) through (10.2-26),are solved by establishing a network of grid points throughout the region $-6 \leq U \leq 6$ and $0 \leq V \leq 8$, with grid spacing $\Delta U = 2/N$, $\Delta V = 1/M$, where M and N are arbitary integers.

11.3 Results and Discussions

In this research, a numerical solution for induced-phase modulation is developed in $\chi^{(3)}$- dispersionless medium where the relative strength of the probe signal to the pump is close to unity. A Mesh (Grid) method, specifically a finite-difference technique, is used to solve the partial differential equations expressed in rectangular coordinates. The asymmetry in the pump and the probe amplitude, phase, and spectral Stokes and anti-Stokes regions are analysed.

In Figures 11.2-1 and 11.2-2, the pump amplitude and the probe amplitude are plotted as a function of U for selected values of εV with $\delta = 1$ and $\sigma = .5, 1$. In Figures 11.2-3 and 11.2-4, the normalized pump phase and probe phase are plotted as a function of U for different values of εV with $\delta = 1$ and $\sigma = .5, 1$.

In Figures 11.2-5 and 11.2-6, the pump amplitude and the probe amplitude are shown for selected values of εV with $\sigma = .5$, $\delta = 0., .5$ and 1. In Figures 11.2-7 and 11.2-8, the normalized pump phase and probe phase are plotted for selected values of εV with $\sigma = .5$, $\delta = 0., .5$ and 1. The spectral distributions of the pump and the probe, with $\delta = 1$, $\sigma = 1$ for selected values of εV, are shown in Figures 11.2-9, 11.2-10. In Figures 11.2-11 and 11.2-12, the spectral distributions of the pump and the probe are plotted for different values of εV with $\delta = 1$ and $\sigma = .5$. In Figures 11.2-13 and 11.2-14, the spectral distributions of the pump and the probe are shown for specific value of εV (= .4) with $\sigma = .5$ and $\delta = 0., 0.5$.

The following features are observed for the pump amplitude (a) probe amplitude (b) pump phase (α), probe phase (β), and, the spectral distributions of the pump and probe $|\tilde{E}|^2$:

<u>On the pump amplitude (a)</u>

1. The self-steepening is more pronounced as εV increases, as is the asymmetry.
2. The position of the value of the amplitude maximum denoted by U and a, respectively, are given by

$$U_a \approx \frac{-3}{2}\varepsilon V \qquad (11.3\text{-}1)$$

$$a_M \approx 1 \qquad (11.3\text{-}2)$$

3. The pump amplitude is independent on the probe width (σ) and the relative strength of strong pulse to the weak pulse (δ).

<u>On the probe amplitude(b)</u>

1. The probe amplitude is asymmetric and skewed towards the trailing edge. Also, the probe amplitude increases as εV increasing.
2. With a fixed value of εV, and where δ is approximately unity,
   (i) the width of the probe amplitude increases with smaller value of σ.
   (ii) the position and the value of the probe maximum denoted by $|U_b|$ and (b_M), respectively, increase with smaller value of σ.

3. For fixed values of εV and σ, the position and the value of the probe maximum, increase with larger value of δ.

<u>On the pump phase (α)</u>

1. The pump pulse is asymmetric with respect to the U-axis. This asymmetry increases as εV increasing.
2. With a fixed value of εV, and where δ is approximately unity
   (i) the width of the pump phase increases with smaller value of σ.
   (ii) the position and value of the phase maximum denoted by $|U_\alpha|$ and (α_M), respectively, increase with smaller value of σ.
   (iii) the sharpness on the edges of the pump phase, increases with larger value of σ. This results into a larger extent on the Stokes and anti-Stokes portions of the pump spectral distribution.
3. For fixed values of εV and σ,
   (i) the position and the value of the phase maximum, increase with larger value of δ.
   (ii) the width of the pump phase increases with larger value of δ.
   (iii) the sharpness on the leading and trailing edges of the pump phase, increases with larger value of δ. This results into a larger extent on the Stokes and anti-Stokes portions of the spectrum.

On the probe phase (β)

1. The probe phase is asymmetric and its maximum is shifted with respect to the $U = 0$.

2. With a fixed value of εV, and where δ is approximately unity,

   (i) the width of the probe phase increases with smaller value of σ.

   (ii) the position and the value of the phase maximum denoted by $|U_\beta|$ and β_M , respectively, are independent on the probe width (σ).

   (iii) the sharpness on the leading and trailing edges of the probe phase, increases with larger value of σ. This results into a larger extent on the Stokes and anti-Stokes portions of the probe spectral distribution.

3. For fixed values of εV and σ,

   (i) the width of the probe phase increases with larger value of δ.

   (ii) the position and the value of the phase maximum increase with larger value of δ.

   (iii) the sharpness on the trailing and leading edges of the probe phase, increases with larger value of δ. This results into a larger extent on the Stokes and anti-Stokes portions of the spectrum.

On the pump and Probe spectral distributions $|\tilde{E}|^2$

1. The spectral distributions of the pump and probe are asymmetric between Stokes and anti-Stokes portions. As εV increases, the spectrum is more asymmetric, and near the Stokes maximum extent the spectrum falls of rapidly.
2. The maximum peak of the spectral distributions of the pump and probe, is shifted to the Stokes side.
3. The number of oscillations of the probe spectral distribution are more than the corresponding one in the pump. This is a result of the proportionality of the number of oscillations with the probe phase (β) and pump phase (α), and (β) is greater than (α) for a fixed value of the pump intensity. Also, the number of oscillations of the spectral distribution increase with increasing εV.
4. The spectral extents of the pump and probe spectral distributions increase with larger value of the probe width (σ). This is a result of the sharpness of α and β curves with larger value of σ.
5. The spectral extents of the pump and probe spectral distribution increase with larger value of (δ). This is a result of the sharpness of α and β curves with larger value of δ.

	$n_2 = 10^{-22}$ (MKS) $= 0.9 \times 10^{-13}$ (emu)			$n_2 = 10^{-20}$ (MKS) $= 0.9 \times 10^{-11}$ (emu)		
P_c Critical power for self focusing	2×10^6 W			2×10^4 W		
P_{in} Pulse input power	10^7W	10^9W	10^{11}W	10^7W	10^9W	10^{11}W
E_0 Maximum amplitude of the incoming pulse	9×10^7V/m	9×10^8V/m	9×10^9V/m	9×10^7V/m	9×10^8V/m	9×10^9V/m
S_f Distance to focusing point	.4m	.04m	.004m	.04m	.004m	.0004m
$\epsilon = \frac{n_2\|E_0\|^2}{n}$ (n = 1.5)	$\frac{2}{3} \times 10^{-6}$	$\frac{2}{3} \times 10^{-4}$	$\frac{2}{3} \times 10^{-2}$	$\frac{2}{3} \times 10^{-4}$	$\frac{2}{3} \times 10^{-2}$	$\frac{2}{3}$
$\epsilon V = \frac{n_2\|E_0\|^2 z}{cT}$ z = 1micron of sample thickness	$\frac{1}{3} \times 10^{-7}$	$\frac{1}{3} \times 10^{-5}$	$\frac{1}{3} \times 10^{-3}$	$\frac{1}{3} \times 10^{-5}$	$\frac{1}{3} \times 10^{-3}$	$\frac{1}{3} \times 10^{-1}$

Table 2.1-1: Range of experimental parameters in super-continuum generation experiments (Source wavelengh = 1 μm, pulse width = 10^{-13} s, and beam diameter at input plane = 1mm

	Amplitude Equation	Phase Equation
Traditional SPM Theory	$\frac{\partial a}{\partial V} = 0$	$\frac{\partial \alpha}{\partial V} = \frac{\epsilon K}{2} a^2$
Slowly varying Amplitude	$\frac{\partial a}{\partial V} - 3\epsilon a^2 \frac{\partial a}{\partial U} = 0$	$\frac{\partial \alpha}{\partial V} - \epsilon a^2 \frac{\partial a}{\partial U} = \frac{\epsilon K}{2} a^2$
Yang and Shen	$\frac{\partial a}{\partial V} - \frac{\epsilon}{2} a^2 \frac{\partial a}{\partial U} = 0$	$\frac{\partial \alpha}{\partial V} - \frac{\epsilon a^2}{2} \frac{\partial a}{\partial U} = \frac{\epsilon K}{2} a^2$
Our results	$\frac{\partial a}{\partial V} - \frac{3}{2} \epsilon a^2 \frac{\partial a}{\partial U} = 0$	$\frac{\partial \alpha}{\partial V} - \frac{\epsilon a^2}{2} \frac{\partial a}{\partial U} = \frac{\epsilon K}{2} a^2 - \frac{\epsilon^2 K}{8} a^4$

Table 3.1-1: Quasi-linear partial differential equations forms for the amplitude and phase of a pulse propagating in a cubic nonlinear medium.

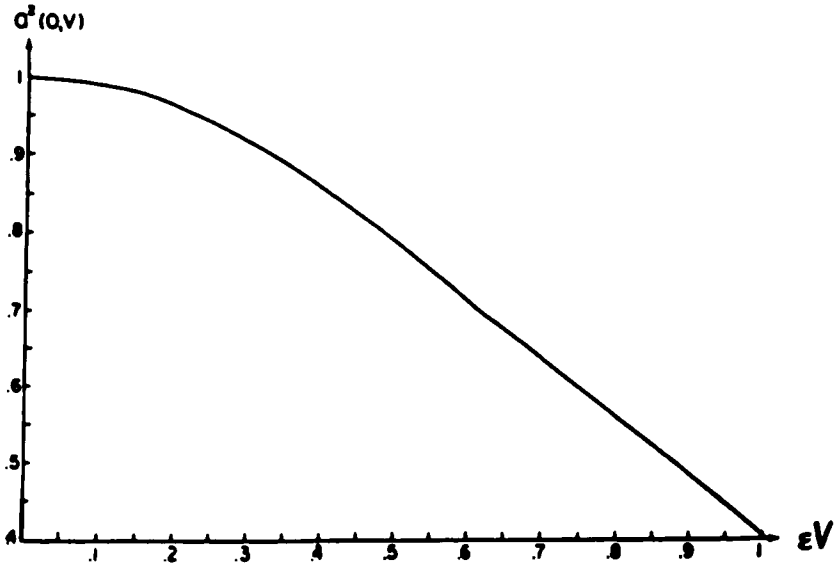

Fig. 4.1-1: The magnitude of the steepenend (amplitude)^2 at U = 0 as function of εV in $\chi^{(3)}$- medium

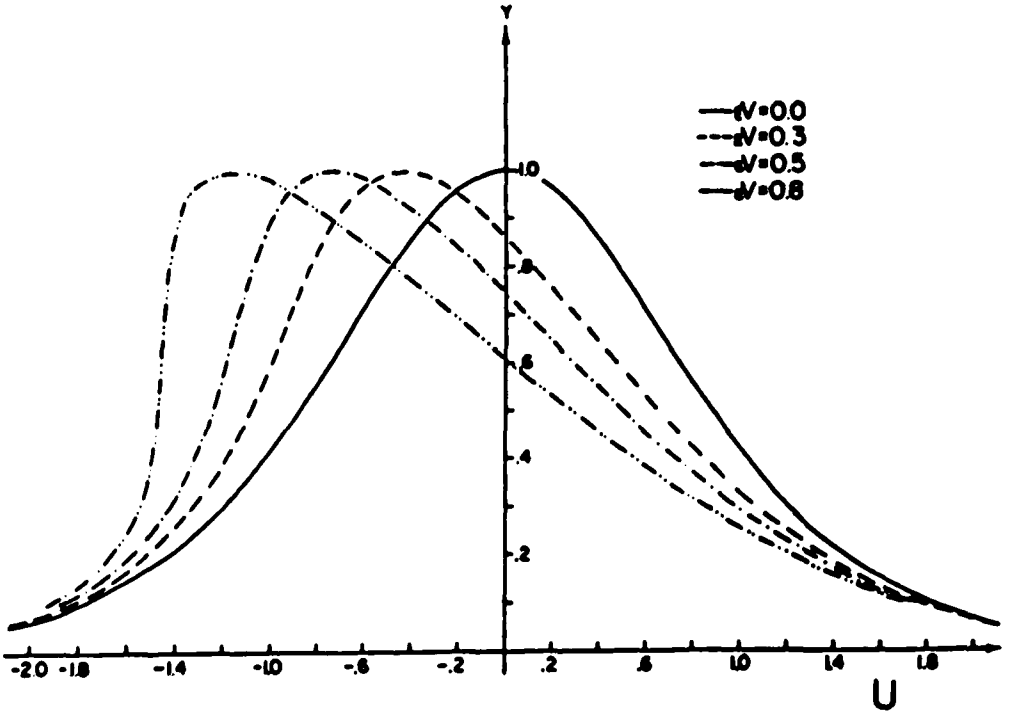

Fig. 4.1-2: The steepend pulse (amplitude)^2 as function of U, with different intensities in $\chi^{(3)}$- medium

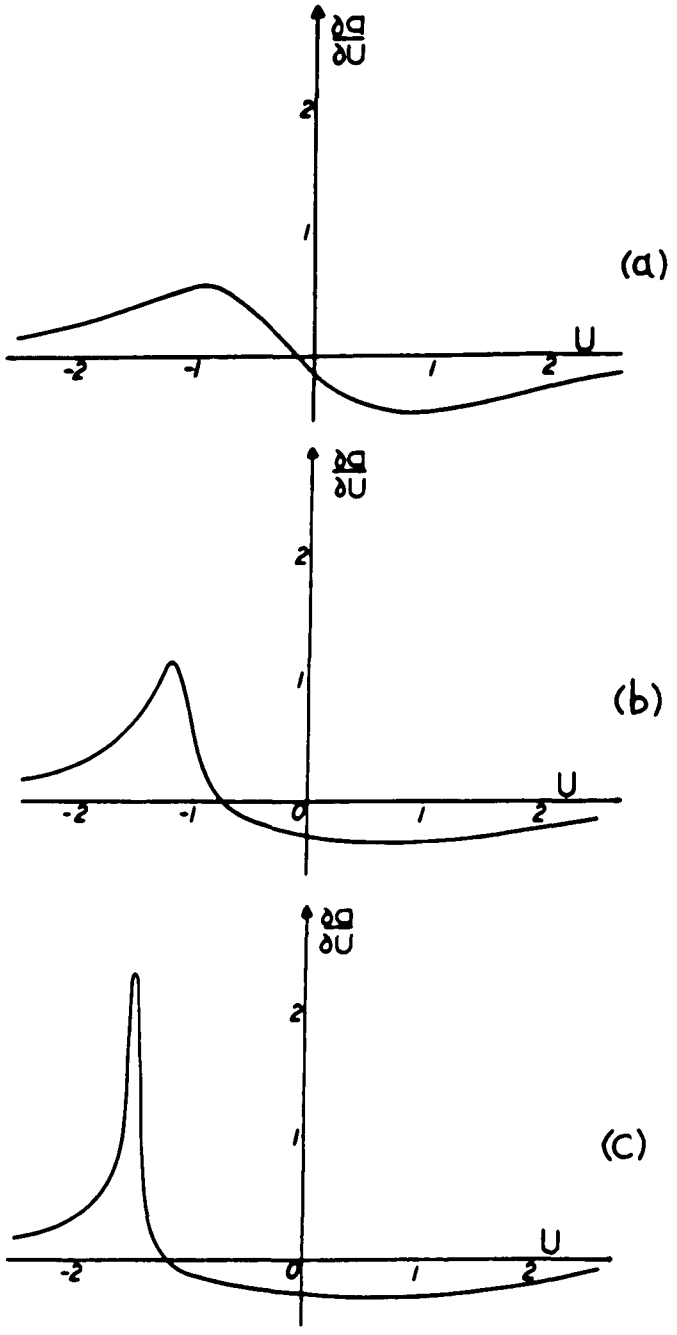

Fig. 4.1-3: The slope of the steepend pulse as function of U in $\chi^{(3)}$- medium.

(a) $\varepsilon V = 0.1$ (b) $\varepsilon V = \varepsilon V$ (c) $\varepsilon V = 0.8$

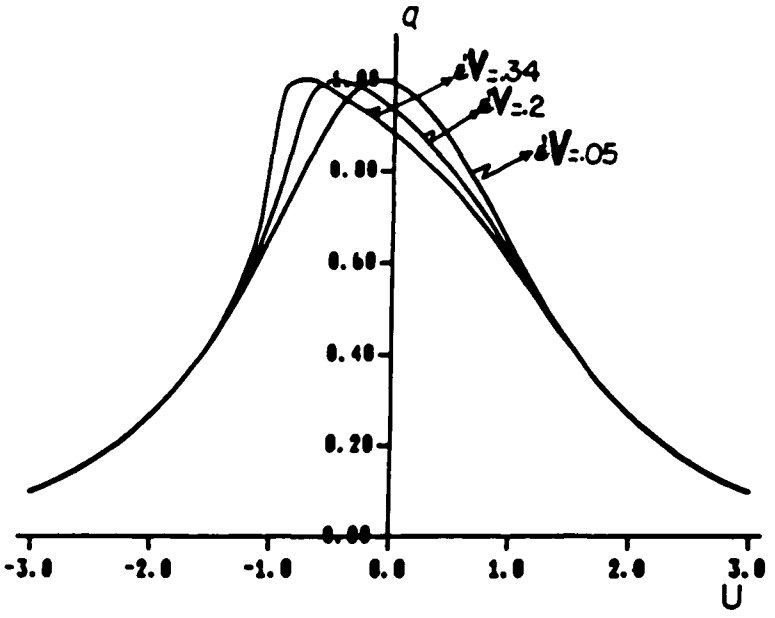

Fig. 4.2-1: The steepend amplitude of a pulse propagating in dispersionless $\chi^{(5)}$- medium as function of U with different intensities

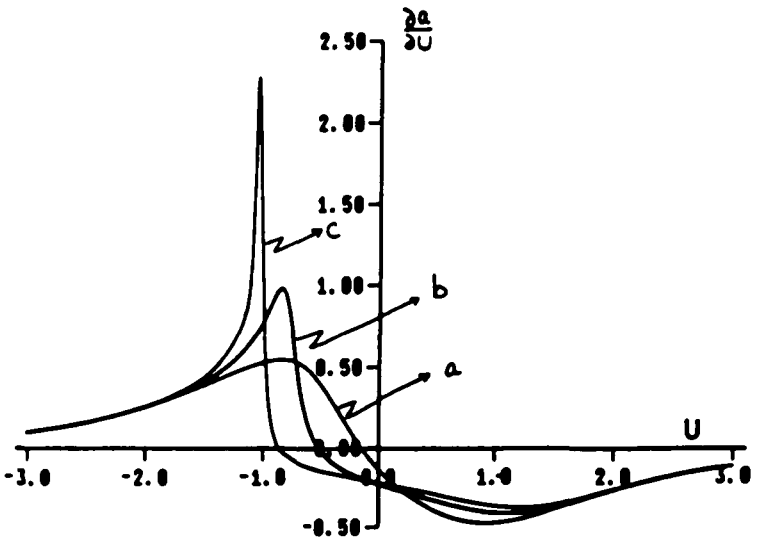

Fig. 4.2-2: The slope of the steepend amplitude of a pulse propagating in dispersionless $\chi^{(5)}$- medium as function of U with different intensities.
(a) $\varepsilon' V = 0.05$ (b) $\varepsilon' V = 0.2$ (c) $\varepsilon' V = 0.34$

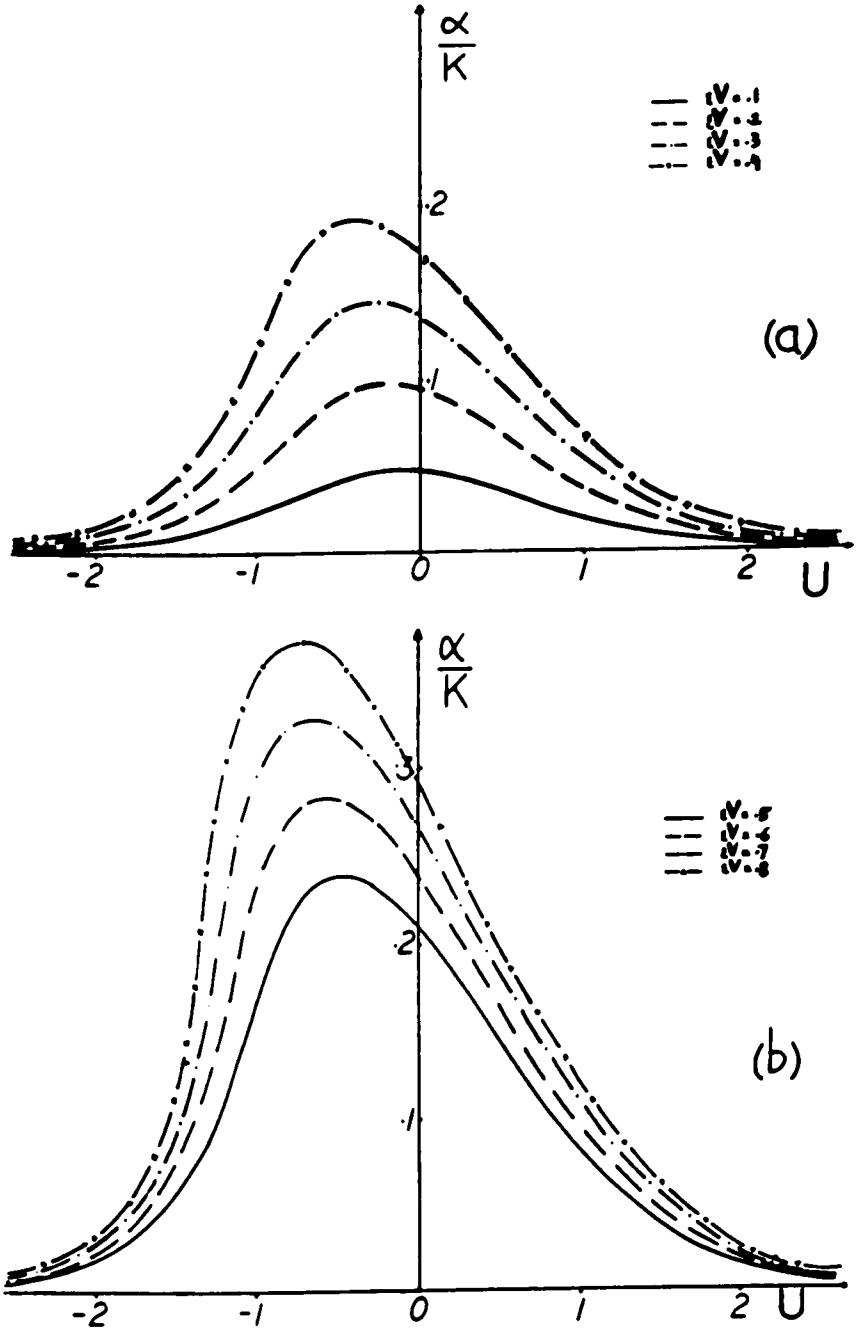

Fig. 5.1-1: The normalized phase of the steepend pulse as function of U in $\chi^{(3)}$- medium.

(a) εV = .1, .2, .3, .4

(b) εV = .5, .6, .7, .8

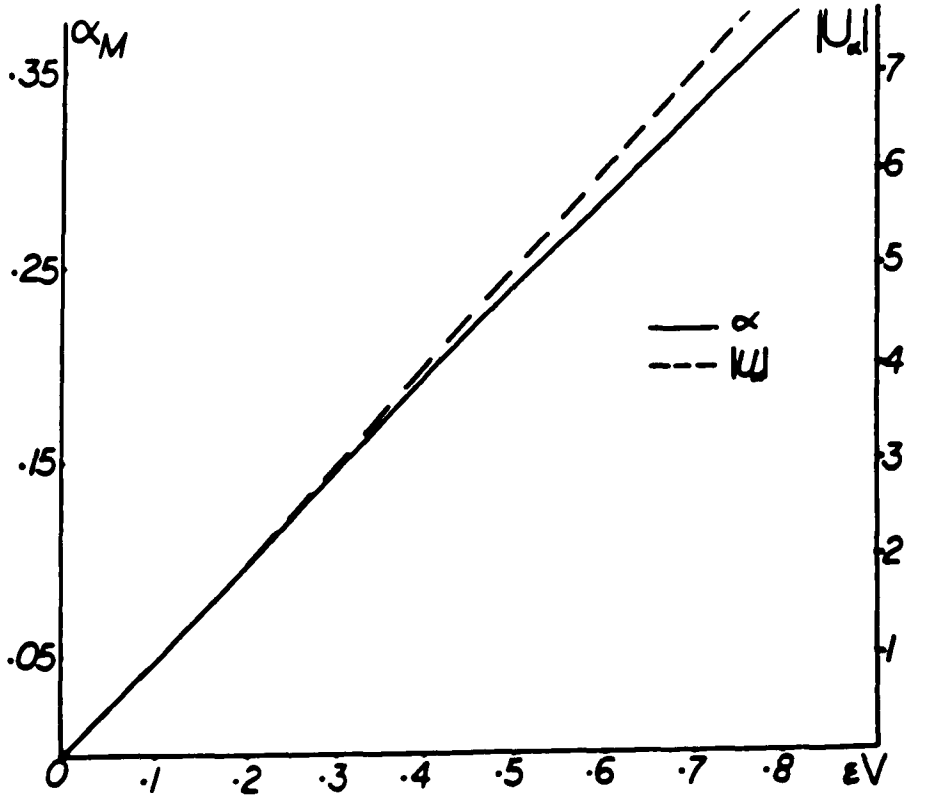

Fig. 5.1-2: The computed magnitude and position of the maximum of the steepened pulse phase as function of εV in $\chi^{(3)}$-medium

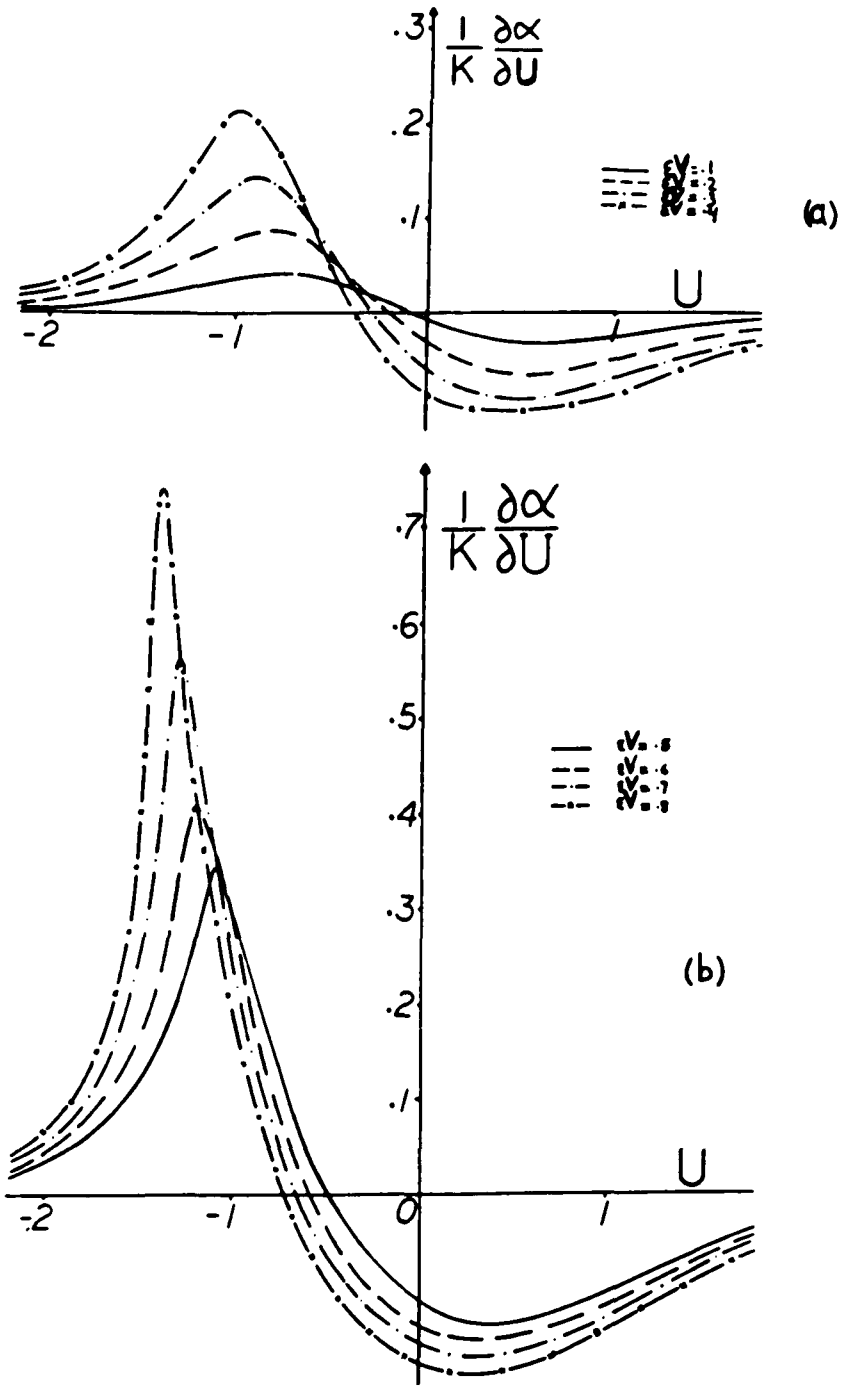

Fig. 5.1-3: The slope of the normalized steepend pulse phase as function of U in $\chi^{(3)}$- medium.

(a) εV = .1, .2, .3, .4

(b) εV = .5, .6, .7, .8

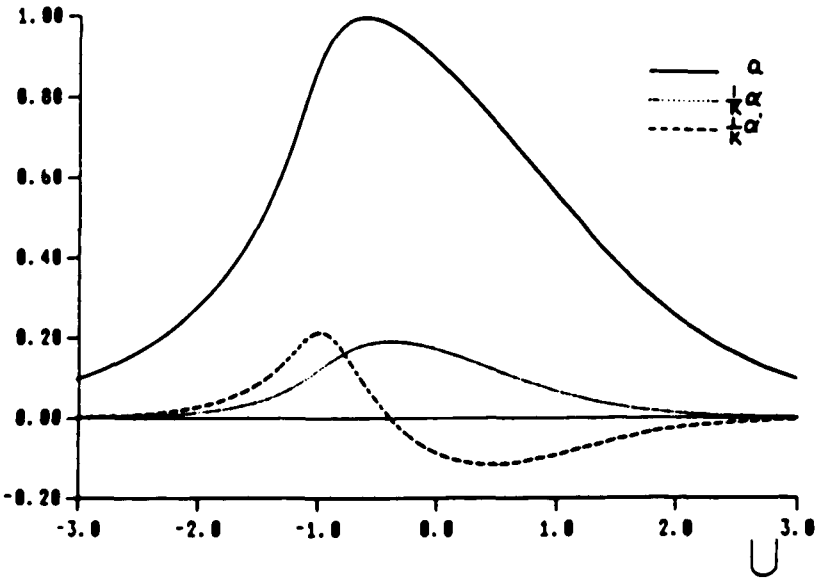

Fig. 5.1-4: The steepened pulse amplitude, phase of the steepened pulse, and slope of the pulse phase as function of U for $\varepsilon V = .4$ in $\chi^{(3)}$- medium .

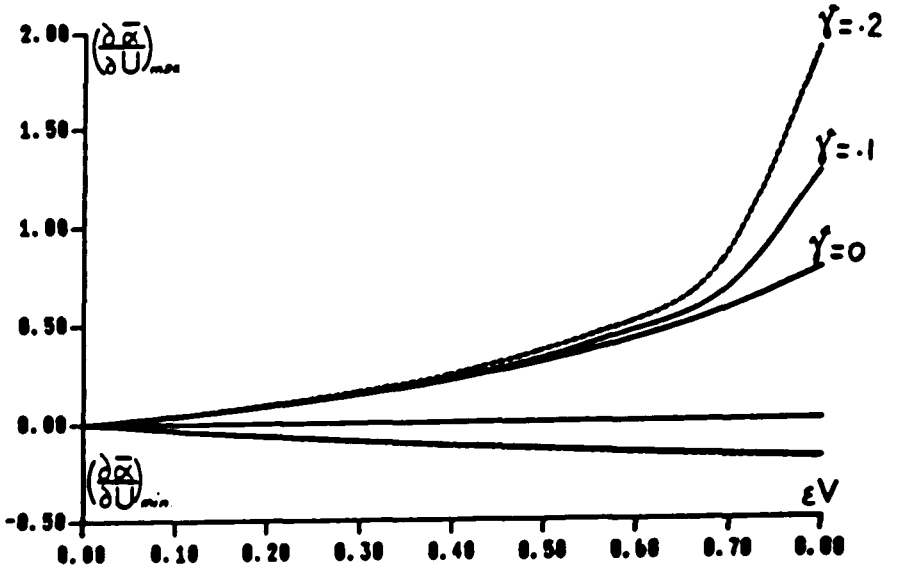

Fig. 5.1-5: The values of the extrema of the slope of the steepened pulse phase for different relaxation time as function of εV in $\chi^{(3)}$ medium .

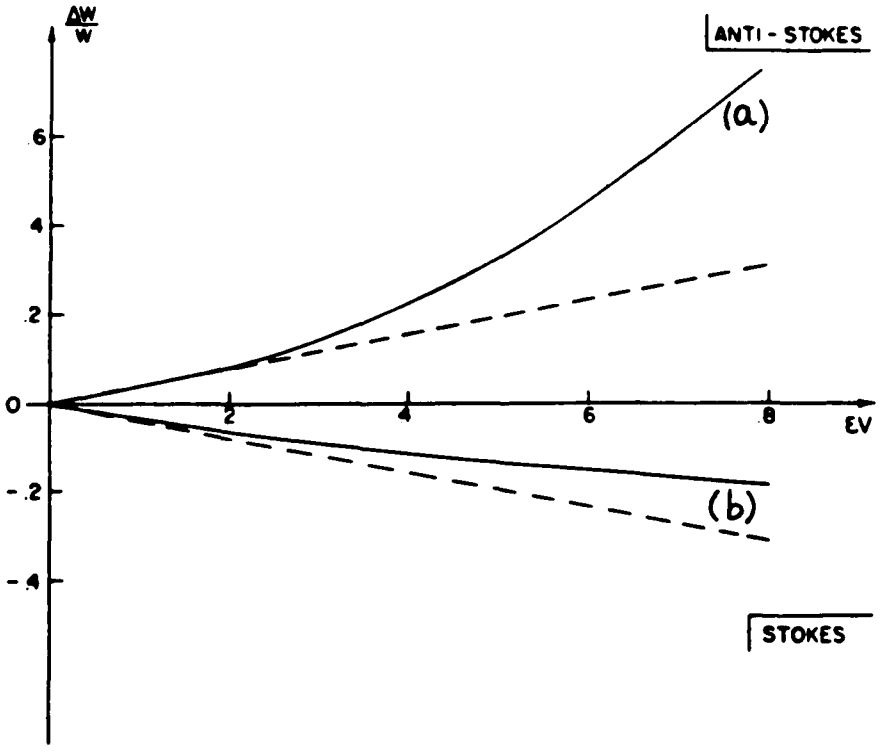

Fig. 5.1-6: The values of the extrema of the slope of the steepened pulse phase as function of εV in $\chi^{(3)}$-medium.

(a) maxima (b) minima

(broken line: conventional SPM, full line: steepened pulse)

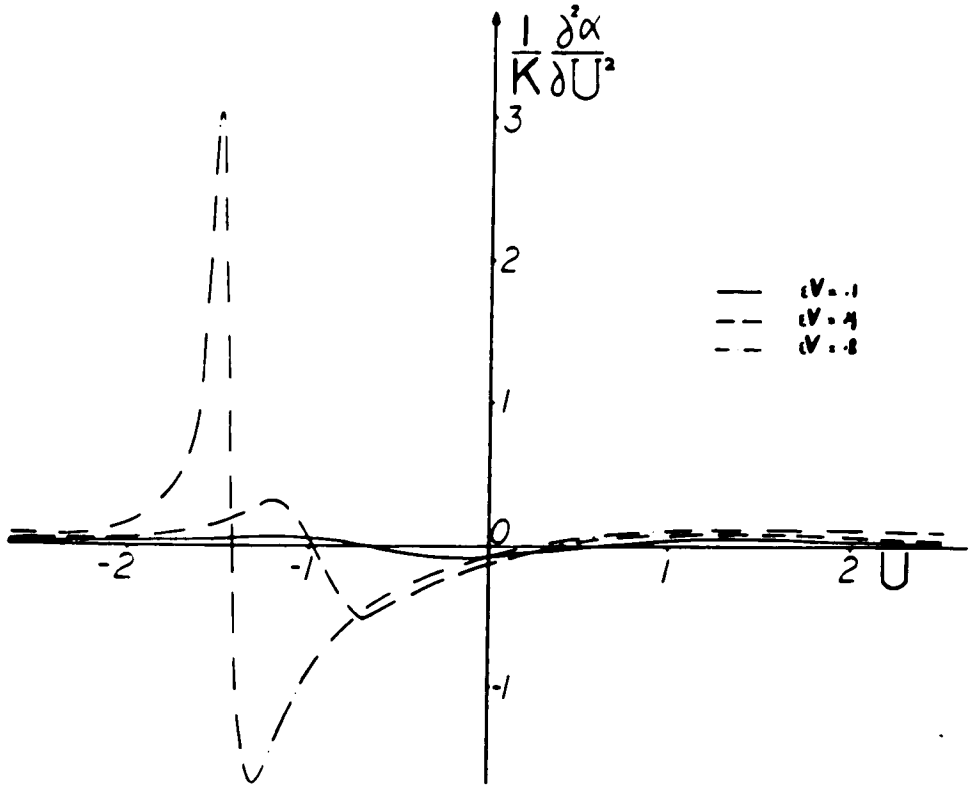

Fig. 5.1-7: The normalized second partial derivative of the pulse phase as function of U with different intensities in $\chi^{(3)}$. medium .

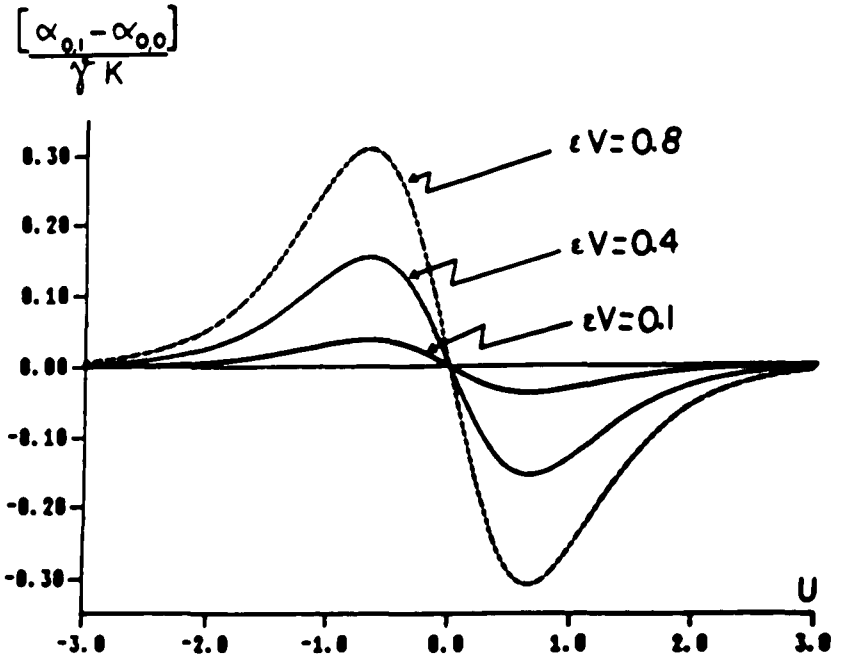

Fig. 5.1-8: The normalized phase portion due to nonzero relaxation time, in the absence of self steepening in dispersionless $\chi^{(3)}$ medium as function of U with different intensities

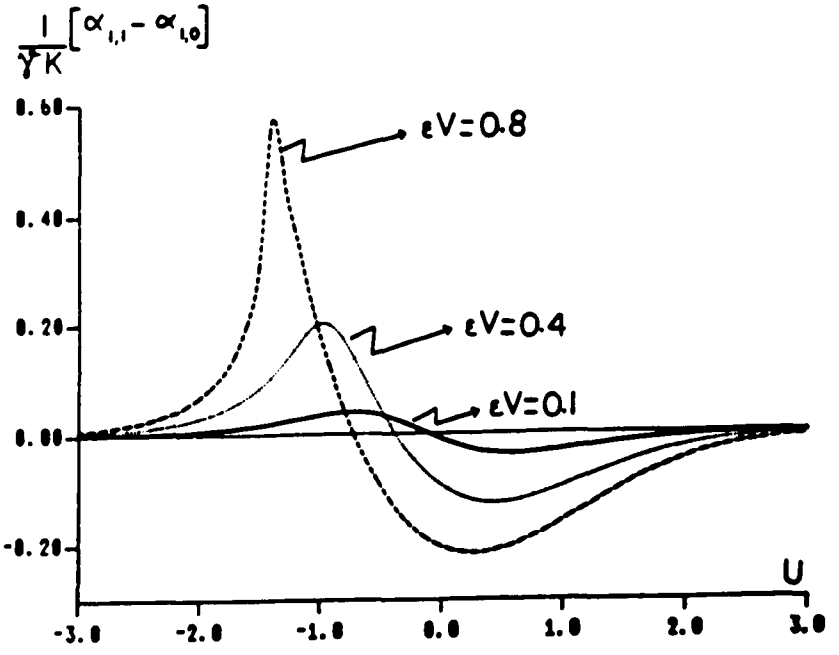

Fig. 5.1-9: The normalized phase portion due to nonzero relaxation time, in the presence of self-steepening as function of U in $\chi^{(3)}$- medium with different intensities

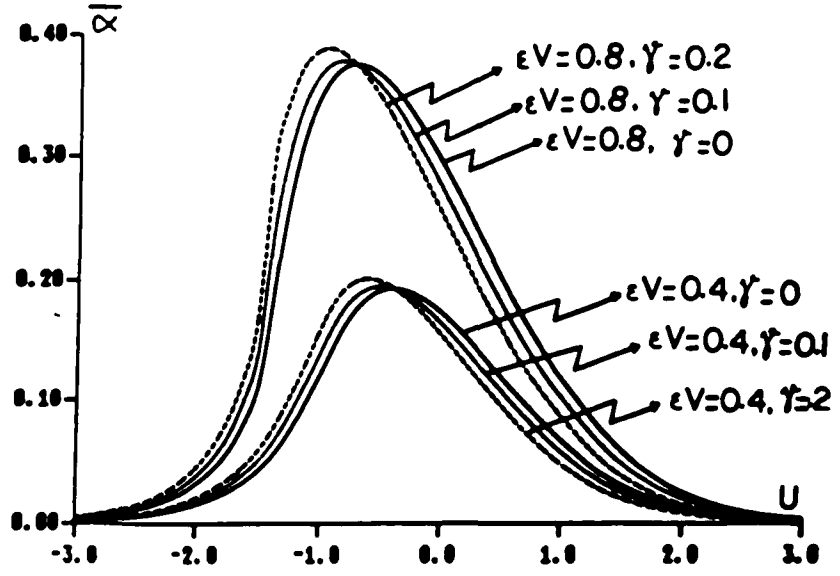

Fig. 5.1-10: The normalized total pulse as function of U with different intensities and relaxation times in $\chi^{(3)}$- medium .

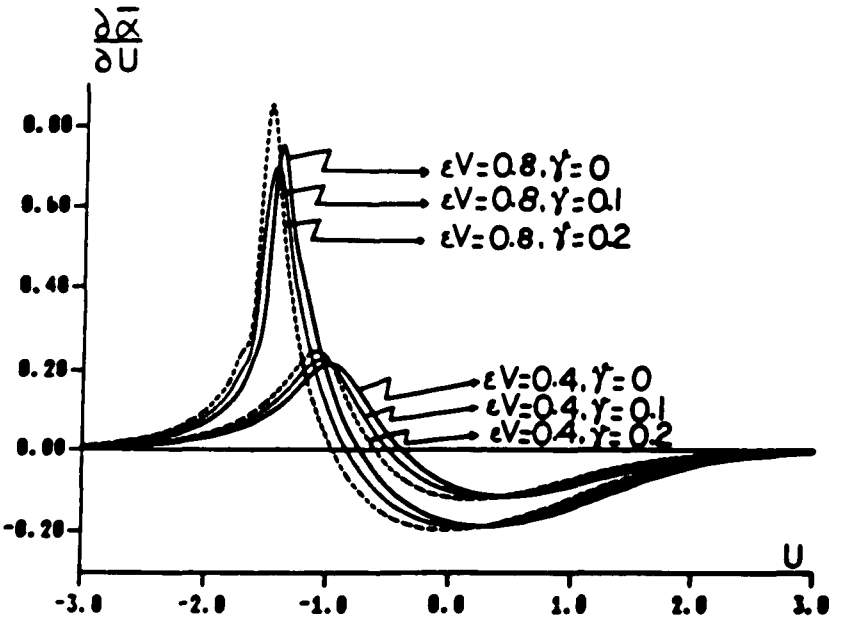

Fig. 5.1-11: The pulse normalized instantaneous frequency sweep as function of U with different intensities and relaxation times in $\chi^{(3)}$- medium .

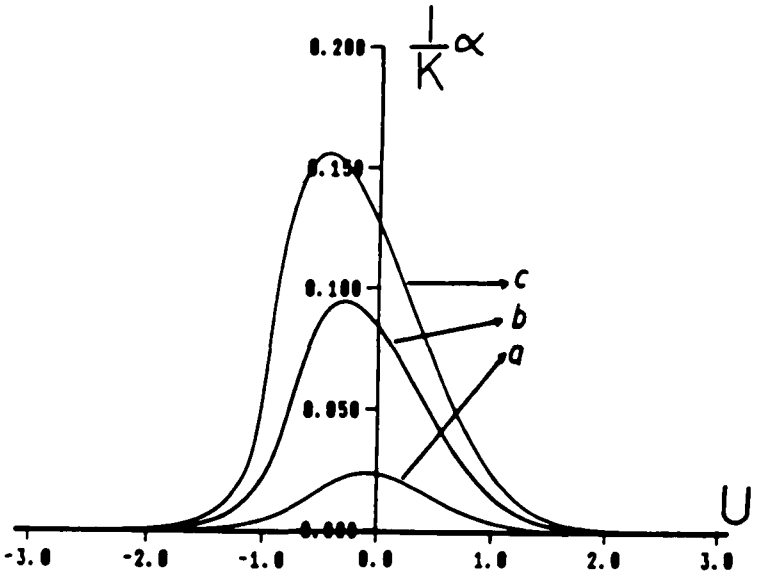

Fig. 5.2-1: The normalized phase of the electric field in dispersionless $\chi^{(5)}$- medium as function of U.
(a) $\varepsilon'V = 0.05$ (b) $\varepsilon'V = 0.2$ (c) $\varepsilon'V = 0.34$

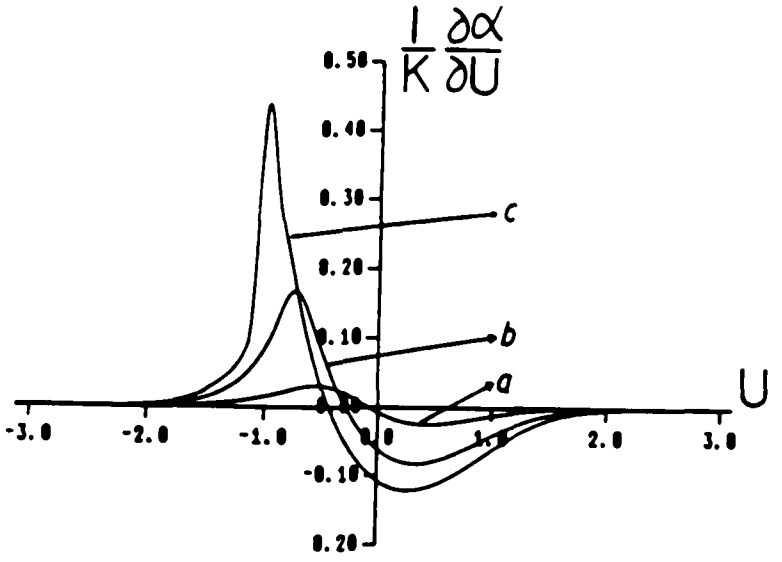

Fig. 5.2-2: The normalized slope of the phase in dispersionless $\chi^{(5)}$- medium as function of U.
(a) $\varepsilon'V = 0.05$ (b) $\varepsilon'V = 0.2$ (c) $\varepsilon'V = 0.34$

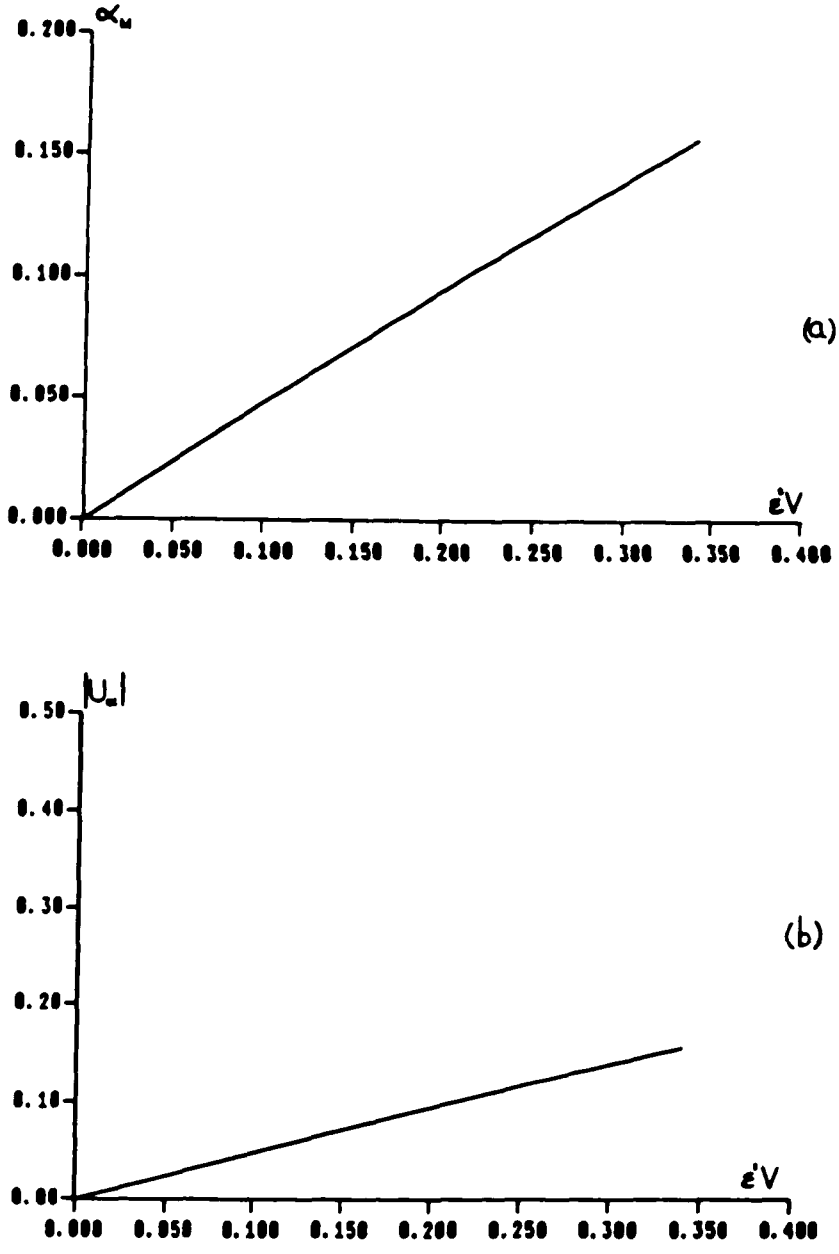

Fig. 5.2-3: (a) The computed magnitude and (b) position of the maximum of the steepened pulse phase as function of $\varepsilon'V$ in $\chi^{(5)}$- medium .

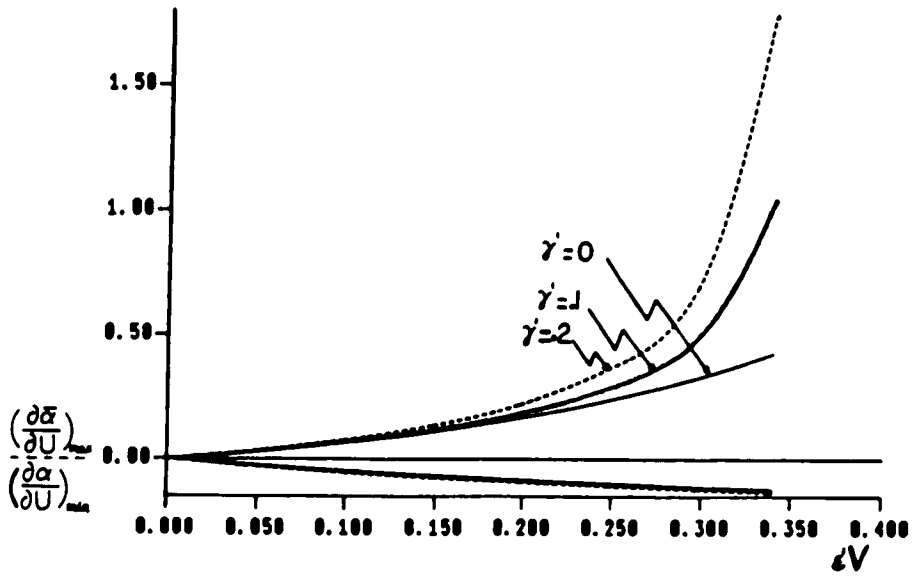

Fig. 5.2-4: The values of the extrema of the slope of the steepened pulse phase in dispersionless $\chi^{(5)}$- medium, for different relaxation times, as function of $\varepsilon'V$.

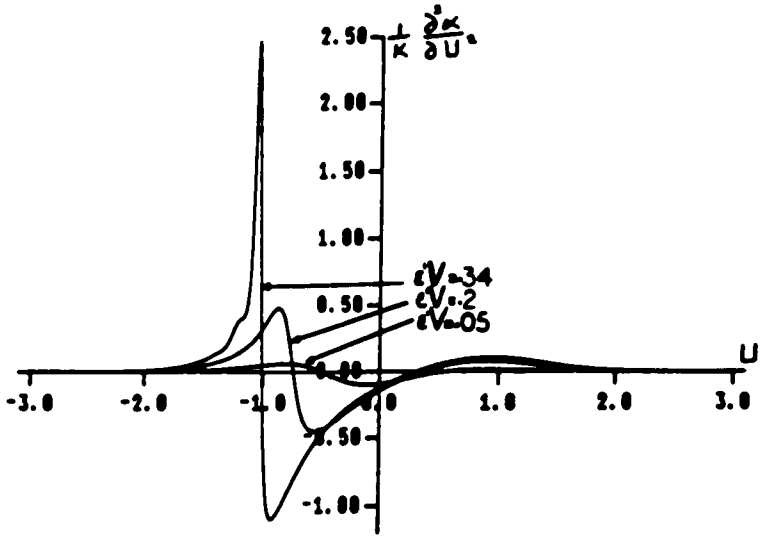

Fig. 5.2-5: The normalized second partial derivative of the phase of a steepened pulse propagating in dispersionless $\chi^{(5)}$-medium as function of U with different intensities .

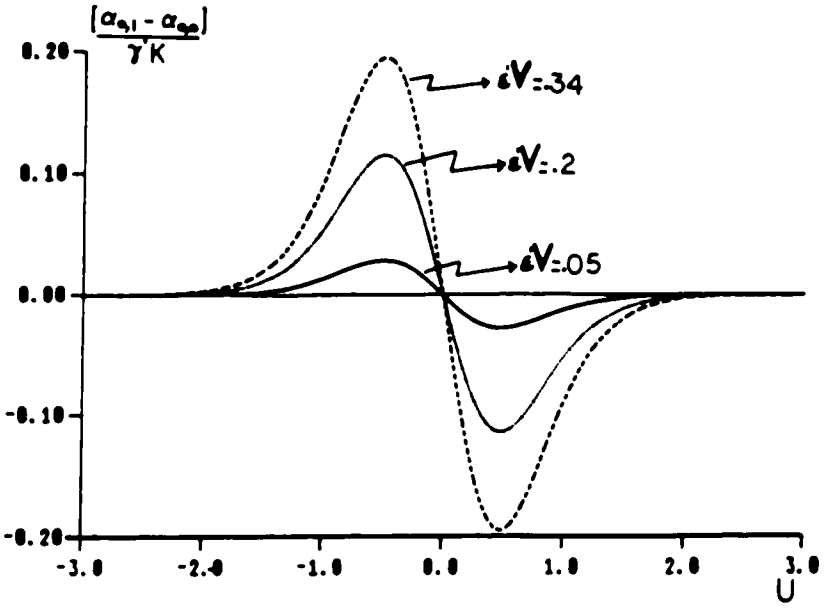

Fig. 5.2-6: The normalized phase portion due to nonzero relaxation time, in the absence of self-steepening in dispersionless $\chi^{(5)}$- medium as function of U with different intensities .

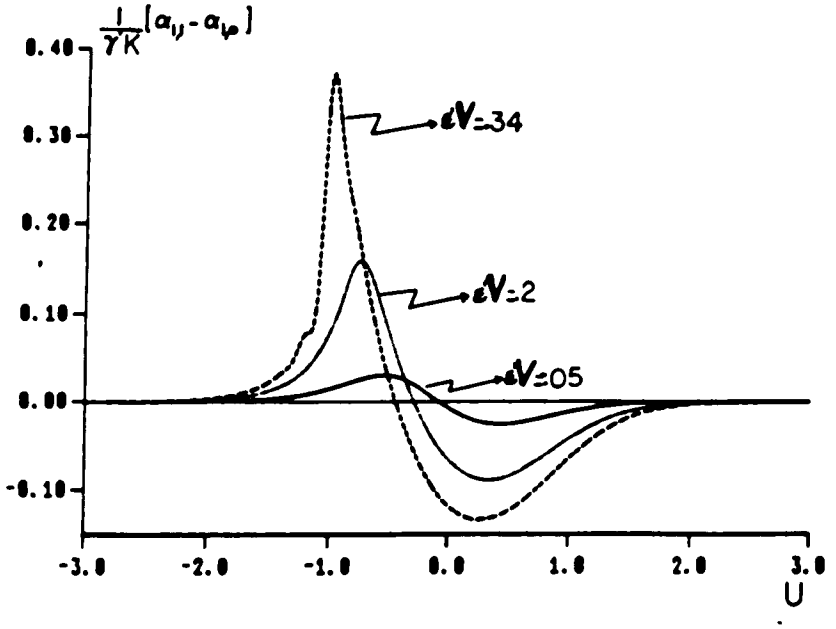

Fig. 5.2-7: The normalized phase portion due to nonzero relaxation time, in the presence of self-steepening in dispersionless $\chi^{(5)}$- medium as function of U with different intensities .

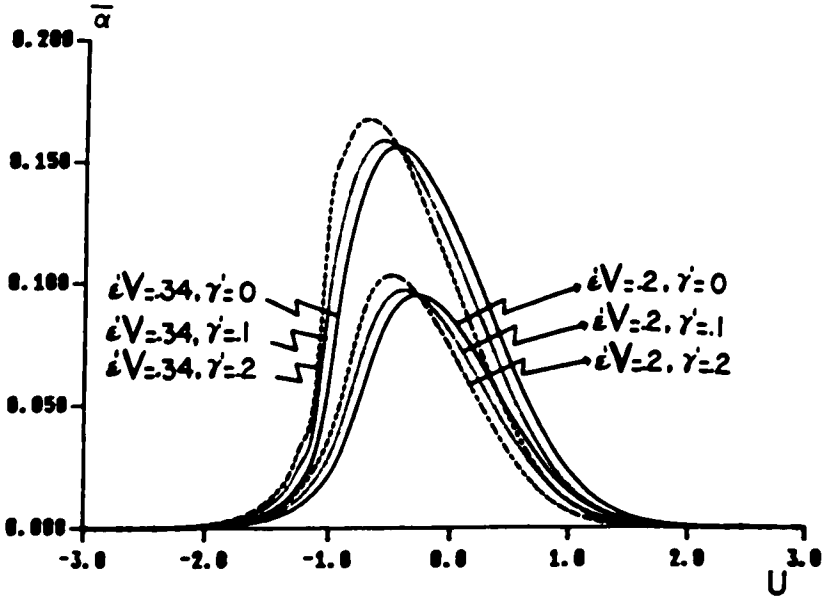

Fig. 5.2-8: The pulse normalized total phase in dispersionless $\chi^{(5)}$- medium as function of U with different intensities and relaxation times

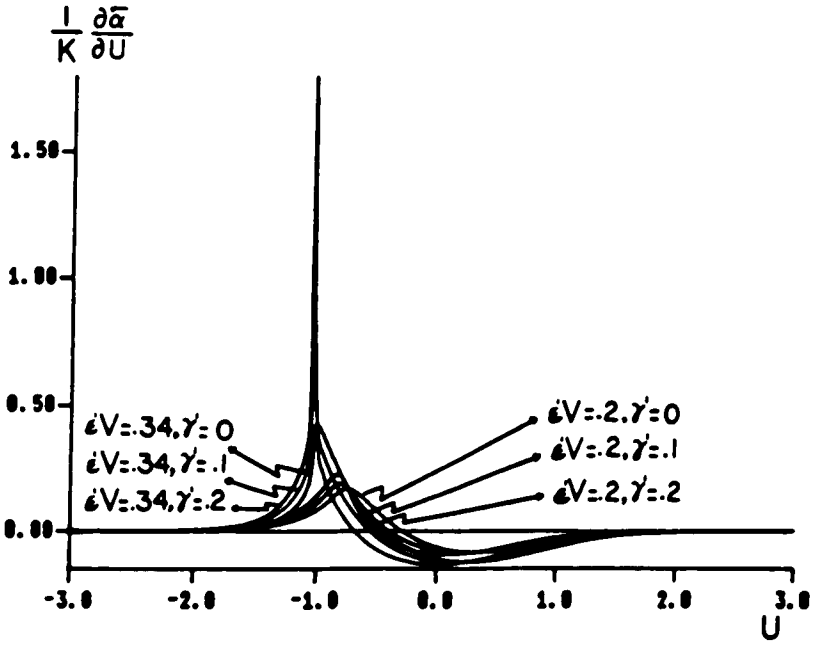

Fig. 5.2-9: The pulse normalized instantaneous frequency sweep in dispersionless $\chi^{(5)}$- medium as function of U with different intensities and relaxation times

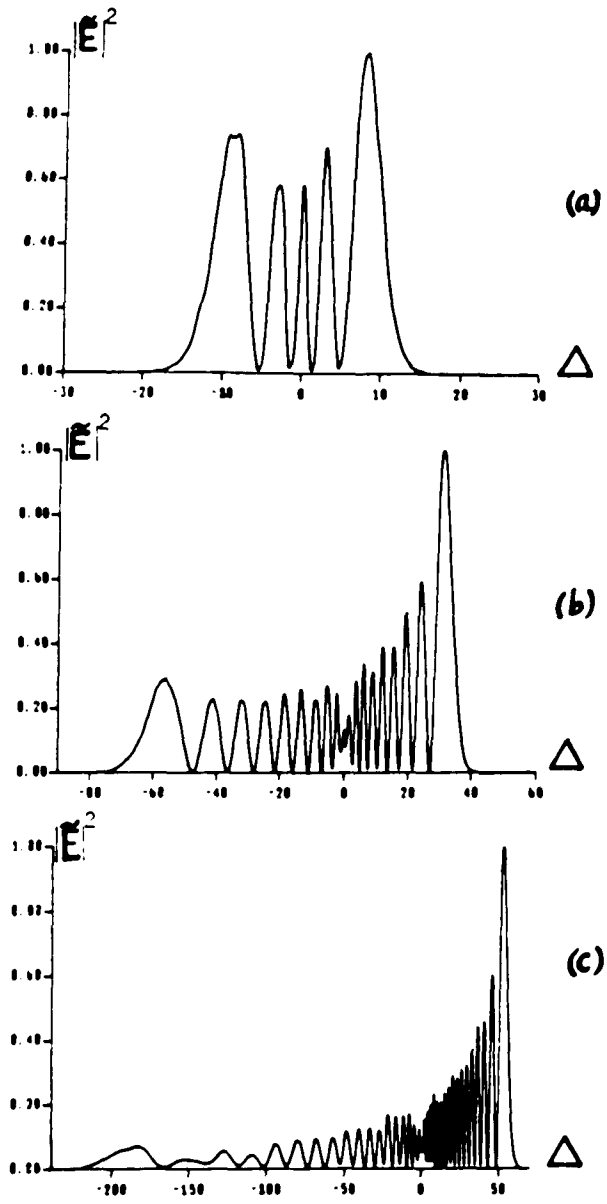

Fig. 6.1-1: The normalized computed spectral distribution of the self-phase modulated steepened pulse as function of the frequency difference multiplied by the pulse duration $\approx 10^{-13}$ s (K= 300) in $\chi^{(3)}$- medium. Left is anti-Stokes side.
(a) $\varepsilon V = 0.1$ (b) $\varepsilon V = 0.4$ (c) $\varepsilon V = 0.8$

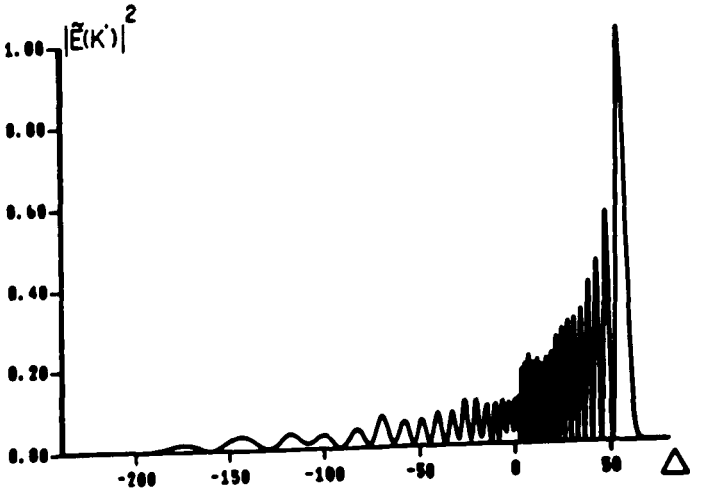

Fig. 6.1-2: The pulse spectral distribution as function of the frequency difference multiplied by the pulse duration in $\chi^{(3)}$-medium. Left is the anti-Stokes side. $K = 300$, $\varepsilon V = 0.8$, $\gamma = 0.2$

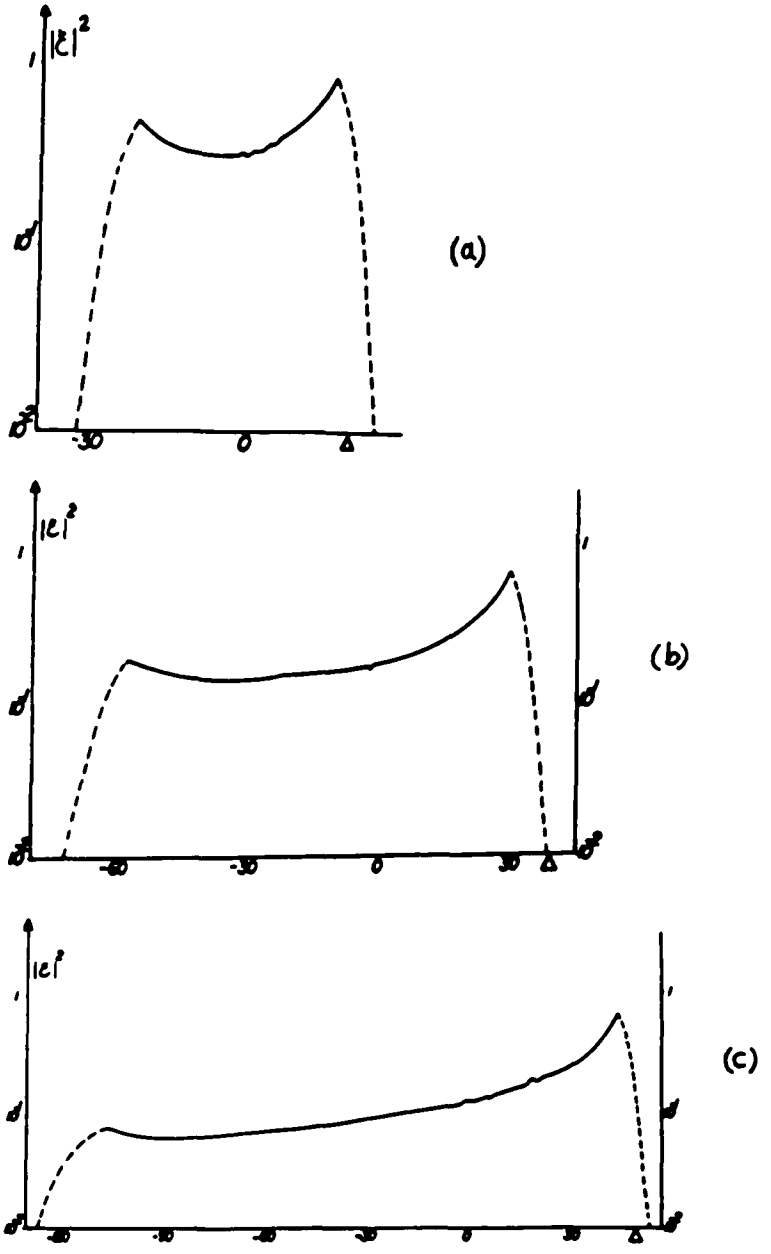

Fig. 6.1-3: The approximate envelopes of the spectra of Fig. 6.1-1 obtained by the method of the stationary phase approximation in $\chi^{(3)}$- medium.

(a) $\varepsilon V = 0.1$ (b) $\varepsilon V = 0.4$ (c) $\varepsilon V = 0.8$

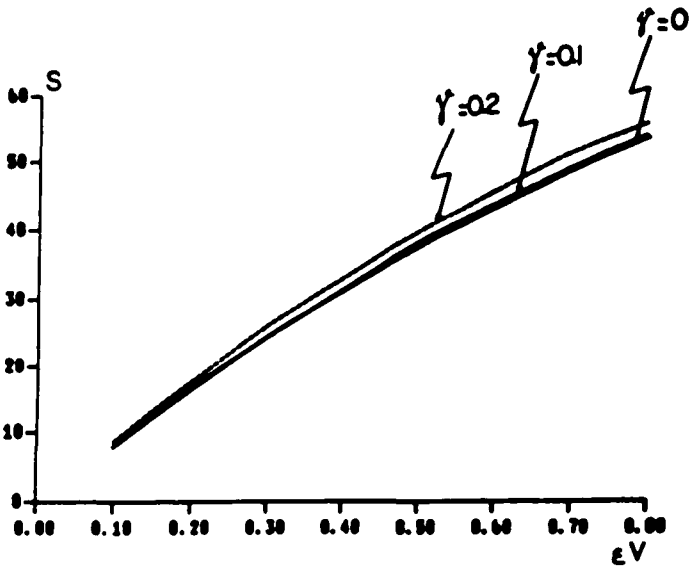

Fig. 6.1-4: The spectral maximum peak position as function of εV , K=300 with different relaxation times in $\chi^{(3)}$- medium.

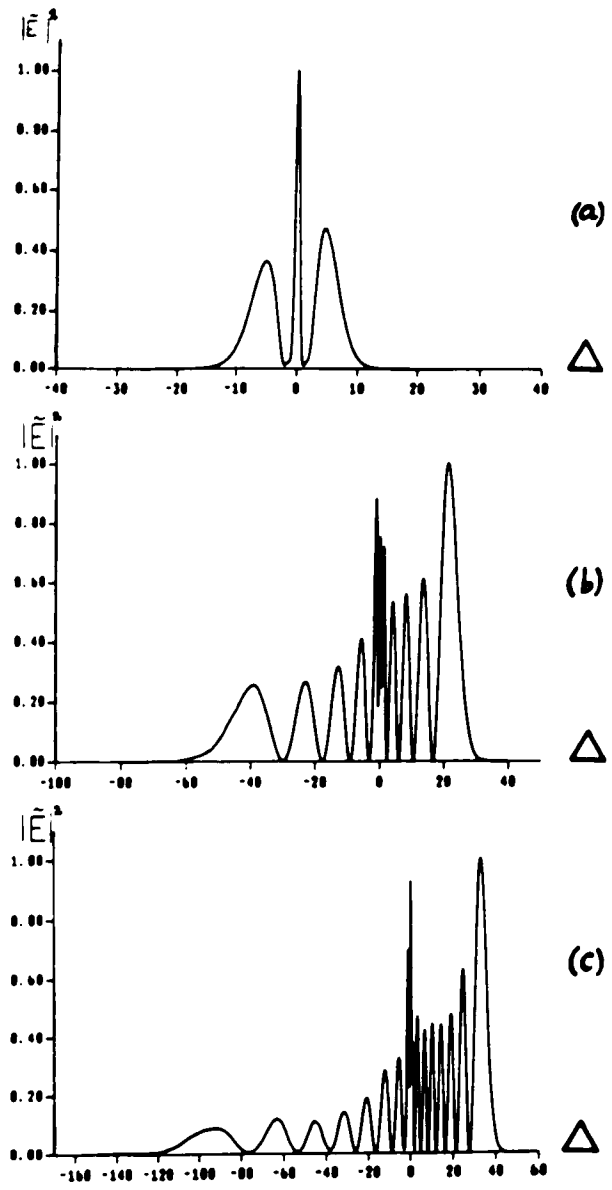

Fig. 6.2-1: The spectral distribution of a steepened pulse outgoing from a dispersionless $\chi^{(5)}$- medium. The zero of Δ is the center frequency of the original pulse.
(a) $\varepsilon' V = 0.05$ (b) $\varepsilon' V = 0.2$ (c) $\varepsilon' V = 0.34$

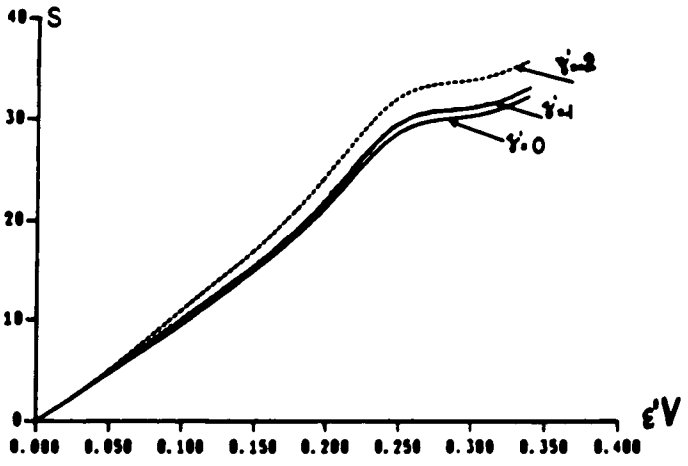

Fig. 6.2-2: The spectral maximum peak position as function of $\varepsilon'V$, K = 300 with different relaxation time in $\chi^{(5)}$- medium .

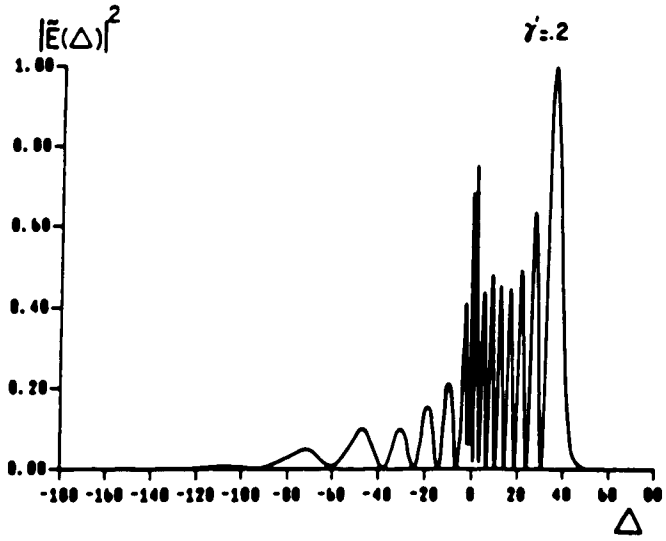

Fig. 6.2-3: The pulse spectral distribution as function of the normalized frequency difference multiplied by pulse duration. Left is the anti-Stokes side. Normalized center frequency .
K = 300, $\varepsilon'V = 0.2$

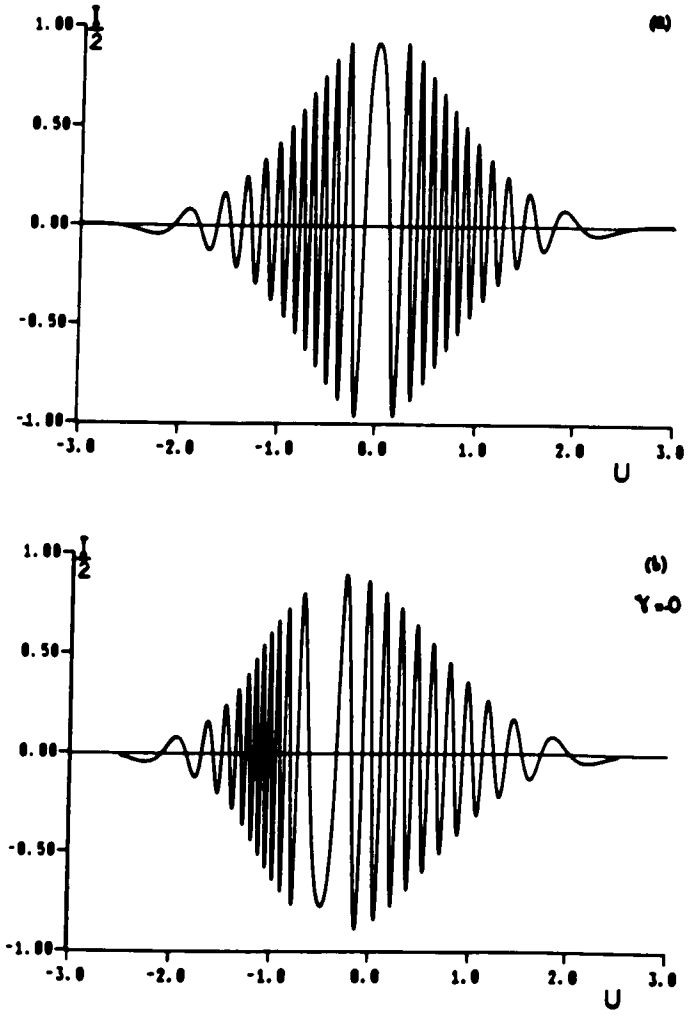

Fig. 7.2-1: The difference signal between the output from a Mach-Zehnder interferometer and the sum of the input pulse to the interferometer, i.e., the SPM pulse, and the reference pulse i.e. sech pulse in $\chi^{(3)}$- medium

K = 300, $\varepsilon V = 0.5$

(a) conventional SPM theory

(b) self-steepened theory

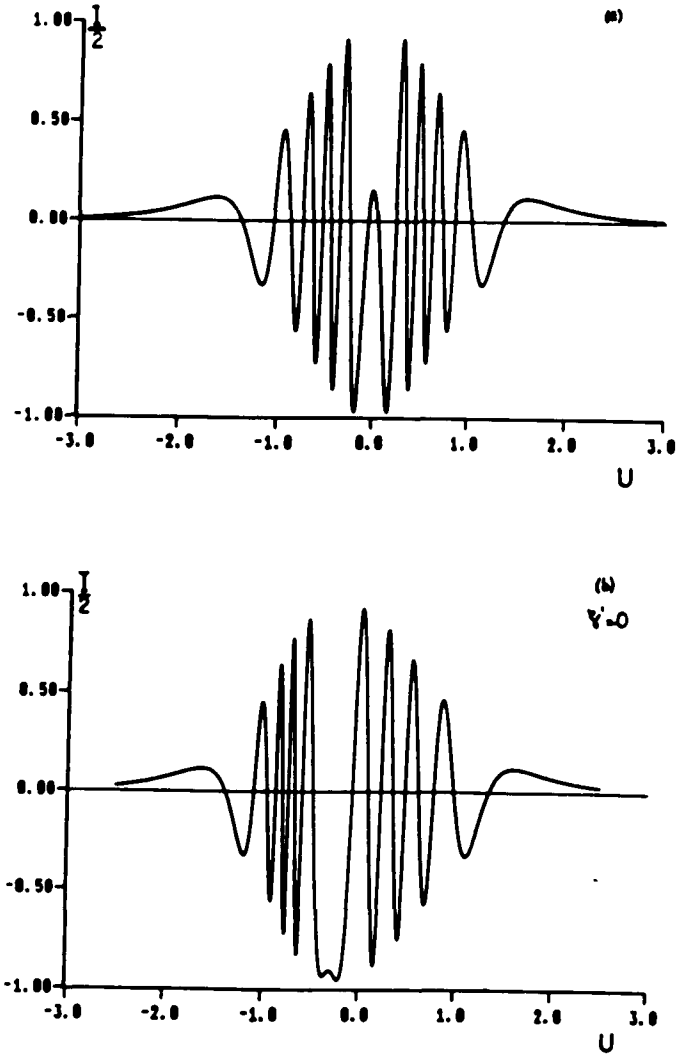

Fig. 7.3-1: The difference signal between the output from a Mach-Zehnder interferometer and the sum of the input pulse to the interferometer, i.e., the SPM pulse, and the reference pulse i.e. sech pulse in $\chi^{(5)}$- medium

$K = 300, \quad \varepsilon' V = .2$

(a) conventional SPM theory

(b) self-steepened theory

	Order				
eV	0	1	2	3	4
0.1	−0.006	−0.016	−0.021	−0.029	−0.034
0.2	−0.018	−0.051	−0.073	−0.045	−0.343
0.3	−0.040	−0.101	−0.010	1.14	2.29
0.4	−0.072	−0.127	1.84	2.02	2.20
0.5	−0.113	0.115	1.74	2.20	3.63
0.6	−0.161	1.29	1.59	3.15	4.59
0.7	−0.213	1.19	2.62	3.84	4.87
0.8	−0.254	1.04	2.51	4.01	5.67

Table 8.2-1: Shifts in the positions of the asymptotic interferometric intensity minima for various orders and ev values.

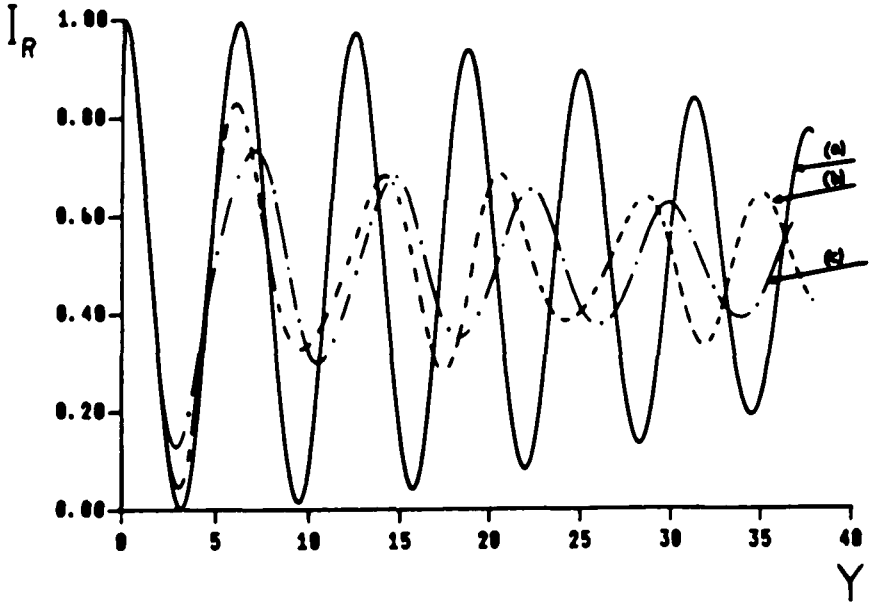

Fig. 8.2-1: The Young/Michaelson normalized interferometric intensity distribution $I_R(y)$, for a steepened self-phase modulated input, as function of $y(= \omega_0\Delta)$, $K = 50$ in $\chi^{(3)}$- medium.

(a) $\varepsilon V = 0.1$ (b) $\varepsilon V = 0.5$ (c) $\varepsilon V = 0.8$

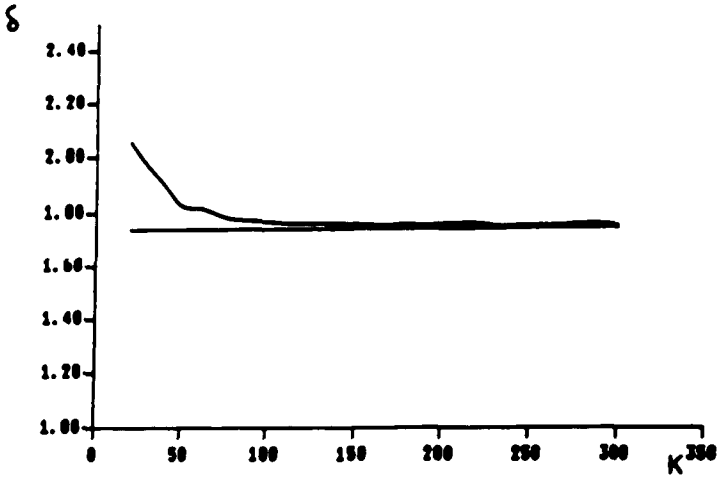

Fig. 8.2-2: The shifts in the position of the Young interiferometric third order minimum, for a steepened self-phase modulated input, $\varepsilon V = 0.5$ as function of $K(= \omega_0 \tau)$ in $\chi^{(3)}$- medium .

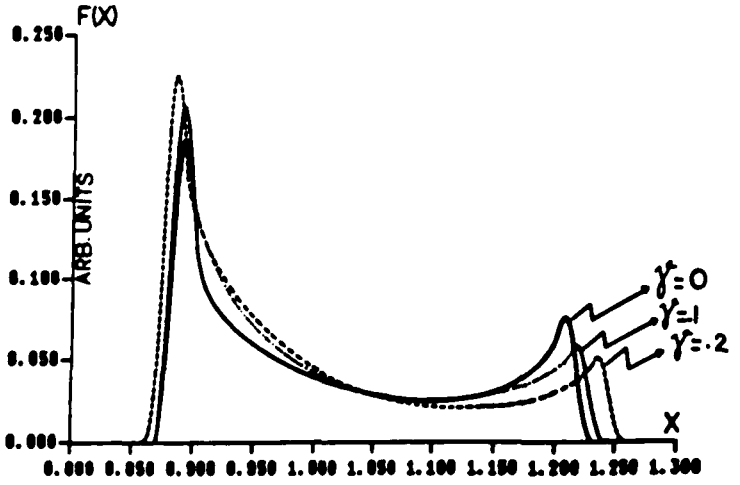

Fig. 8.2-3: The envelope of the Fourier transform of the Young visibility function with different relaxation times in $\chi^{(3)}$- medium .

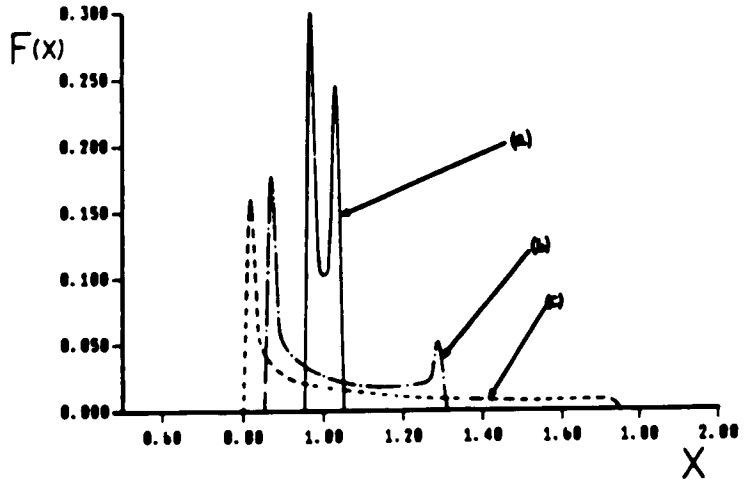

Fig. 8.2-4: The Fourier transform of the Young interferometer intensity distribution for a steepened SPM pulse as function of X in $\chi^{(3)}$- medium.
(a) $\varepsilon V = 0.1$ (b) $\varepsilon V = 0.5$ (c) $\varepsilon V = 0.8$

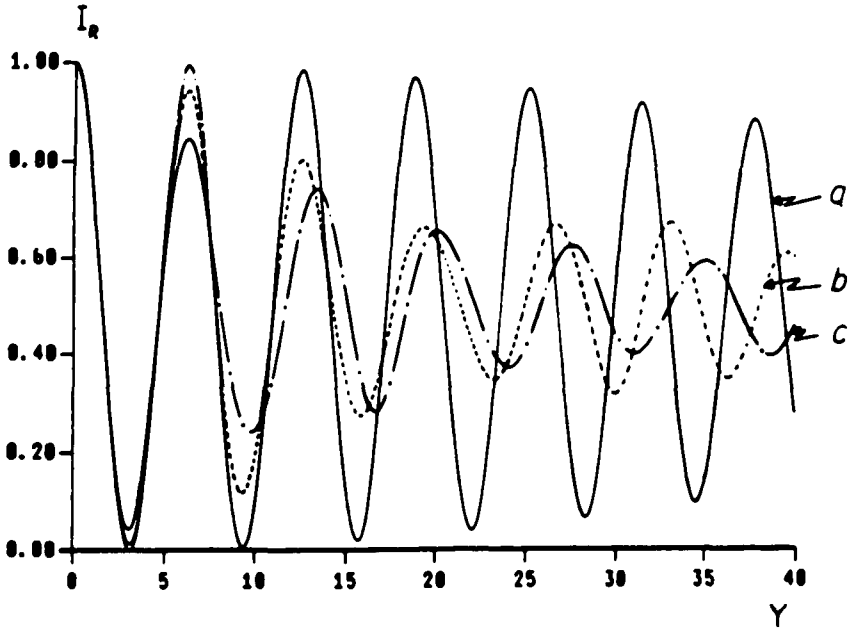

Fig. 8.3-1: The Young/Michaelson normalized interferometric intensity distribution $I_R(y)$, for a steepened self-phase modulated input in $\chi^{(5)}$- dispersionless medium as function of $y(= \omega_0\Delta)$, K = 50.

(a) $\varepsilon'V = 0.05$ (b) $\varepsilon'V = 0.2$ (c) $\varepsilon'V = 0.34$

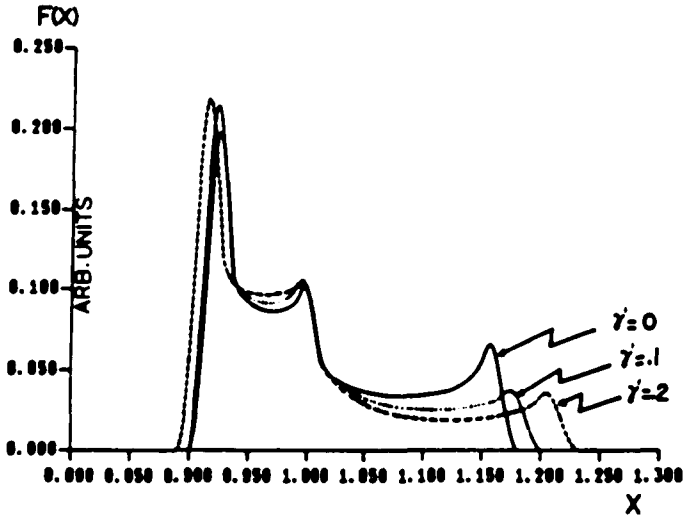

Fig. 8.3-2: The envelope of the Fourier transform of the Young visibility function in dispersionless $\chi^{(5)}$- medium with different relaxation times .

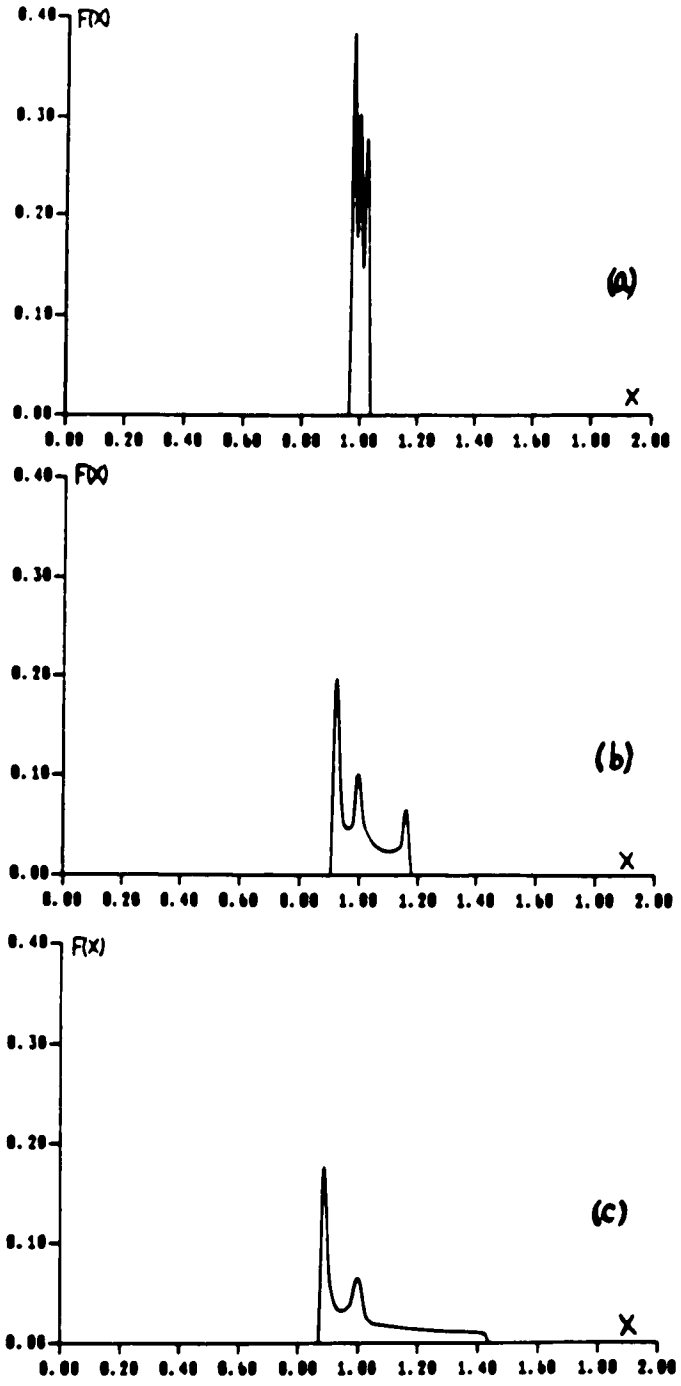

Fig. 8.3-3: The Fourier transform of the Young interferometer intensity distribution for a steepened SPM pulse in dispersionless $\chi^{(5)}$- medium as function of X.

(a) $\varepsilon'V = 0.05$ (b) $\varepsilon'V = 0.2$ (c) $\varepsilon'V = 0.34$

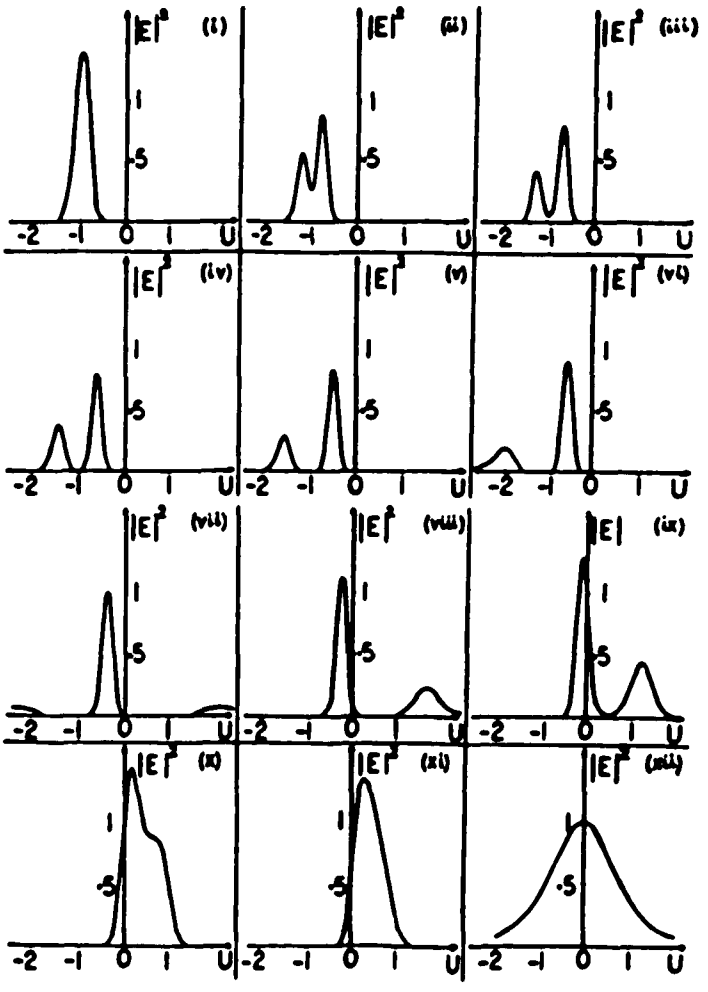

Fig. 9.2-1: The field intensity outgoing from an amplitude filter, where the input is a steepened SPM signal ($K = 300$, $\varepsilon V = 0.4$, $\Delta_f \tau = 5$) in $\chi^{(3)}$- medium. All the intensities are normalized to the maximum value of the pulse resulting from the filter with the same center frequency as the incoming pulse

(i) $K - K_f = -60$ (ii) $K - K_f = -50$ (iii) $K - K_f = -40$

(iv) $K - K_f = -30$ (v) $K - K_f = -20$ (vi) $K - K_f = -10$

(vii) $K - K_f = 0$ (viii) $K - K_f = 10$ (ix) $K - K_f = 20$

(x) $K - K_f = 30$ (xi) $K - K_f = 34$ (xii) normalized sech^2 pulse .

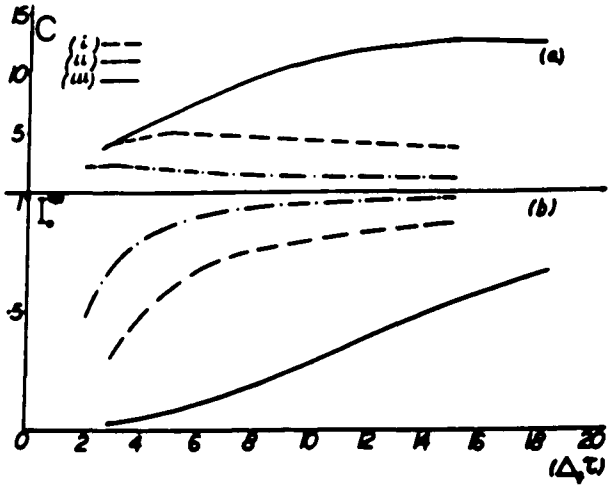

Fig. 9.2-2: (a) The compression ratio and (b) the intensity magnitude of the steepened SPM pulses outgoing from a filter as function of $(\Delta_f \tau)$ in $\chi^{(3)}$- medium

(i) $K = 300$, $\varepsilon V = 0.4$, $K - K_f = -60$

(ii) $K = 30$, $\varepsilon V = 0.4$, $K - K_f = -6$

(iii) $K = 300$, $\varepsilon V = 0.8$, $K - K_f = -210$

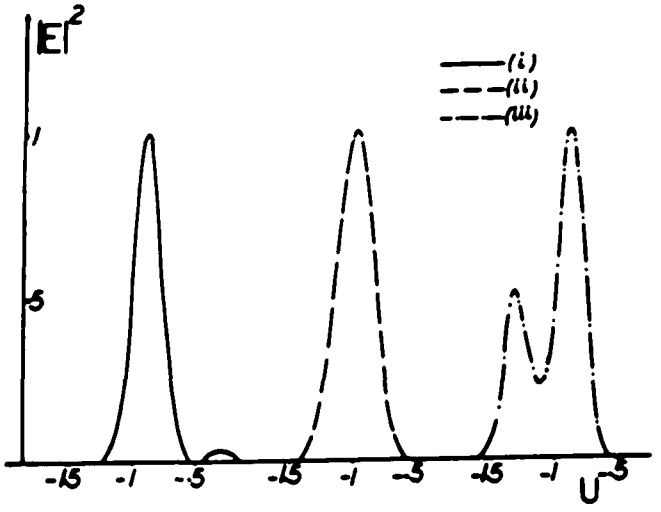

Fig. 9.2-3: The effects of fluctuation εV (i.e. laser intensity) on the shape of the filter output in $\chi^{(3)}$- medium
($K = 300$, $K - K_f = -60$, $\Delta_f \tau = 5$)

(i) $\varepsilon V = 0.3$ (ii) $\varepsilon V = 0.4$ (iii) $\varepsilon V = 0.5$

The peak intensities are, respectively:
8.27×10^{-3}, 6.03×10^{-2}, 2.54×10^{-1}

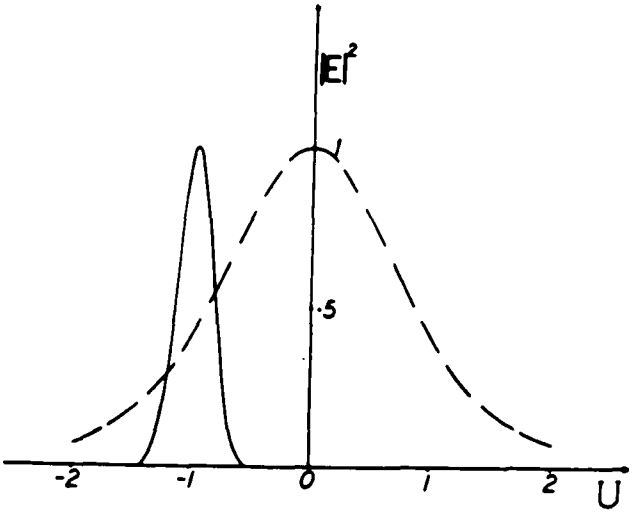

Fig. 9.2-4: The computed normalized intensity, shape and position of SPM pulse outgoing from an optimum compression filter and the normalized intensity shape of the incoming pulse prior to SPM and filtering in $\chi^{(3)}$- medium .

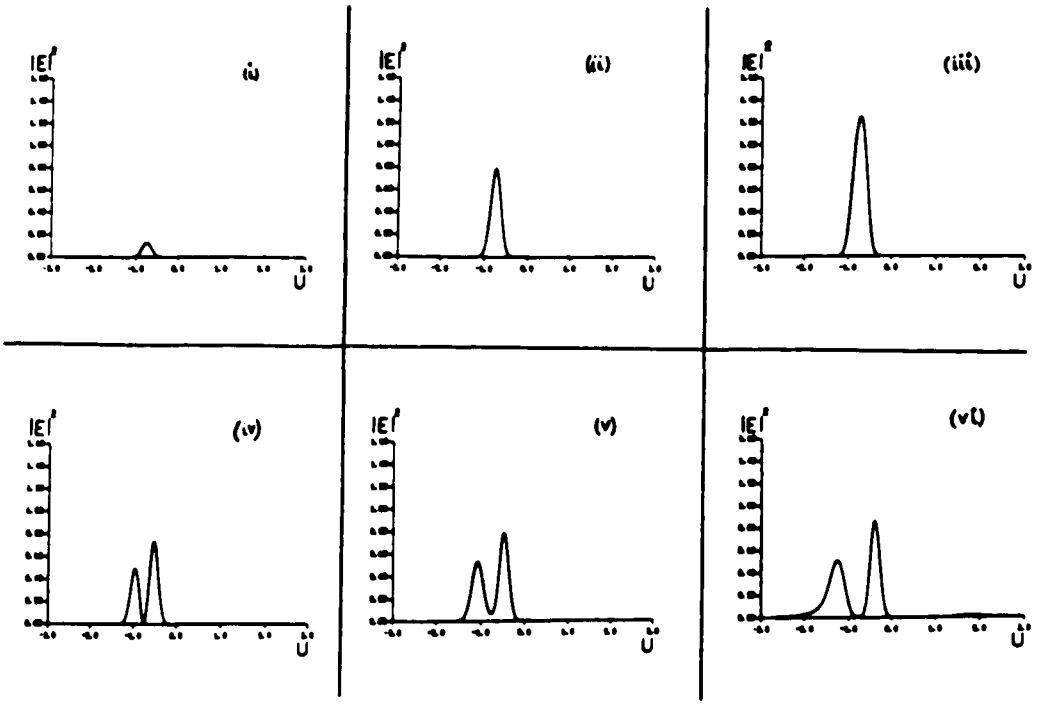

Fig. 9.3-1: The field intensity outgoing from an amplitude filter, where the input is a steepened SPM signal ($K = 300$, $\varepsilon' V = 0.2$ in dispersionless $\chi^{(5)}$- medium. All the intensities are normalized to the maximum value of the pulse resulting from the filter with the same center frequency as the incoming pulse.

(i) $K - K_f = -60$ (ii) $K - K_f = -50$ (iii) $K - K_f = -40$

(iv) $K - K_f = -30$ (v) $K - K_f = -20$ (vi) $K - K_f = -10$

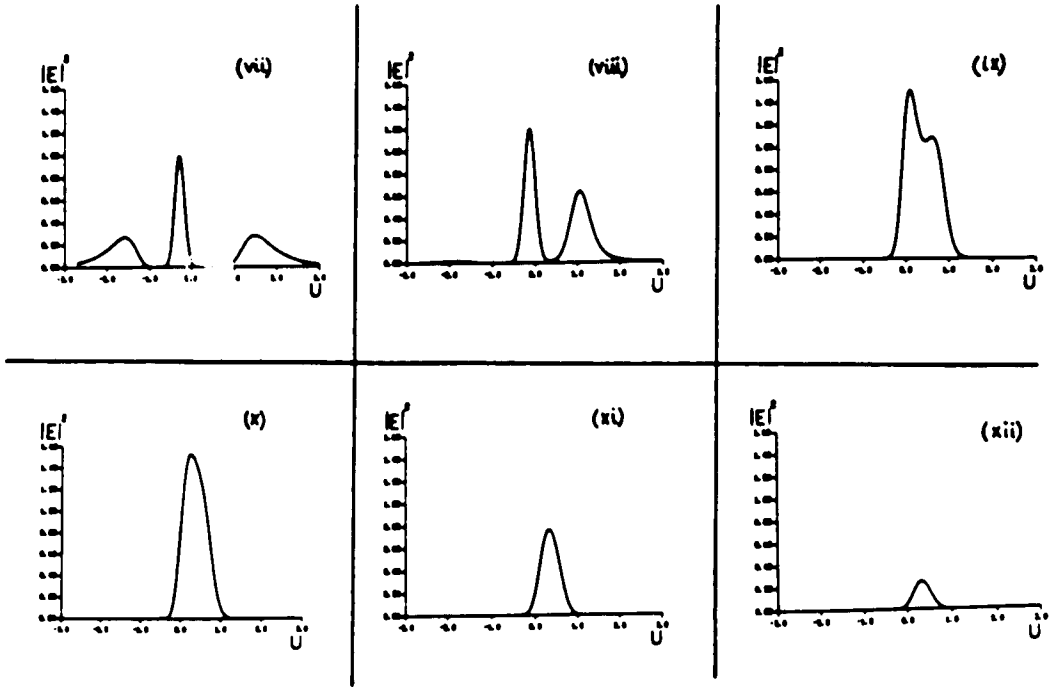

Fig. 9.3-1: The field intensity outgoing from an amplitude filter, where the input is a steepened SPM signal ($K = 300$, $\varepsilon' V = 0.2$ in dispersionless $\chi^{(5)}$- medium. All the intensities are normalized to the maximum value of the pulse resulting from the filter with the same center frequency as the incoming pulse.

(vii) $K - K_f = 0$ (viii) $K - K_f = 10$ (ix) $K - K_f = 20$

(x) $K - K_f = 24$ (xi) $K - K_f = 30$ (xii) $K - K_f = 34$

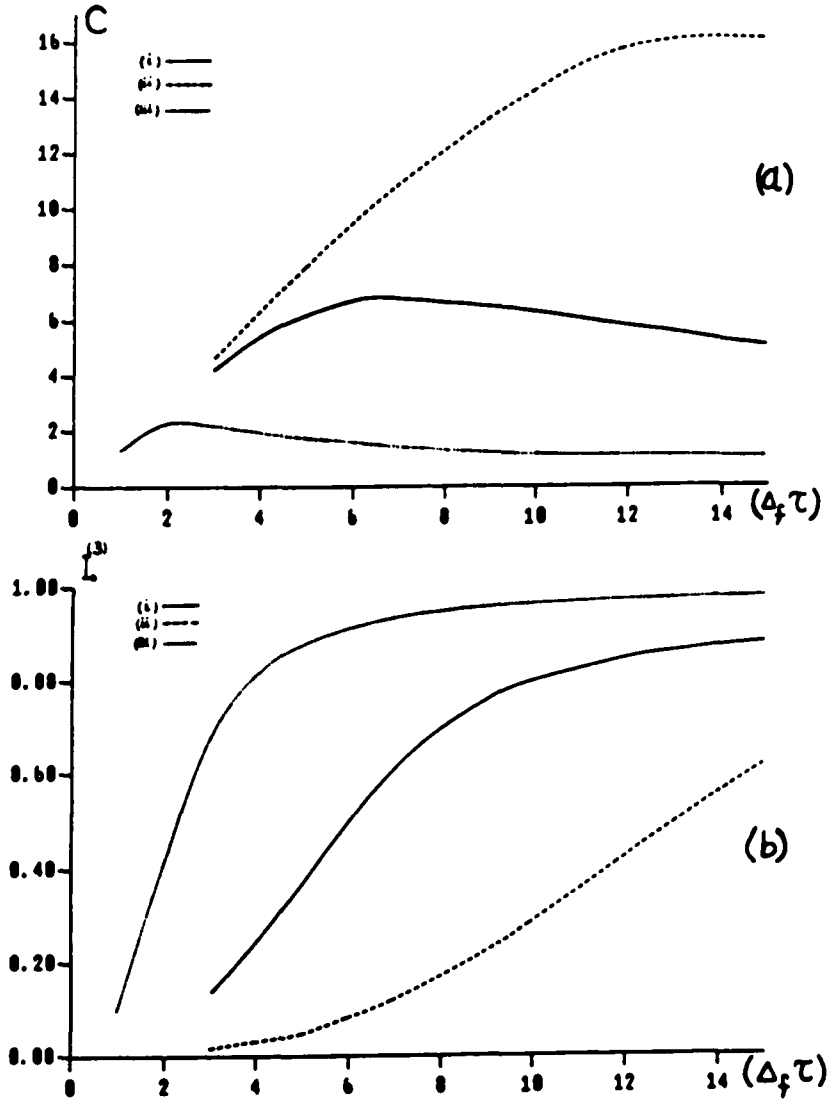

Fig. 9.3-2: (a) The compression ratio and (b) the intensity magnitude of the steepened SPM pulses outgoing from a filter as function of ($\Delta_f \tau$) in dispersionless $\chi^{(5)}$- medium.

(i) $K = 300$, $\varepsilon' V = 0.2$, $K - K_f = -50$

(ii) $K = 30$, $\varepsilon' V = 0.2$, $K - K_f = -5$

(iii) $K = 300$, $\varepsilon' V = 0.34$, $K - K_f = -210$

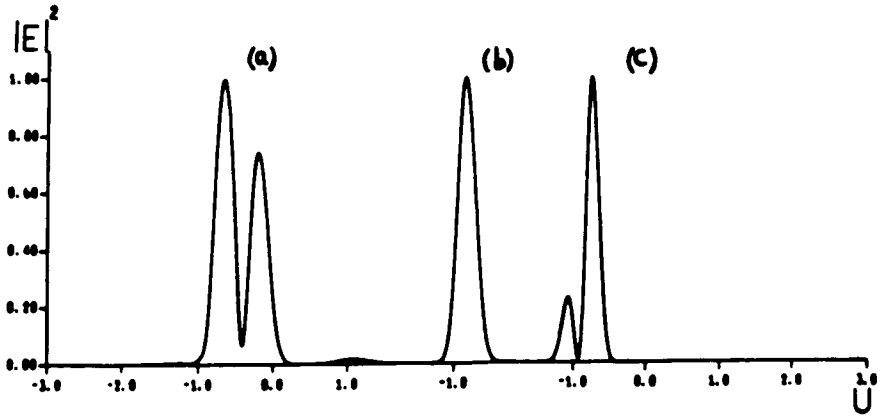

Fig. 9.3-3: The effects of fluctuation εV (i.e. laser intensity) on the shape of the filter output. ($K = 300$, $K - K_f = -50$, $\Delta_f \tau = 5$) in $\chi^{(5)}$- dispersionless medium

(a) $\varepsilon' V = 0.15$ (b) $\varepsilon' V = 0.2$ (c) $\varepsilon' V = 0.25$

The peak intensities are, respectively:

0.123×10^{-2} , 0.4711×10^{-1} , 0.357×10^{0}

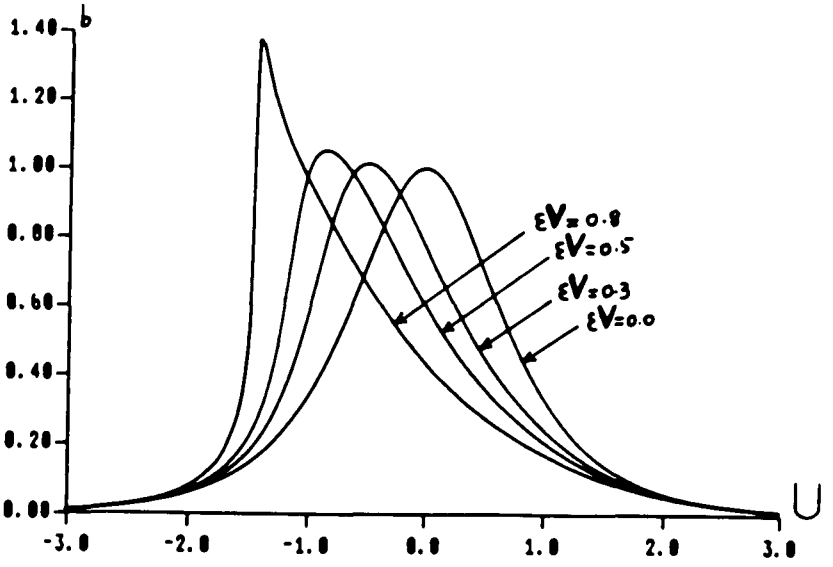

Fig. 10.2-1: The amplitude of the induced phase modulated steepened second harmonic pulse as function of U with different intensities with n = 1.76 .

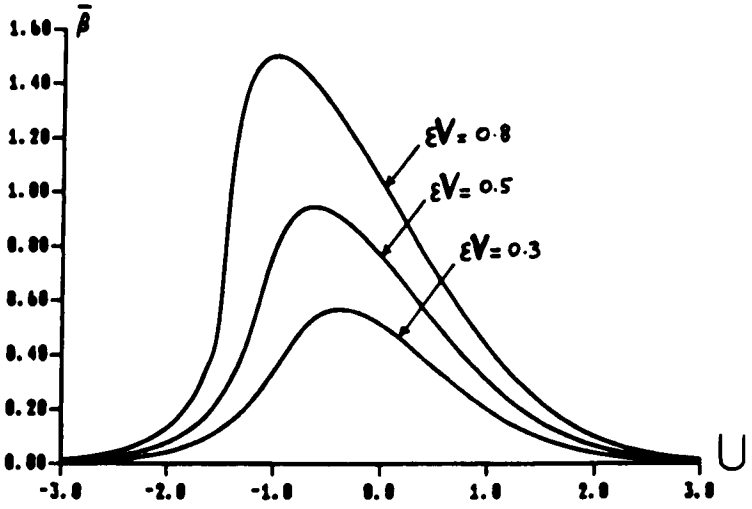

Fig. 10.2-2: The normalized phase of the induced phase modulated steepened second harmonic pulse as function of U with different intensities with n = 1.76 .

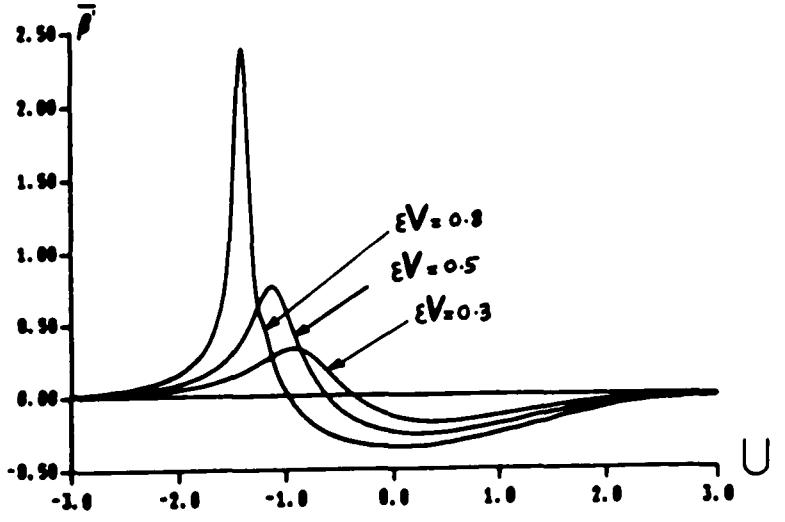

Fig. 10.2-3: The derivative of the normalized phase of the induced phase modulated steepened second harmonic pulse as function of U with different intensities with n = 1.76 .

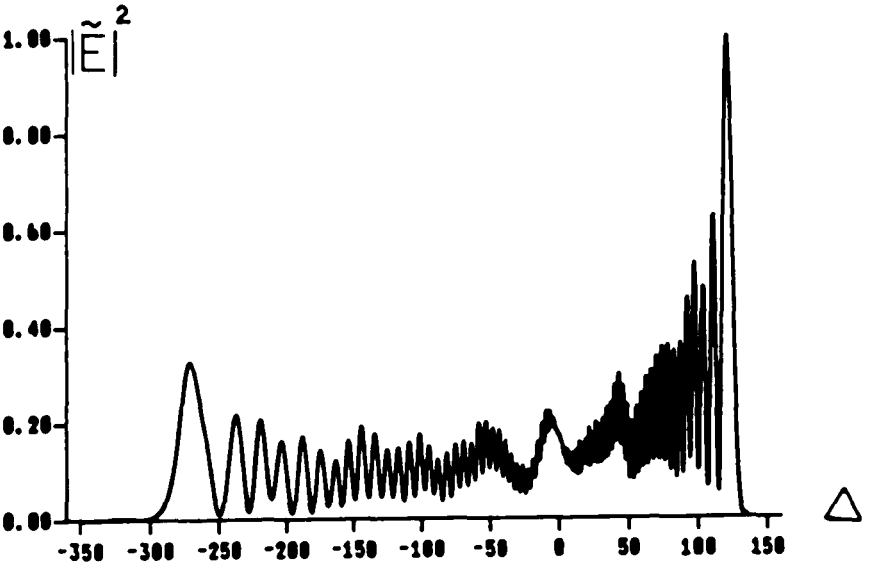

Fig. 10.2-4: The spectral distribution of the induced phase modulated steepened second harmonic pulse as function of Δ with $\varepsilon V = .5$ with $n = 1.76$.

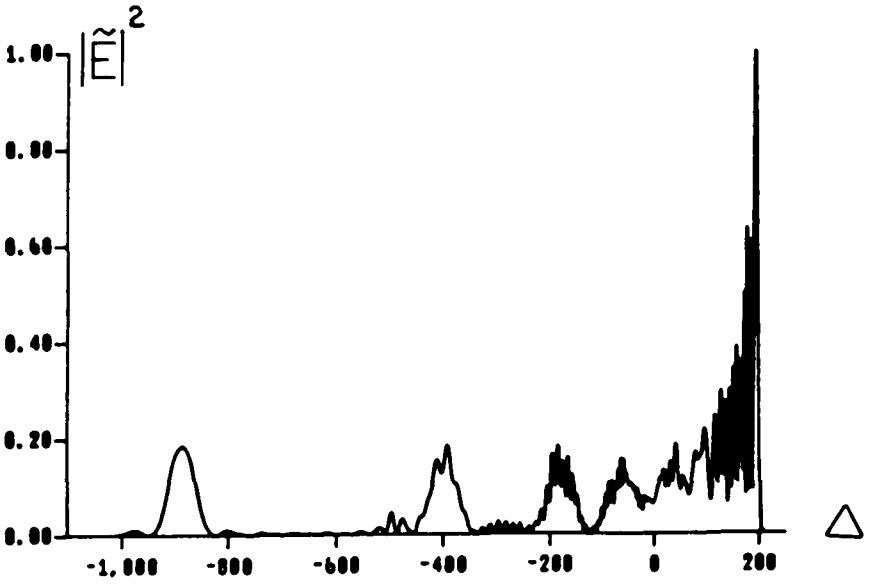

Fig. 10.2-5: The spectral distribution of the induced phase modulated steepened second harmonic pulse as function of Δ with $\varepsilon V = .8$ with $n = 1.76$.

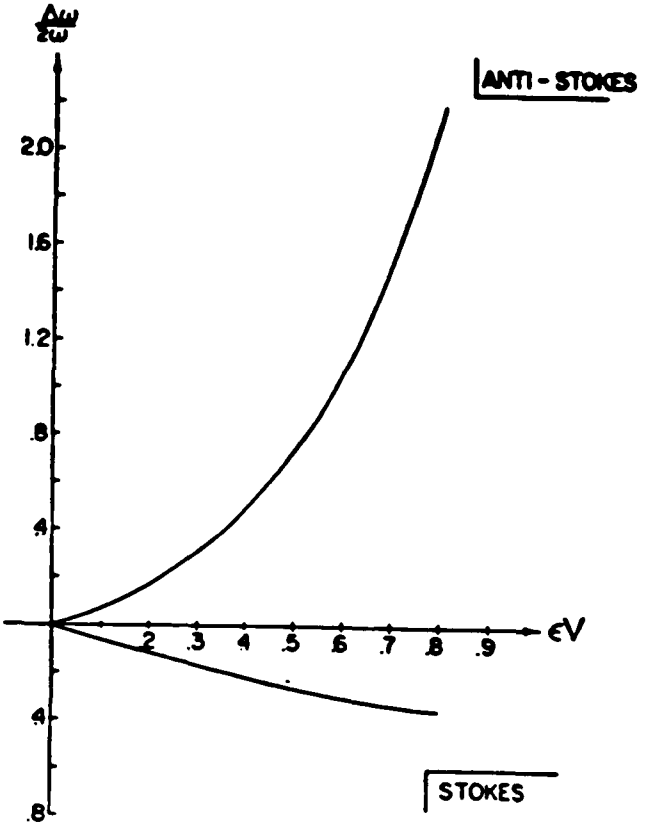

Fig. 10.2-6: The induced frequency sweep extents (maxima and minima of the derivative of the induced phase) for a steepened second harmonic pulse in dispersionless $\chi^{(3)}$- medium as function of εV.

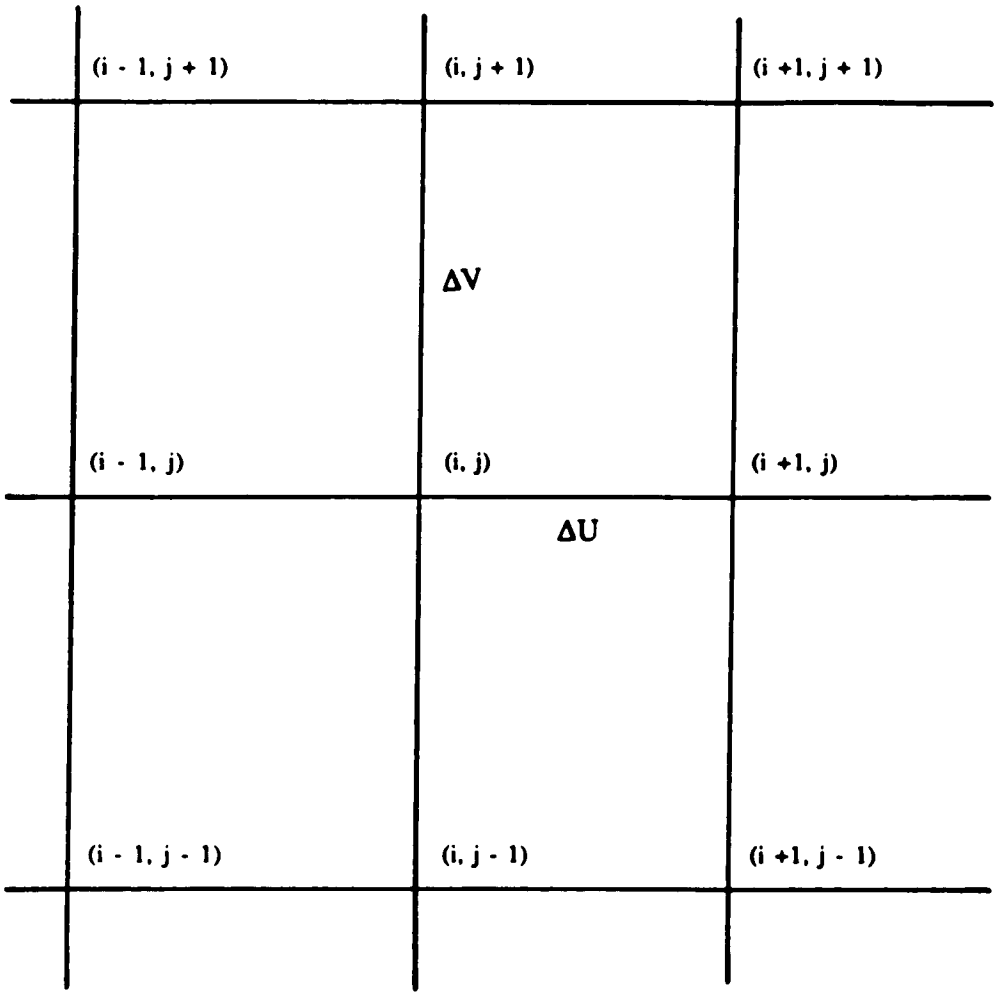

Fig. 11.1-1: Rectangular grid

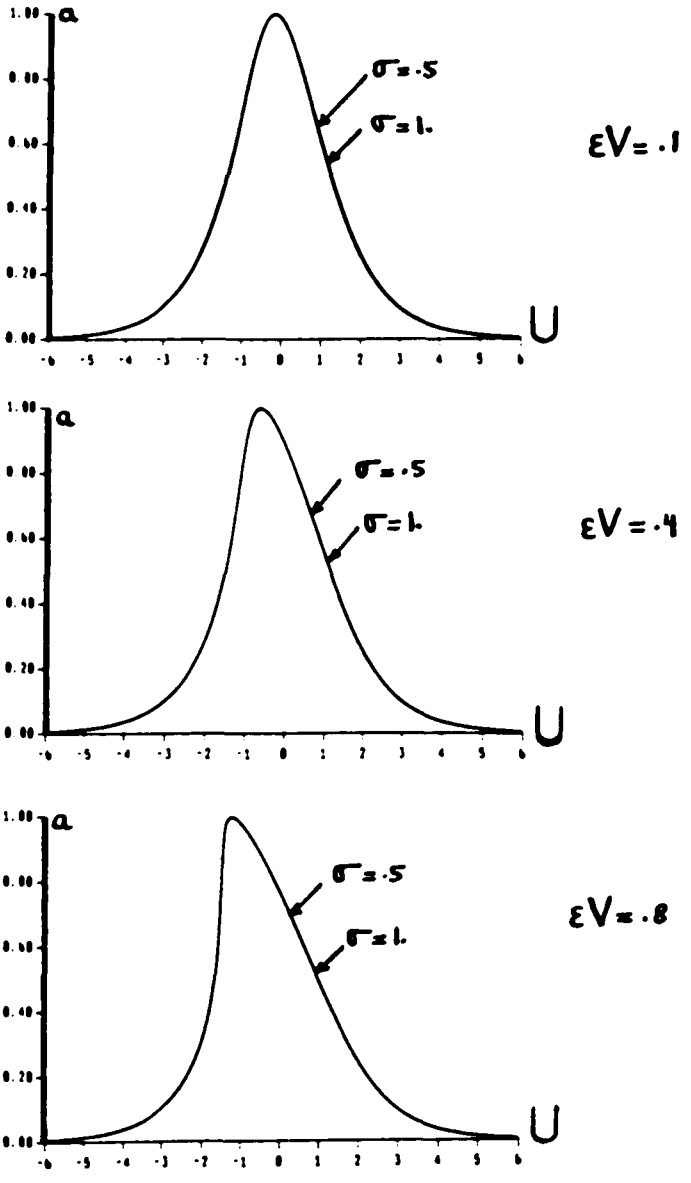

Fig. 11.2-1: The pump amplitude as a function of U for $\delta = 1$ and $\sigma = .5, 1$ with $\varepsilon V = .1, .4, .8$

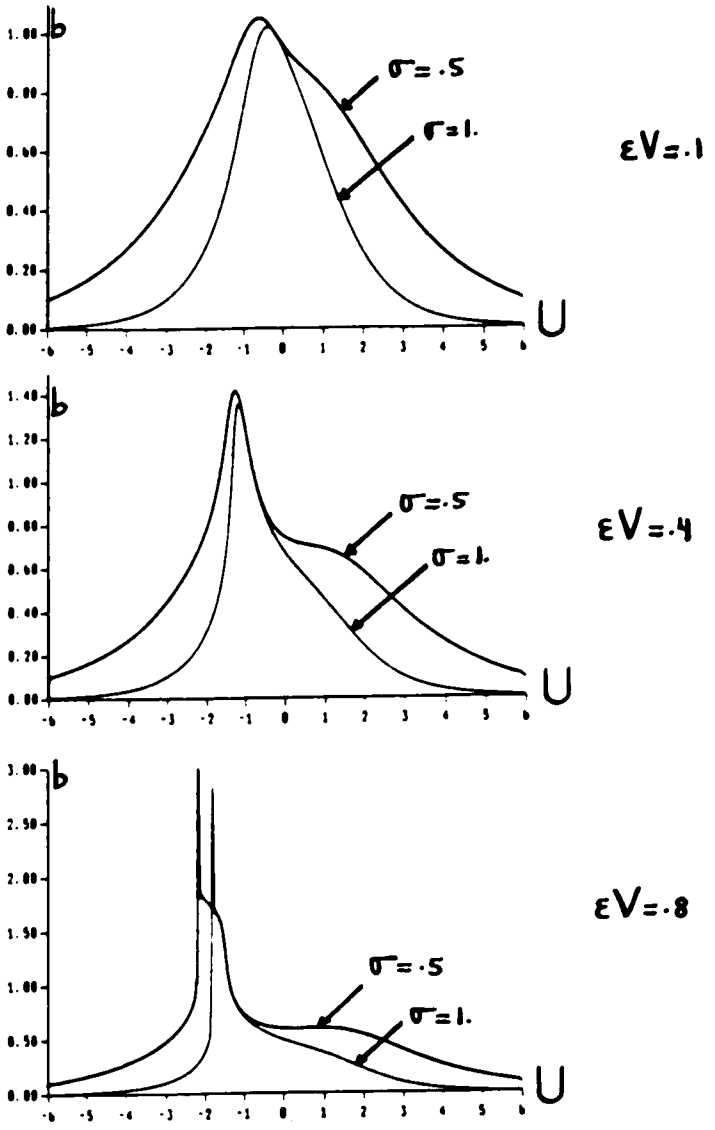

Fig. 11.2-2: The probe amplitude as a function of U for $\delta = 1$ and $\sigma = .5, 1$ with $\varepsilon V = .1, .4, .8$

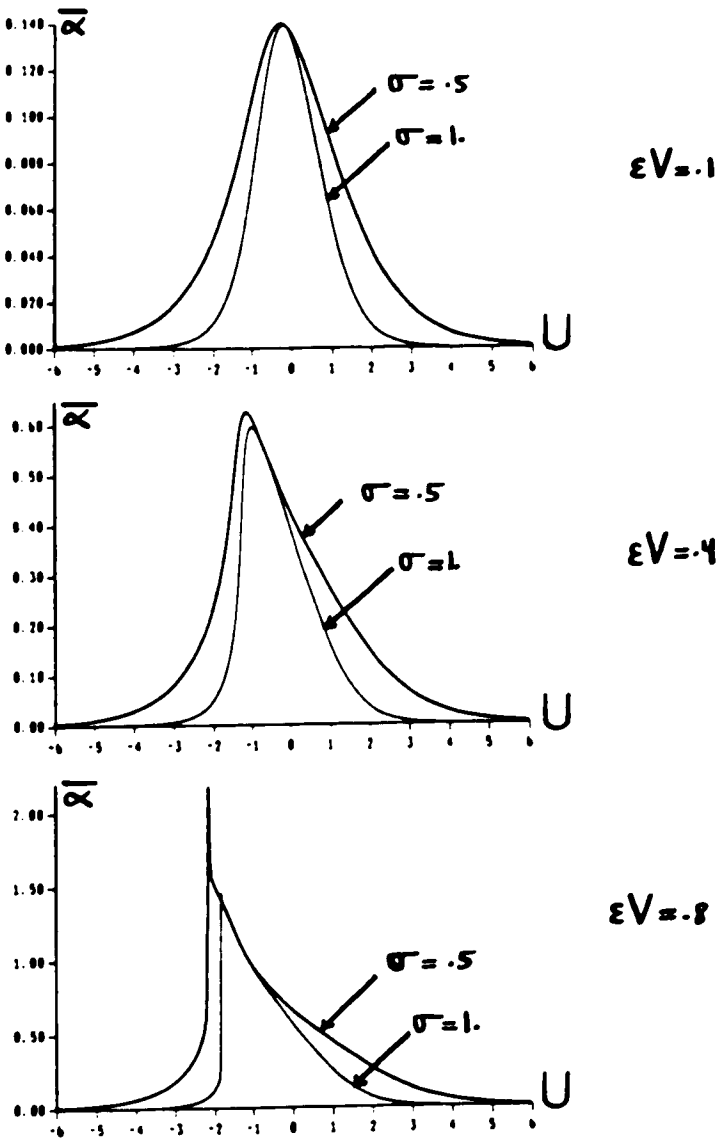

Fig. 11.2-3: The normalized pump phase as a function of U $\delta = 1$ and $\sigma = .5, 1$ with $\varepsilon V = .1, .4, .8$

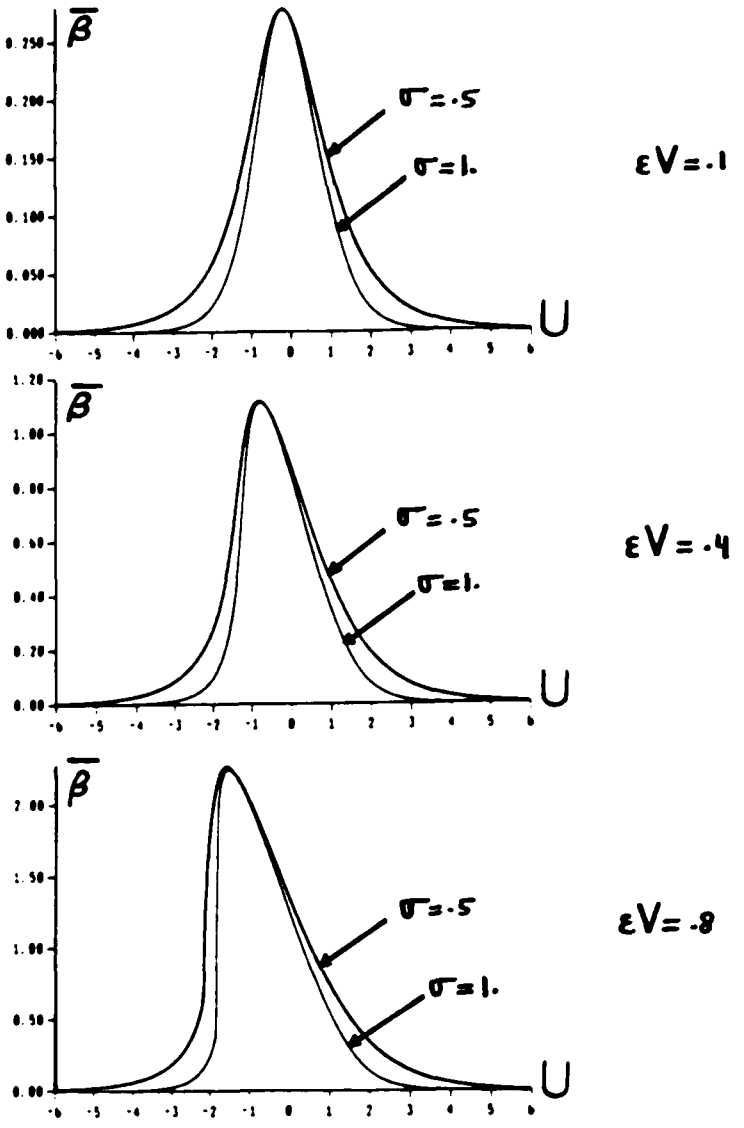

Fig. 11.2-4: The normalized probe phase as a function of U for $\delta = 1$ and $\sigma = .5, 1$ with $\varepsilon V = .1, .4, .8$

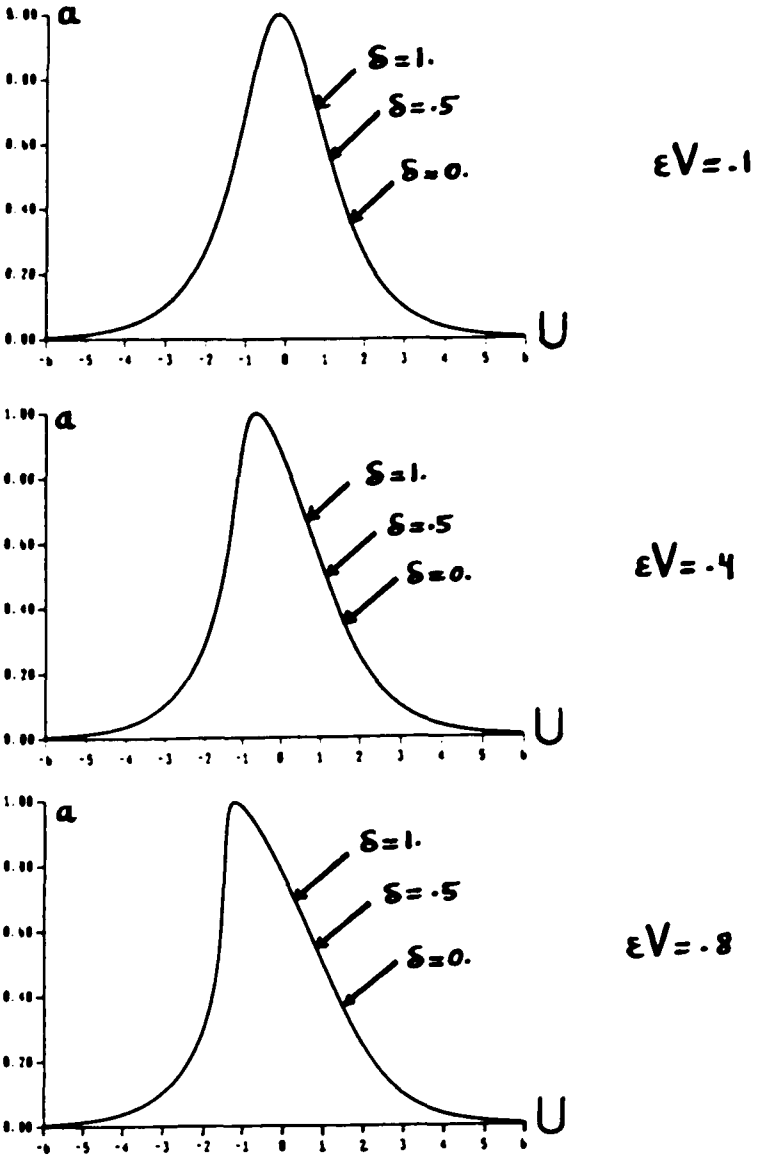

Fig. 11.2-5: The pump amplitude as a function of U for $\sigma = .5$ and $\delta = 0., .5, 1$ with $\varepsilon V = .1, .4, .8$

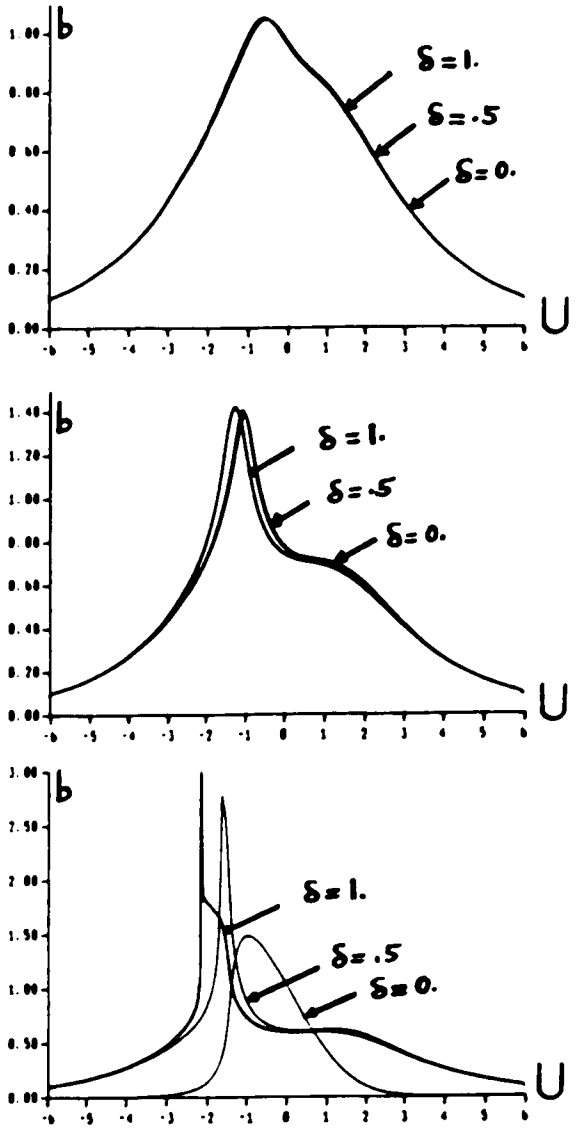

Fig. 11.2-6: The probe amplitude as a function of U for $\sigma = .5$ and $\delta = 0., .5, 1$ with $\varepsilon V = .1, .4, .8$

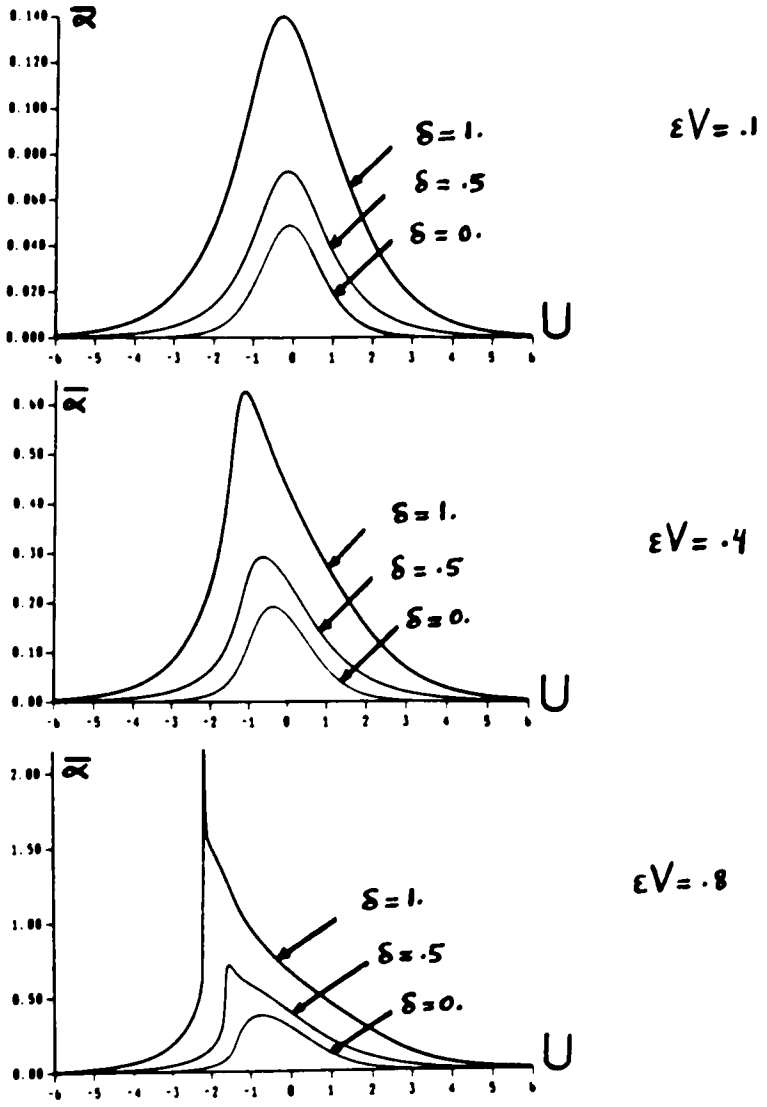

Fig. 11.2-7: The normalized pump phase as a function of U for σ = .5 and δ = 0., .5, 1 with εV = . 1, .4, .8

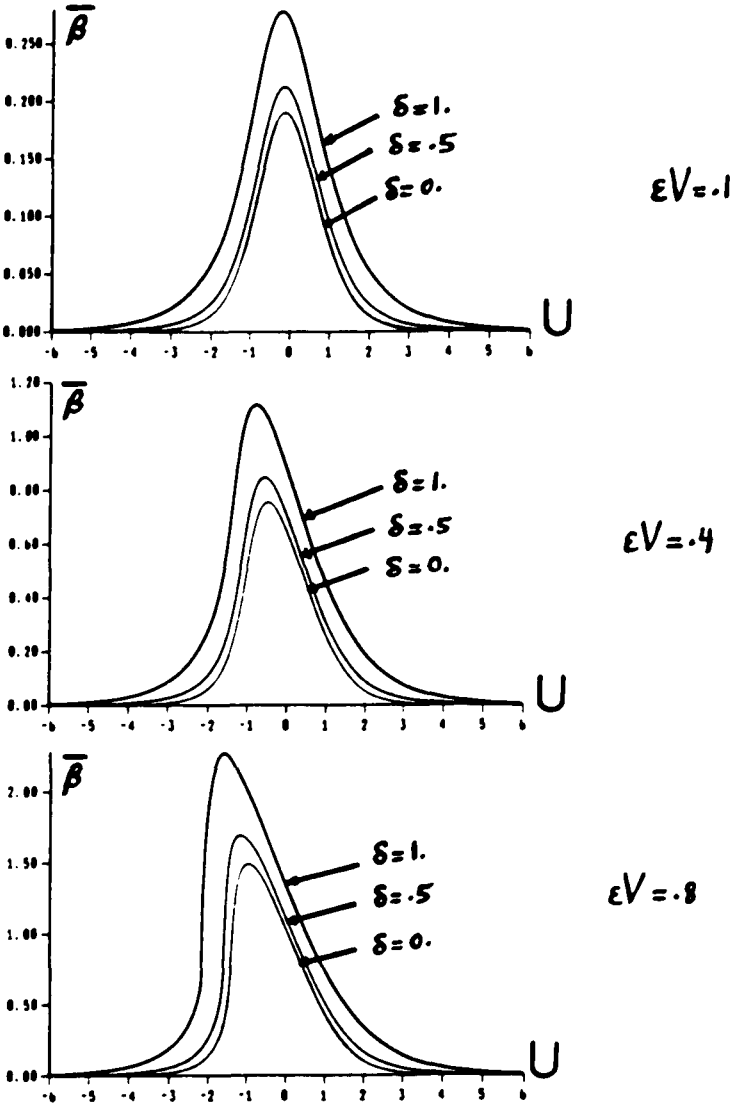

Fig. 11.2-8: The normalized probe phase as a function of U for $\sigma = .5$ and $\delta = 0., .5, 1$ with $\varepsilon V = .1, .4, .8$

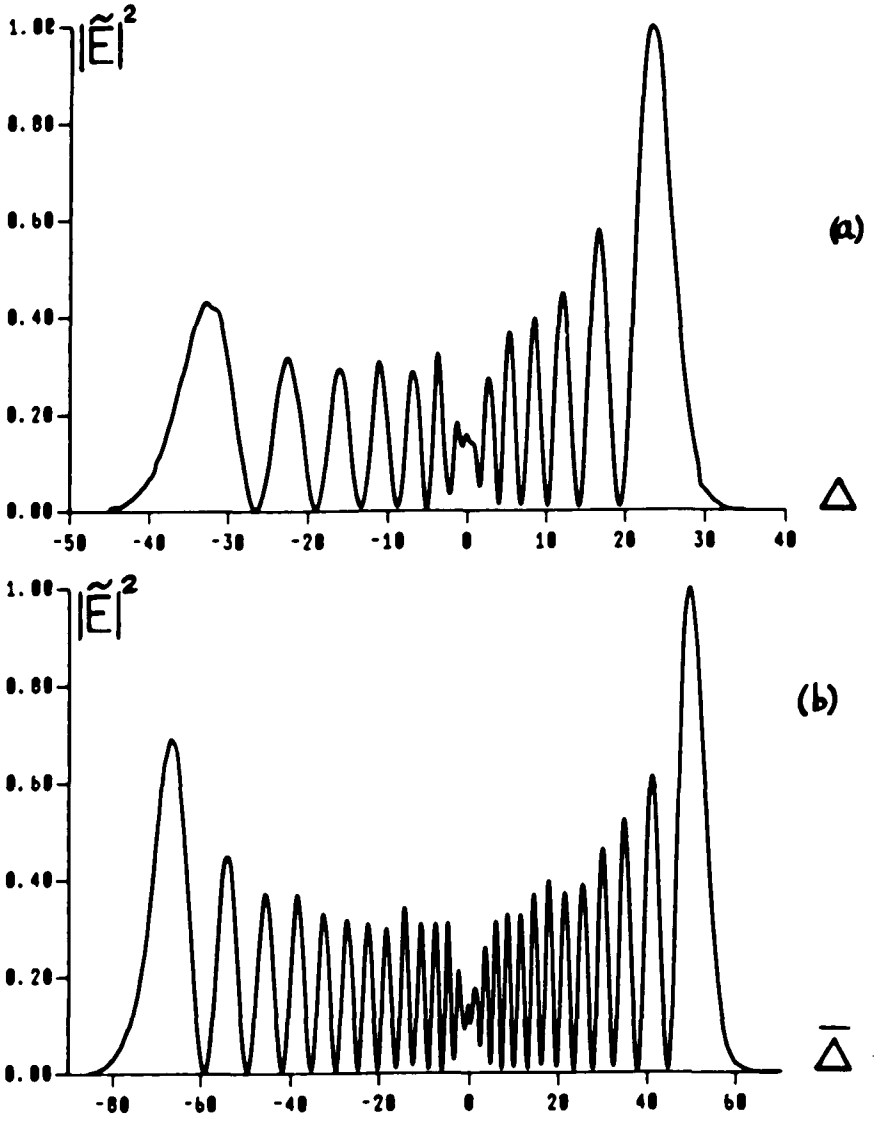

Fig. 11.2-9: The normalized spectral distributions of the pump and the probe as a function of Δ and $\bar{\Delta}$ and respectively, for $\delta = 1$, $\sigma = 1$ and $\varepsilon V = .1$

(a) pump spectral distribution

(b) probe spectral distribution

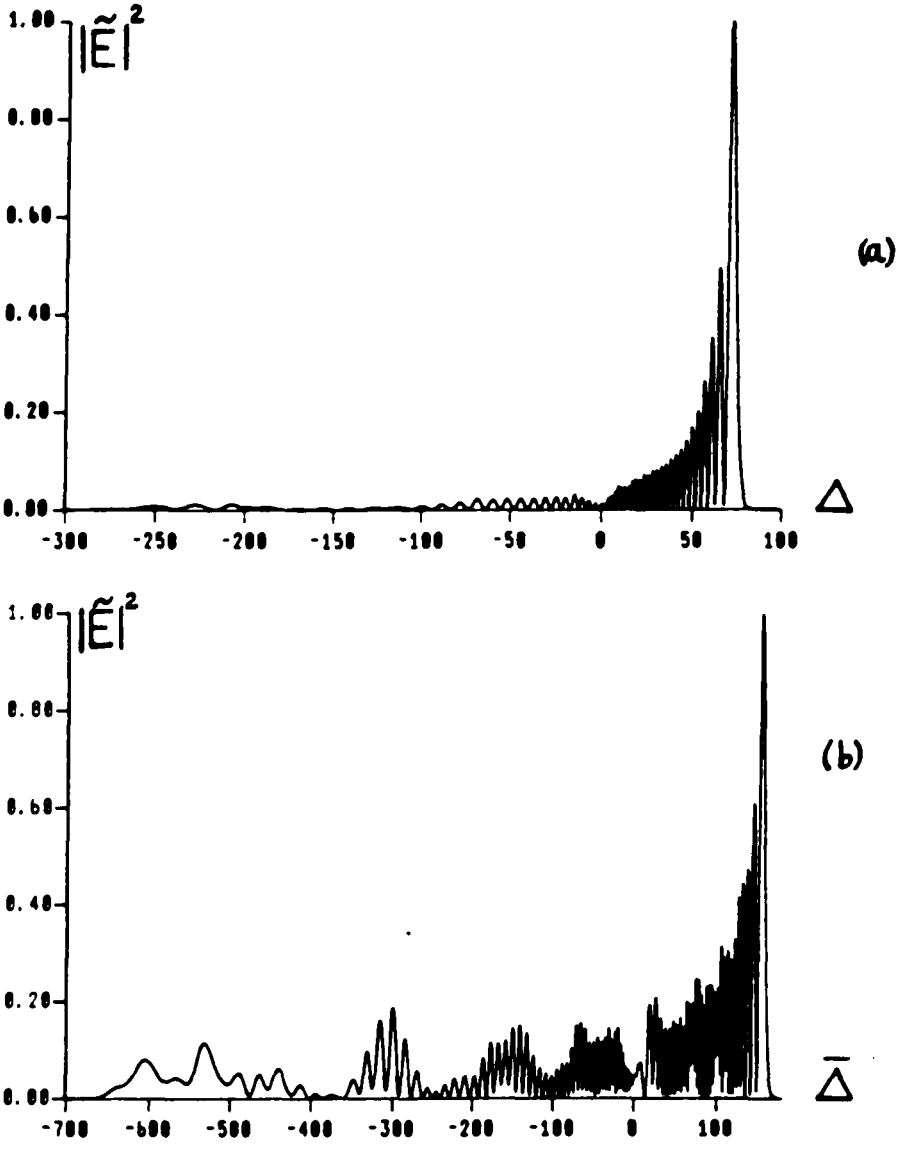

Fig. 11.2-10: The normalized spectral distributions of the pump and the probe as a function of Δ and $\bar{\Delta}$ respectively, for $\delta = 1$, $\sigma = 1$ and $\varepsilon V = .4$

(a) pump spectral distribution

(b) probe spectral distribution

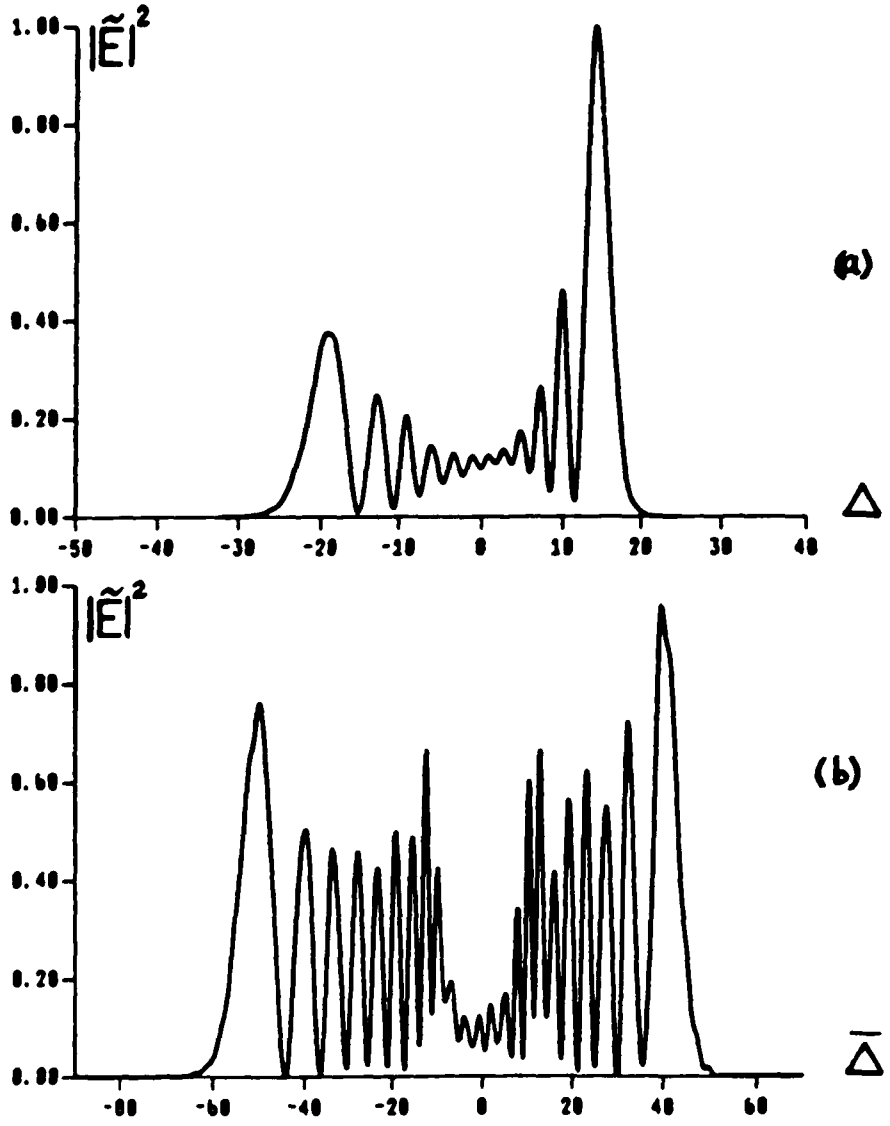

Fig. 11.2-11: The normalized spectral distributions of the pump and the probe as a function of Δ and $\bar{\Delta}$ respectively, for $\delta = 1$, $\sigma = .5$ and $\epsilon V = .1$

(a) pump spectral distribution

(b) probe spectral distribution .

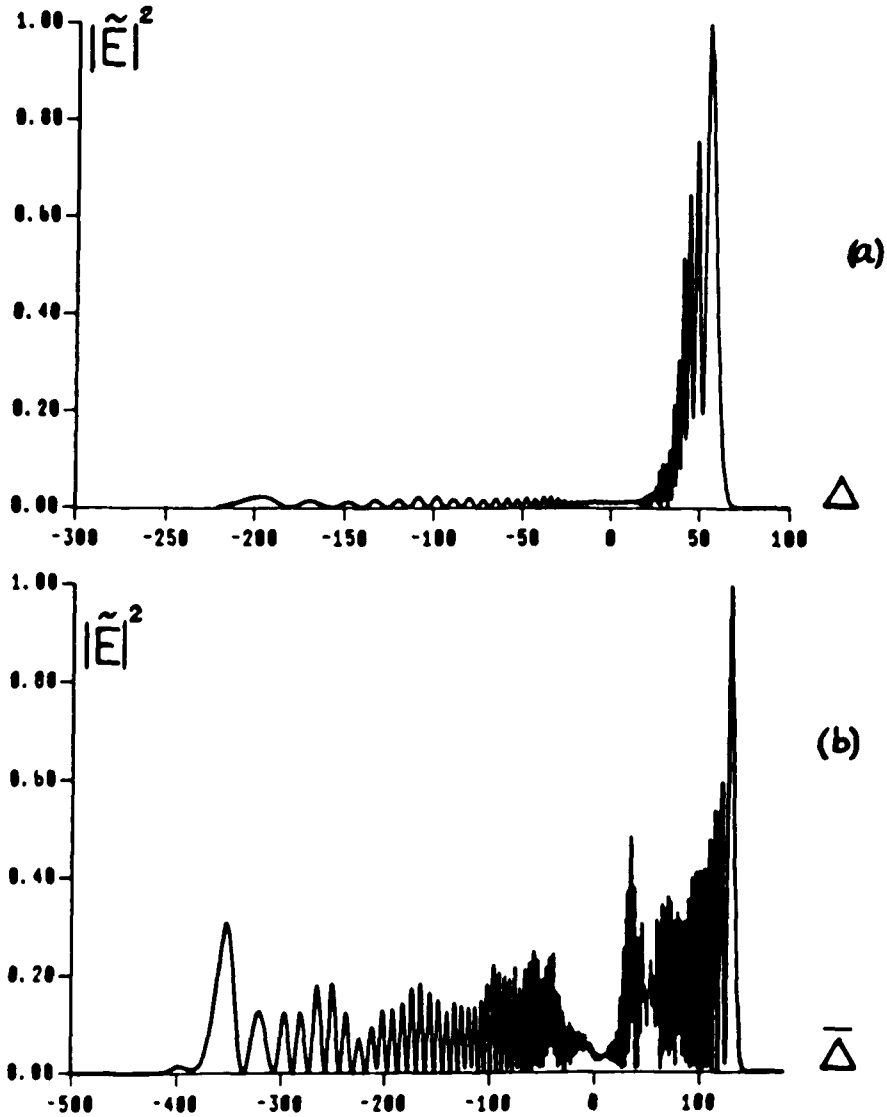

Fig. 11.2-12: The normalized spectral distributions of the pump and the probe as a function of Δ and $\bar{\Delta}$ respectively, for $\delta = 1$, $\sigma = .5$ and $\varepsilon V = .4$

(a) pump spectral distribution

(b) probe spectral distribution .

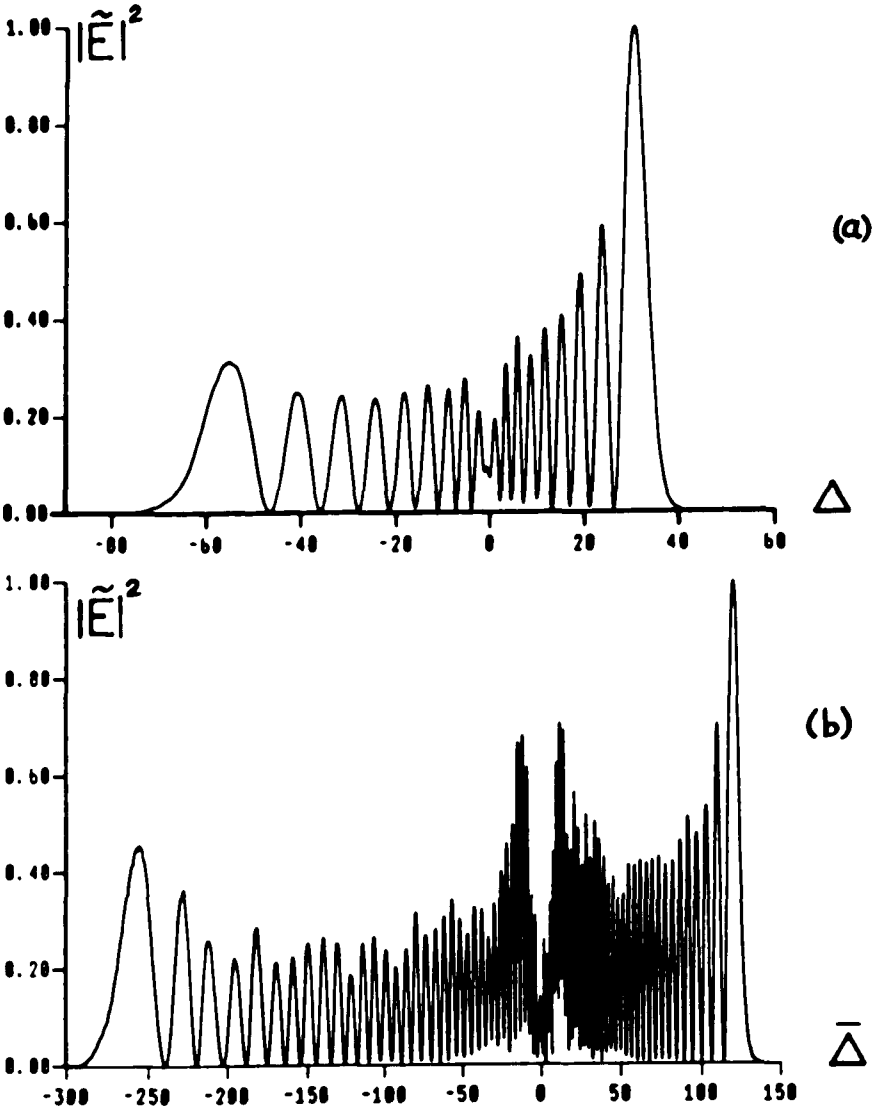

Fig. 11.2-13: The normalized spectral distributions of the pump and the probe as a function of Δ and $\bar{\Delta}$ respectively, for $\delta = 0$, $\sigma = .5$ and $\varepsilon V = .4$

(a) pump spectral distribution

(b) probe spectral distribution .

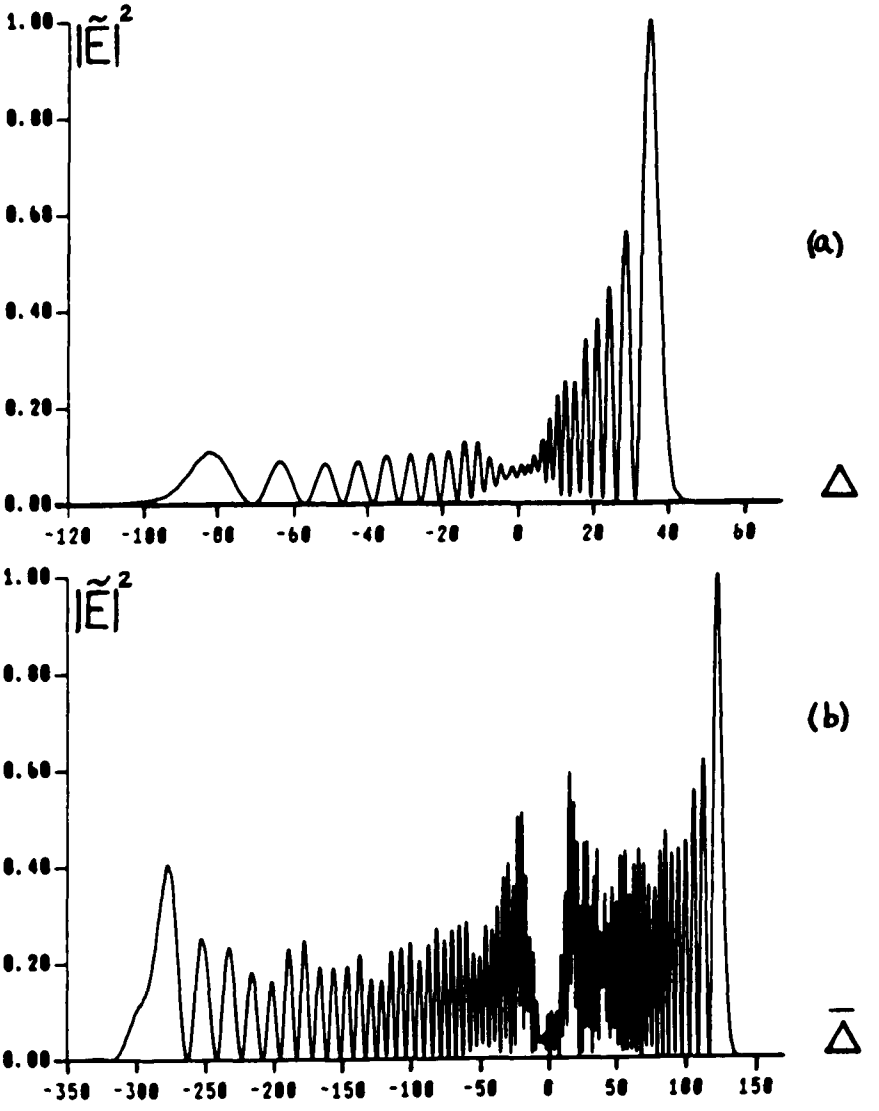

Fig. 11.2-14: The normalized spectral distributions of the pump and the probe as a function of Δ and $\bar{\Delta}$ respectively, for $\delta = .5$, $\sigma = .5$ and $\varepsilon V = .4$

(a) pump spectral distribution

(b) probe spectral distribution .

REFERENCES

1. J.T. Manassah, M.A. Mustafa, R.R. Alfano, and P.P. Ho,"Spectral Extent and Pulse Shape of the Supercontinuum for Ultrashort Laser Pulses", IEEE J. of Quantum Electronics QE-22, 197 (1986).

2. J.T. Manassah and M.A. Mustafa, "The Phase, Spectral Shape and Frequency Shift of a Self-Phase Modulation Pulse", Phys. Lett. A, 133, 51 (1988).

3. J.T. Manassah and M.A. Mustafa, "Analytical Solution for a Self-Phase Modulated Pulse Propagating in a $\chi^{(3)}$- Medium in the Presence of Self-Steepening and Material Relaxation", JOSA, B 6, June (1989).

4. J.T. Manassah and M.A. Mustafa, "The Supercontinuum Generated by Six-Photon Mixing", Opt. Lett. 13, 862 (1988).

5. J.T. Manassah and M.A. Mustafa, "Analytical Solution for a Self-phase Modulated Pulse Propagating in a Medium $\chi^{(5)}$- with Material Relaxation", Invited talk to Lasers '88, Nevada.

6. J.T. Manassah and M.A. Mustafa, "Interference Pattern of the Supercontinuum Generated by Self-phase Modulation", Opt. Lett. 13, 752 (1988).

7. J.T. Manassah and M.A. Mustafa," Effects of Amplitude Filters on Self-Phase Modulated Pulses: A Compression Scheme for Ultrashort Pulses", App. Opt. 27, 807 (1988).

8. R.R. Alfano and S.L. Shapiro, "Observation of Self-phase Modulation and Small-Scale Filaments in Crystals and Glasses", Phys. Rev. Lett. 24, 592 (1970).

9. R.R. Alfano, "The Ultrafast Supercontinuum Laser Source"' printed from proceedings of the international conference on lasers '85. December 2-6, 1985.

10. R.L. Fork, C.V. Shank, C. Hirlimann, R. Yen, and W.J. Tomlinson, "Femtosecond White-light Continuum Pulses", Opt. Lett 8, 1 (1983).

11. J.T. Manassah, P.P. Ho, A. Katz, and R.R. Alfano, "Ultrafast Supercontinuum Laser Source", Photonics Spectra, 53 (1984).

12. P.B. Corkum, P.P. Ho, R.R. Alfano, and J.T. Manassah, "Generation of Infrared Supercontinuum Covering 3-14 μm in Dielectrics and Semiconductors", Opt. Lett. 10, 624 (1985).

13. G. Yang and Y.R. Shen, "Spectral Broadening of Ultrashort Pulses in a Nonlinear Medium", Opt. Lett 9, 510 (1984).

14. R.R. Alfano, Ed., "Biological Events Probed by Ultrafast Laser Spectroscopy", Academic Press, New York, (1983).

15. R.A. Fisher, Ed., "Optical Phase Conjugation", Academic press, New York, (1983).

16. J.T. Manassah, M.A. Mustafa, R.R. Alfano and P.P. Ho, "Induced Supercontinuum and Steepening of an Ultrafast Laser Pulse", Phys. Lett. 113A, 242 (1985).

17. F. Shimizu, "Frequency Broadening in Liquid by a Short Light Pulse", Phys. Rev. Lett. 19, 1097 (1967).

18. R.R. Alfano, L.L. Hope, and S.L. Shapiro, "Electronic Mechanism for Production of Self-Phase Modulation", Phys. Rev. A6, 433 (1972).

19. P.L. Baldeck, P.P. Ho and R.R. Alfano, "Effects of Self, Induced and Cross Phase Modulation on the Generation of Picosecond and

Femtosecond White Light Supercontinua", Phys. Rev. Lett. 22, 1677 (1987).

20. E.P. Ippen, C.V. Shank, and T.K. Gustafson, "Self-Phase Modulation of Picosecond Pulses in Optical Fibers", App. Phys. Lett. 24, 190 (1974).

21. Y.R. Shen, "The Principles of Nonlinear Optics", Wiley, New York, 1984.

22. R.H. Stolen and C. Lin, "Self-Phase-Modulation in Silica Optical Fibers", Phys. Rev., A17, 1448 (1978).

23. F. DeMartini, C.H. Townes, T.K. Gustafson and P.L. Kelley, "Self-Steepening of Light Pulses", Phys. Rev. 164, 312 (1967).

24. D. Grischkowsky, E. Courtens, and J.A. Armstrong, "Observation of Self-Steepening of Optical Pulses with Possible Shock Formation", Phys. Rev. Lett. 31, 422 (1973).

25. T.K. Gustafson, J.P. Taran, H.A. Haus, J.R. Lifsitz, and P.L. Kelley, "Self- Modulation, Self-Steepening, and Spectral Development of Light in Small-Scale Trapped Filaments", Phys. Rev. 177, 306 (1969).

26. D. Anderson and M. Lisak, "Nonlinear Asymmetric Self-Phase Modulation and Self-Steepening of Pulses in Long Optical Waveguides"Phys. Rev. 164, 312 (1967).

27. J.P. Gordon, "Theory of the Soliton Self-Frequency Shift"' Opt. Lett. 11, 662 (1986).

28. J.H. Marburger, "Self-Focusing Theory", Prog. Quantum Electron. 4, 35 (1975).

29. A.H. Nayfeh, "Introduction to Perturbation Techniques", Wiley, New York, 1981.

30. F.B. Hilderbrand, "Advanced Calculus for Applications", Prentice-Hall, New Jersey, 1976.

31. W. Zhao and E. Bourkoff, "Femtosecond Pulse Propagation in Optical Fibers: Higher Order Effects", IEEE J. of Quantum Electronics QE-24, 365 (1988).

32. S.M. Kay and A. Maitland, "Quantum Optics", Academic Press, New York, (1970).

33. D. Mesidagh and M. Haelterman, "Spectral Super-Broadening of Ultra-Short Pulses in a Nonlinear Kerr Medium; Effect of Relaxation", Opt. Comm. 61, 291 (1987).

34. N. Bloembergen, "Nonlinear Optics", Benjamin, New York, (1965).

35. G.F. Carrier, M. Krook and C.E. Pearson, "Functions of a Complex Variable", McGraw-Hill, New York, (1966).

36. E. Zauderer, "Partial Differential Equations of Applied Mathmatics", Wiley, New York, (1983).

37. J.E. Rothenberg and D. Grischkowsky, "Measurement of Optical Phase with Subpicosecond Resolution by Time-Domain Interferometry", Opt. Lett. 12, 99 (1987).

38. J.M. Stone, "Radiation and Optics". McGraw Hill, New York, (1963).

39. J.T. Manassah, "Interferometric Characterization of Chirped Ultrafast Pulses", App. Opt. 25, 2480 (1986).

40. W.H. Knox, N.M. Pearson, K.D. Li, and C.A. Hirlimann, "Interferometric Measurements of Femtosecond Group Delay in Optical Components", Opt. Lett. 13, 574 (1988).

41. M. Born and E. Wolf, "Principles of Optics", 5th Edition, Pergamon,

New York, (1975).

42. J.T. Manassah, R.R. Alfano, M.A. Mustafa, and P.P. Ho, "Spectral Distribution of an Ultrafast Supercontinuum Laser Source", Phys. Lett. 107A, 305 (1985).

43. R.R. Alfano, Q.X. Li, T. Jimbo, J.T. Manassah and P.P. Ho, "Induced Spectral Broadening of a Weak Picosecond Pulse in Glass Produced by an Intense Picosecond Pulse", Opt. Lett. 11, 626 (1986).

44. D.W. Peaceman, "Fundamentals of Numerical Reservoir Simulation", Developments in Petroleum Science 6.

45. W. Cheney and D. Kincaid, "Numerical Mathematics and Computing", Brooks/Cole publi, Monterey, 1985.

46. B. Carnahan, H.A. Luther and J.O. Wilkes, "Applied Numerical Methods", Wiley, New York, 1969.

47. L. Saaty, "Modern Nonlinear Equations", Dover, New York, 1982.

BIBLIOGRAPHY

1. Alfano R.R., "The Ultrafast Supercontinuum Laser Source"' printed from proceedings of the international conference on lasers '85. December 2-6, 1985.

2. Alfano R.R., Ed., "Biological Events Probed by Ultrafast Laser Spectroscopy", Academic Press, New York, (1983).

3. Alfano R.R., L.L. Hope, and S.L. Shapiro, "Electronic Mechanism for Production of Self-Phase Modulation", Phys. Rev. A6, 433 (1972).

4. Alfano R.R., Q.X. Li, T. Jimbo, J.T. Manassah and P.P. Ho, "Induced Spectral Broadening of a Weak Picosecond Pulse in Glass Produced by an Intense Picosecond Pulse", Opt. Lett. 11, 626 (1986).

5. Alfano R.R. and S.L. Shapiro, "Observation of Self-phase Modulation and Small-Scale Filaments in Crystals and Glasses", Phys. Rev. Lett. 24, 592 (1970).

6. Anderson D. and M. Lisak, "Nonlinear Asymmetric Self-Phase Modulation and Self-Steepening of Pulses in Long Optical Waveguides "Phys. Rev. 164, 312 (1967).

7. Baldeck P.L., P.P. Ho and R.R. Alfano, "Effects of Self, Induced and Cross Phase Modulation on the Generation of Picosecond and Femtosecond White Light Supercontinua", Phys. Rev. Lett. 22, 1677 (1987).

8. Bloembergen N., "Nonlinear Optics", Benjamin, New York, (1965).

9. Born M. and E. Wolf, "Principles of Optics", 5th Edition, Pergamon, New York, (1975).

10. Carnahan B., H.A. Luther and J.O. Wilkes, "Applied Numerical Methods", Wiley, New York, 1969.

11. Carrier G.F., M. Krook and C.E. Pearson, "Functions of a Complex Variable", McGraw-Hill, New York, (1966).

12. Cheney W. and D. Kincaid, "Numerical Mathematics and Computing", Brooks/Cole publi, Monterey, 1985.

13. Corkum P.B., P.P. Ho, R.R. Alfano, and J.T. Manassah, "Generation of Infrared Supercontinuum Covering 3-14 μm in Dielectrics and Semiconductors", Opt. Lett. 10, 624 (1985).

14. DeMartini F., C.H. Townes, T.K. Gustafson and P.L. Kelley, "Self-Steepening of Light Pulses", Phys. Rev. 164, 312 (1967).

15. Fisher R.A., Ed., "Optical Phase Conjugation", Academic press, New York, (1983).

16. Fork R.L., C.V. Shank, C. Hirlimann, R. Yen, and W.J. Tomlinson, "Femtosecond White-light Continuum Pulses", Opt. Lett 8, 1 (1983).

17. Gordon J.P., "Theory of the Soliton Self-Frequency Shift"' Opt. Lett. 11, 662 (1986).

18. Grischkowsky D, E. Courtens, and J.A. Armstrong, "Observation of Self-Steepening of Optical Pulses with Possible Shock Formation", Phys. Rev. Lett. 31, 422 (1973).

19. Gustafson T.K., J.P. Taran, H.A. Haus, J.R. Lifsitz, and P.L. Kelley, "Self- Modulation, Self-Steepening, and Spectral Development of Light in Small-Scale Trapped Filaments", Phys. Rev. 177, 306 (1969).

20. Hilderbrand F.B., "Advanced Calculus for Applications", Prentice-Hall, New Jersey, 1976.

21. Ippen E.P., C.V. Shank, and T.K. Gustafson, "Self-Phase Modulation of Picosecond Pulses in Optical Fibers", App. Phys. Lett. 24, 190 (1974).

22. Kay S.M. and A. Maitland, "Quantum Optics", Academic Press, New York, (1970).

23. Knox W.H., N.M. Pearson, K.D. Li, and C.A. Hirlimann, "Interferometric Measurements of Femtosecond Group Delay in Optical Components", Opt. Lett. 13, 574 (1988).

24. Manassah J.T., "Interferometric Characterization of Chirped Ultrafast Pulses", App. Opt. 25, 2480 (1986).

25. Manassah J.T., R.R. Alfano, M.A. Mustafa, and P.P. Ho, "Spectral Distribution of an Ultrafast Supercontinuum Laser Source", Phys. Lett. 107A, 305 (1985).

26. Manassah J.T., P.P. Ho, A. Katz, and R.R. Alfano, "Ultrafast Supercontinuum Laser Source", Photonics Spectra, 53 (1984).

27. Manassah J.T., M.A. Mustafa, R.R. Alfano and P.P. Ho, "Induced Supercontinuum and Steepening of an Ultrafast Laser Pulse", Phys. Lett. 113A, 242 (1985).

28. Manassah J.T., M.A. Mustafa, R.R. Alfano, and P.P. Ho,"Spectral Extent and Pulse Shape of the Supercontinuum for Ultrashort Laser Pulses", IEEE J. of Quantum Electronics QE-22, 197 (1986).

29. Manassah J.T. and M.A. Mustafa, "The Phase, Spectral Shape and Frequency Shift of a Self-Phase Modulation Pulse", Phys. Lett. A, 133, 51 (1988).

30. Manassah J.T. and M.A. Mustafa," Effects of Amplitude Filters on Self-Phase Modulated Pulses: A Compression Scheme for Ultrashort Pulses", App. Opt. 27, 807 (1988).

31. Manassah J.T. and M.A. Mustafa, "The Supercontinuum Generated by Six-Photon Mixing", Opt. Lett. 13, 862 (1988).

32. Manassah J.T. and M.A. Mustafa, "Analytical Solution for a Self-phase Modulated Pulse Propagating in a Medium $\chi^{(5)}$ with Material Relaxation", Invited talk to Lasers '88, Nevada.

33. Manassah and M.A. Mustafa, "Interference Pattern of the Supercontinuum Generated by Self-phase Modulation", Opt. Lett. 13, 752 (1988).

34. Manassah J.T. and M.A. Mustafa, "Interference Pattern of the Supercontinuum Generated by Self-phase Modulation", Opt. Lett. 13, 752 (1988).

35. Marburger J.H., "Self-Focusing Theory", Prog. Quantum Electron. 4, 35 (1975).

36. Mestdagh D. and M. Haelterman, "Spectral Super-Broadening of Ultra-Short Pulses in a Nonlinear Kerr Medium; Effect of Relaxation", Opt. Comm. 61, 291 (1987).

37. Nayfeh A.H., "Introduction to Perturbation Techniques", Wiley, New York, 1981.

38. Peaceman D.W., "Fundamentals of Numerical Reservoir Simulation", Developments in Petroleum Science 6.

39. Rothenberg J.E. and D. Grischkowsky, "Measurement of Optical Phase with Subpicosecond Resolution by Time-Domain Interferometry", Opt. Lett. 12, 99 (1987).

40. Saaty L., "Modern Nonlinear Equations", Dover, New York, 1982.

41. Shen Y.R. , "The Principles of Nonlinear Optics", Wiley, New York, 1984.

42. Shimizu F., "Frequency Broadening in Liquid by a Short Light Pulse", Phys. Rev. Lett. 19, 1097 (1967).

43. Stolen R.H. and C. Lin, "Self-Phase-Modulation in Silica Optical Fibers", Phys. Rev., A17, 1448 (1978).

44. Stone J.M., "Radiation and Optics". McGraw Hill, New York, (1963).

45. Yang G. and Y.R. Shen, "Spectral Broadening of Ultrashort Pulses in a Nonlinear Medium", Opt. Lett 9, 510 (1984).

46. Zauderer E., "Partial Differential Equations of Applied Mathmatics", Wiley, New York, (1983).

47. Zhao W. and E. Bourkoff, "Femtosecond Pulse Propagation in Optical Fibers: Higher Order Effects", IEEE J. of Quantum Electronics QE-24, 365 (1988).